



**PEDRO JORGE MEDIÇÃO DE PROPRIEDADES TERMOFÍSICAS DE
MARQUES CARVALHO PERFLUOROCARBONETOS E LÍQUIDOS IÓNICOS**

**MEASUREMENTS OF THERMOPHYSICAL
PROPERTIES OF PERFLUOROCARBONS AND IONIC
LIQUIDS**



PEDRO JORGE MARQUES CARVALHO **MEDIÇÃO DE PROPRIEDADES TERMOFÍSICAS DE
PERFLUOROCARBONETOS E LÍQUIDOS IÓNICOS**

**MEASUREMENTS OF THERMOPHYSICAL
PROPERTIES OF PERFLUOROCARBONS AND IONIC
LIQUIDS**

Dissertação apresentada à Universidade de Aveiro para cumprimento dos requisitos necessários à obtenção do grau de Mestre em Engenharia Química, realizada sob a orientação científica do Dr. João A. P. Coutinho, Professor associado com agragação do Departamento de Química da Universidade de Aveiro e do Dr. António José do Nascimento Queimada, Investigador Assistente da Faculdade de Engenharia da Universidade do Porto

Aos meus pais, à Fatolas e aos meus orientadores.

“Acima de tudo, na vida, temos necessidade de alguém que nos obrigue a realizar aquilo de que somos capazes.”

“Diz-me, e eu esquecerei; ensina-me e eu lembrar-me-ei; envolve-me, e eu aprenderei.”

o júri

presidente

Prof. Dr. Carlos Pascoal Neto
Professor catedrático da Universidade de Aveiro

Prof. Dr. João A. P. Coutinho
Professor associado com agregação da Universidade de Aveiro

Prof. Dr. Abel Gomes Martins Ferreira
Professor auxiliar da Faculdade de Ciências e Tecnologia da Universidade de Coimbra

Prof. Dra. Isabel Maria Delgado Jana Marrucho Ferreira
Professora auxiliar da Universidade de Aveiro

Dr. António José do Nascimento Queimada
Investigador assistente da Faculdade de Engenharia da Universidade do Porto

agradecimentos

Aos meus orientadores, Prof. Dr. João Coutinho, Dra. Isabel Marrucho e Dr. António Queimada, por acreditarem, investirem, incentivarem e me desafiarem diariamente a construir este caminho recheado de subtilezas que me deixam vidrado com o mundo da ciência. A eles, ao serem um exemplo a seguir, devo o construído até aqui e agradeço maravilhado os passos dados rumo a desafios futuros.

A todos os membros do grupo PATH que além de colegas se tornaram amigos (Ana Caço, Ana Dias, Mara Martins, António Queimada, Nuno Pedrosa, Fatima Varanda, Fátima Mirante, Maria Jorge, Mariana Belo, Mariana Costa, Carla Gonçalves, Nelson Oliveira, Ramesh, Sónia Ventura, Machado e aos restantes membros de projectos e seminários: Catarina, Cláudia, ...) o meu mais profundo agradecimento pelos bons momentos passados e por tornarem este grupo um excelente e divertido local de trabalho. Ao Prof. Dr. Avelino um especial obrigado pelos desafios, pela confiança e pelos divertidos momentos passados acompanhados pelo doce aroma do café.

Deste magnífico grupo tenho que destacar alguns, que pela sua especial envolvimento deram um toque especial a esta caminhada. Ao Tózé agradeço muito do que sei hoje, desde o passar do testemunho (Tensiómetro), ao conhecimento transmitido, ao espírito crítico até ao interpretar os resultados “outsiders”, e por ser um exemplo a seguir. À Mara, mais que uma colega e amiga, tornou-se também um exemplo. Ao acompanhar o trabalho ao incentivar e especialmente a me desafiar para novas trilhas e novos projectos, muito obrigado. À Ana Caço ao ser uma peça vital neste taboleiro devo um especial obrigado, não só por aturar a minha bagunça mas também pela enorme paciência e sentido de humor mesmo quando usava imenso material que nem sempre lavava prontamente (especialmente os copos com petróleo e os funis de vidro). À Ana Dias, ao Nuno, à Mariana Costa, à Mara e à Fatima agradeço as divertidíssimas noitadas passadas ao fim de semana.

Pour le groupe du LHP au Laboratoire des Fluides Complexes de l'Université de Pau (Jean Luc Daridon, Jérôme Pauly e Hervé Carrier) par l'amitié et par la connaissance transmise, qui a aidé à compléter le travail ici développé. Et, bien sure, aussi de m'avoir introduit au Jurançon et à la cuisine française.

Estou agradecido a todos os amigos que fiz, por todas as pessoas que conheci, por todas as oportunidades que tive para viajar e alargar os horizontes. Mas nada disto teria sido possível sem o apoio dos meus pais e da Fatolas. Obrigado por estarem sempre perto, mesmo quando a distância é grande, pelo apoio, pelo amor... por serem vocês mesmos.

palavras-chave

tensões interfaciais, densidades, perfluorocarbonetos, líquidos iônicos, dependência com a temperatura, dependência com a pressão, influência do conteúdo de água, concentração iônica efectiva, condutividade molar, temperatura crítica, compressibilidade isotérmica, expansividade isobárica, entropia de superfície, entalpia de superfície, correlação de Faizullin.

resumo

No presente trabalho propõe-se estudar a tensão superficial de vários perfluorocarbonetos lineares, cíclicos, aromáticos e α -substituídos bem como líquidos iônicos com o catião imidazolium em comum.

Apesar do seu interesse inerente, informação sobre esta propriedade para os compostos seleccionados é escassa e quando disponível apresenta discrepâncias consideráveis entre si. As medições foram realizadas no intervalo de temperaturas (283 to 353) K usando o método do anel de Du Noüy.

Para os fluorocarbonetos, os dados experimentais demonstram que a estrutura molecular é o factor primordial no comportamento da superfície uma vez que os fluorocarbonetos aromáticos apresentam a tensão superficial mais elevada, seguida pelos fluorocarbonetos cíclicos e substituídos. Os perfluorocarbonetos lineares apresentam os menores valores de tensão superficial, aumentando ligeiramente com o aumento do número de carbonos.

Os líquidos iônicos estudados foram seleccionados com o objectivo de fornecerem um estudo compreensivo sobre a influência do tamanho da cadeia alquílica do catião, o número de substituições no catião e a influência do anião. A influência do conteúdo de água na tensão superficial foi estudada em função da temperatura e da fracção molar de água para o líquido iónico mais hidrofóbico, [omim][PF6], e para o mais higroscópico, [bmim][PF6].

As funções termodinâmicas de superfície, como a entropia e entalpia de superfície, foram derivadas a partir da dependência da tensão superficial com a temperatura.

Os dados obtidos para o fluorocarbonetos foram comparados com a correlação proposta por Faizullin, apresentando um desvio inferior a 4 % e demonstrando a sua aplicabilidade para com esta classe de compostos.

A metodologia adoptada neste trabalho requer o conhecimento das densidades dos compostos de modo a aplicar a necessária correcção hidrostática. Contudo, para os líquidos iónicos esta informação é limitada ou mesmo inexistente. Por este motivo realizaram-se medições de densidade em função da pressão ($0.10 < p/\text{MPa} < 10.0$) e da temperatura ($293.15 < T/\text{K} < 393.15$). Desta dependência, as propriedades termodinâmicas, tais como compressibilidade isotérmica, expansividade isobárica, coeficiente térmico da pressão e dependência da capacidade calorífica com a pressão foram investigadas.

A influência do teor de água na densidade foi também estudada para o líquido iónico mais hidrofóbico, [omim][PF6].

Um modelo simples de volume-ideal foi aplicado de forma preditiva para os volumes molares dos líquidos iónicos, em condições ambientais, descrevendo bem os dados experimentais.

keywords

interfacial tension, densities, perfluorocarbons, ionic liquids, temperature dependence, pressure dependence, water content, effective ionic concentration, molar conductivity, critical temperature, isothermal compressibility, isobaric expansivity, surface entropy, surface enthalpy, Faizullin correlation.

abstract

This work aims at studying the surface tension of some linear, cyclic, aromatic, α -substituted perfluorocarbons and imidazolium based ionic liquids.

Despite its fundamental interest, information about this property for these compounds is scarce and the available data present strong discrepancies among each other. The measurements were carried out in the temperature range (283 to 353) K with the Du Noüy ring method.

For the fluorocarbons, the analysis of the experimental data shows that the molecular structure is the main factor in the surface since the aromatic fluorocompounds present the highest surface tensions, followed by the cyclic and substituted fluorocompounds. The linear n-perfluoroalkanes exhibit the lowest surface tension values, slightly increasing with the carbon number.

The set of selected ionic liquids was chosen to provide a comprehensive study of the influence of the cation alkyl chain length, the number of cation substitutions and the anion on the properties under study. The influence of water content in the surface tension was studied for several ILs as a function of the temperature as well as a function of water mole fraction, for the most hydrophobic IL investigated, [omim][PF₆], and one hygroscopic IL, [bmim][PF₆].

The surface thermodynamic functions such as surface entropy and enthalpy were derived from the temperature dependence of the surface tension values.

The perfluorocarbons experimental data were compared against the Faizullin correlation, and it is shown that this correlation describes the measured surface tensions with deviations inferior to 4 %.

The methodology adopted in this work requires the knowledge of the densities of the compounds under study in order to apply an hydrostatic correction. However, for ionic liquids these information is scarce and in some cases unavailable. Therefore, experimental measurements of the pressure ($0.10 < p/\text{MPa} < 10.0$) and temperature ($293.15 < T/\text{K} < 393.15$) dependence of the density and derived thermodynamic properties, such as the isothermal compressibility, the isobaric expansivity, the thermal pressure coefficient, and the pressure dependence of the heat capacity of several imidazolium-based ionic were determined. The influence of water content in the density was also studied for the most hydrophobic IL used, [omim][PF₆]. A simple ideal-volume model was employed for the prediction of the imidazolium molar volumes at ambient conditions, which proved to agree well with the experimental results.

Contents

List of Tables	III
List of Figures	IV
1. General Introduction	1
1.1. General Context.....	5
1.2. Scope and Objectives.....	10
2. Fluorocarbons	11
2.1. Introduction.....	15
2.2. Experimental Section.....	15
2.2.1. Materials.....	15
2.2.2. Apparatus and Procedure.....	16
2.3. Results and Discussion.....	17
2.3.1. Surface Tension Measurements.....	17
2.3.2. Thermodynamic Properties.....	20
2.3.3. The Methodology of Thermodynamic Similarity.....	22
2.4. Conclusions.....	25
3. Ionic Liquids	27
3.1. Introduction.....	31
3.2. High Pressure Densities.....	32
3.2.1. Introduction.....	32
3.2.2. Materials.....	32
3.2.3. Results and Discussion.....	34
3.2.3.1. Density Measurements.....	34
3.2.3.2. Thermodynamic Properties.....	40
3.2.4. Conclusions.....	51
3.3. Surface Tensions.....	51
3.3.1. Introduction.....	51
3.3.2. Experimental Section.....	52
3.3.2.1. Materials.....	52

3.3.2.2. Apparatus and Procedure.....	54
3.3.3. Results and Discussion.....	55
3.3.3.1. Surface Tension Measurements.....	55
3.3.3.2. Thermodynamic Properties.....	59
3.3.3.3. Mass Spectrometry and Hydrogen Bonding.....	61
3.3.3.4. Influence of the Water Content on the Surface Tension of Ionic Liquids	62
3.3.3.5. Estimated Critical Temperatures.....	67
3.3.3.6. Effective Ionic Concentration and Surface Tension Relation.....	69
3.3.4. Conclusions.....	70
4. Final Remarks and Future Work.....	73
5. References.....	79

List of Tables

Table 2.1. Experimental surface tension (γ) of linear perfluoroalkanes.....	18
Table 2.2. Experimental surface tension (γ) of cyclic and substituted fluoroalkanes.....	18
Table 2.3. Experimental surface tension (γ) of aromatic perfluoroalkanes.....	19
Table 2.4. Surface thermodynamic functions for the FCs.....	21
Table 2.5. Properties required for the faizullin correlation ^[65]	24
Table 3.1. Experimental density data, ρ , for [C ₄ mim][BF ₄], [C ₈ mim][BF ₄] and [C ₄ mim][CF ₃ SO ₃].....	36
Table 3.2. Experimental density data, ρ , for [C ₄ C ₁ mim]PF ₆ , [C ₆ mim]PF ₆] and dry and water saturated [C ₈ mim][PF ₆].....	37
Table 3.3. Effective molar volume of anion, V_a^* , cation, V_c^* , and estimated molar volumes, V_m , at 298.15 K.....	40
Table 3.4. Coefficients of the Tait equation (eq 3.5) for the density at each isotherm between 0.10 and 10.0 MPa for [C ₄ mim][BF ₄], [C ₈ mim][BF ₄] and [C ₄ mim][CF ₃ SO ₃]....	41
Table 3.5. Coefficients of the Tait equation (eq 3.5) for the density at each isotherm between 0.10 and 10.0 MPa for [C ₄ C ₁ mim]PF ₆ , [C ₆ mim]PF ₆] and [C ₈ mim][PF ₆].....	42
Table 3.6. Coefficients of the Tait equation (eq 3.5) for the density at each isotherm between 0.10 and 10.0 MPa for water saturated [C ₈ mim][PF ₆].....	43
Table 3.7. Parameters of the isobaric second-order polynomial fitting (eq 3.8) for [C ₄ mim][BF ₄], [C ₈ mim][BF ₄] and [C ₄ mim][CF ₃ SO ₃].....	46
Table 3.8. Parameters of the isobaric second-order polynomial fitting (eq 3.8) for [C ₄ C ₁ mim][PF ₆], [C ₆ mim][PF ₆] and dry and water saturated [C ₈ mim][PF ₆].....	47
Table 3.9. Experimental surface tension, γ , of the dry ionic liquids studied.....	57
Table 3.10. Surface thermodynamic functions for the ionic liquids studied.....	60
Table 3.11. Experimental surface tension, γ , of water saturated ionic liquids.....	63
Table 3.12. Experimental surface tension, γ , of ILs as a function of the water mole fraction (x_{H_2O}) at 303.15 K.....	63
Table 3.13. Estimated critical temperatures, T_c , using both Eötvös ^[107] (Eot) and Guggenheim ^[108] (Gug) equations, comparison and relative deviation from literature data.....	68

List of Figures

Figure 1.1. Green Chemistry logo.....	5
Figure 1.2. An optimised structure of a 1-methyl-3-octadecylimidazolium cation showing the structural regions.....	7
Figure 1.3. Exponential growth of ionic liquid publications, 1986-2006 ^[22]	7
Figure 1.4. The BASIL jet stream reactor (©BASF 2007).....	8
Figure 1.5. Exponential growth of ionic liquid patents, 1986-2006 ^[22]	8
Figure 2.1. Nima DST 9005 tensiometer from NIMA Technology, Ltd.....	16
Figure 2.2. Surface tensions as a function of temperature for the FCs: ◆, C ₆ F ₁₄ ; ■, C ₇ F ₁₆ ; ▲, C ₈ F ₁₈ ; ◇, C ₉ F ₂₀ ; ×, C ₇ F ₁₄ ; Δ, C ₁₀ F ₁₈ ; ○, C ₆ F ₆ ; □, C ₇ F ₈ ; -, C ₈ F ₁₇ Br.....	17
Figure 2.3. Relative deviations between the experimental surface tension data of this work and those reported in the literature. (a) ○, C ₆ F ₁₄ , ^[53] ◇, C ₆ F ₁₄ , ^[52] □, C ₆ F ₁₄ , ^[45] +, C ₆ F ₁₄ , ^[48] *, C ₇ F ₁₆ , ^[52] ●, C ₇ F ₁₆ , ^[45] ▲, C ₇ F ₁₆ , ^[50] —, C ₈ F ₁₈ , ^[52] ◆, C ₈ F ₁₈ , ^[45] ■, C ₈ F ₁₈ , ^[48] Δ, C ₈ F ₁₈ , ^[47] (b) X, C ₉ F ₂₀ , ^[52] *, C ₉ F ₂₀ , ^[45] Δ, C ₉ F ₂₀ , ^[47] ◇, C ₁₀ F ₁₈ , ^[47] □, C ₆ F ₆ , ^[45]	19
Figure 2.4. Surface tension vs. vaporization enthalpy correlation: ■, C ₆ F ₁₄ ; ●, C ₇ F ₁₆ ; ×, C ₈ F ₁₈ ; *, C ₉ F ₂₀ ; ▲, C ₆ F ₆ ; —, C ₇ F ₈ ; +, C ₇ F ₁₄ ; ◆, C ₁₀ F ₁₈ ; ○, C ₈ F ₁₇ Br; ◇, C ₈ H ₁₈ . The solid line represents the Faizullin correlation ^[65]	23
Figure 2.5. Relative deviations between the experimental reduced surface tensions and those calculated with the Faizullin correlation ^[65] : ■, C ₆ F ₁₄ ; ●, C ₇ F ₁₆ ; ×, C ₈ F ₁₈ ; *, C ₉ F ₂₀ ; ▲, C ₆ F ₆ ; —, C ₇ F ₈ ; +, C ₇ F ₁₄ ; ◆, C ₁₀ F ₁₈ ; ○, C ₈ F ₁₇ Br; ◇, C ₈ H ₁₈	24
Figure 3.1. Experimental setup for the measurement of ionic liquid densities at high pressures. 1, Julabo FP-50 thermostatic bath; 2, DMA 60 (Anton Paar) device for the measuring the period of oscillation; 3, measuring cell DMA 512P (Anton Paar); 4, syringe for sample introduction; 5, pressure generator model HIP 50-6-15; 6, Pt probe; 7, pressure transducer WIKA, S-10.....	34
Figure 3.2. Relative deviations between the experimental density data of this work and those reported in the literature as a function of temperature. (a) [C ₄ mim][BF ₄] at 0.10 MPa: ▲, Fredakle et al. ^[84] ; □, Tokuda et al. ^[86] ; ◇, Azevedo et al. ^[98] ; ○, Zhou et al. ^[99] ; [C ₄ mim][BF ₄] at 10.0 MPa: -, Azevedo et al. ^[98] ; (b) [C ₄ mim][CF ₃ SO ₃] at 0.10 MPa: ▲, Fredakle et al. ^[84] ; □, Tokuda et al. ^[86] ; [C ₈ mim][BF ₄] at 0.10 MPa: ✱, Gu and Brennecke ^[100] ; -, Harris et al. ^[101] ; [C ₆ mim][PF ₆] at 0.10 MPa: Δ, Pereiro et al. ^[102] ; ○, Dzyuba and Bartsch ^[103] ; [C ₈ mim][PF ₆] at 0.10 MPa: ■, Gu and Brennecke ^[100] ; +, Harris et al. ^[101] ; ◆, Dzyuba and Bartsch ^[103]	38
Figure 3.3. Isotherms of the experimental density of [C ₄ mim][CF ₃ SO ₃]: ◆, 293.15 K; ▲, 303.15 K; ×, 313.15 K; ■, 323.15 K; ✱, 333.15 K; -, 343.15 K; +, 353.15 K; □, 363.15 K; ◇, 373.15 K; ○, 383.15 K; Δ, 393.15 K. The lines correspond to the fit of the data by eq 3.5.....	43

Figure 3.4. Isothermal compressibilities of $[C_6mim][PF_6]$: \blacklozenge , 293.15 K; \blacktriangle , 303.15 K; \times , 313.15 K; \blacksquare , 323.15 K; \blackstar , 333.15 K; $-$, 343.15 K; $+$, 353.15 K; \square , 363.15 K; \diamond , 373.15 K; \circ , 383.15 K; Δ , 393.15 K.....44

Figure 3.5. Isotherms for the isobaric expansivity of $[C_8mim][BF_4]$: \blacktriangle , 303.15 K; \times , 313.15 K; \blacksquare , 323.15 K; \blackstar , 333.15 K; \blacklozenge , 343.15 K; $+$, 353.15 K; \square , 363.15 K; \diamond , 373.15 K; \circ , 383.15 K.....48

Figure 3.6. Isotherms for the thermal pressure coefficient of $[C_8mim][PF_6]$: \blacktriangle , 303.15 K; \times , 313.15 K; \blacksquare , 323.15 K; \blackstar , 333.15 K; $-$, 343.15 K; $+$, 353.15 K; \square , 363.15 K; \diamond , 373.15 K; \circ , 383.15 K.....49

Figure 3.7. (a) Isothermal compressibility at 5.0 MPa as a function of temperature; (b) Thermal expansion coefficient at 5.0 MPa as a function of temperature: \diamond , $[C_4mim][BF_4]$; \circ , $[C_8mim][BF_4]$; \blackstar , $[C_4mim][CF_3SO_3]$; $+$, $[C_4C_1mim][PF_6]$; Δ , $[C_6mim][PF_6]$; \square , $[C_8mim][PF_6]$ dried; $-$, $[C_8mim][PF_6]$ saturated with water at 293.15 K.....50

Figure 3.8. Experimental surface tension as a function of temperature for the dry ionic liquids studied: \circ , $[C_4mim][BF_4]$; \diamond , $[C_4mim][PF_6]$; $+$, $[C_4mim][Tf_2N]$; \square , $[C_4mim][CF_3SO_3]$; \blacklozenge , $[C_6mim][PF_6]$; \blacksquare , $[C_8mim][PF_6]$; \blacktriangle , $[C_4C_1mim][PF_6]$; $-$, $[C_8mim][BF_4]$56

Figure 3.9. Relative deviations between the experimental surface tension data of this work and those reported in literature: \square , $[C_4mim][BF_4]^{[110]}$; $+$, $[C_4mim][BF_4]^{[113]}$; \blacktriangledown , $[C_4mim][BF_4]^{[41]}$; \blacksquare , $[C_4mim][BF_4]^{[118]}$; \oplus , $[C_4mim][BF_4]^{[114]}$; \diamond , $[C_4mim][PF_6]^{[113]}$; \blacktriangledown , $[C_4mim][PF_6]^{[41]}$; $-$, $[C_4mim][PF_6]^{[118]}$; \oplus , $[C_4mim][PF_6]^{[119]}$; \blacklozenge , $[C_4mim][PF_6]^{[103]}$; \blacktriangle , $[C_4mim][PF_6]^{[115]}$; \times , $[C_4mim][PF_6]^{[114]}$; \circ , $[C_8mim][PF_6]^{[113]}$; \oplus , $[C_8mim][PF_6]^{[41]}$; \oplus , $[C_8mim][PF_6]^{[118]}$; Δ , $[C_8mim][PF_6]^{[119]}$; \star , $[C_8mim][PF_6]^{[103]}$; \oplus , $[C_8mim][PF_6]^{[114]}$; \oplus , $[C_8mim][BF_4]^{[113]}$; \blacktriangledown , $[C_8mim][BF_4]^{[118]}$; \blacksquare , $[C_8mim][BF_4]^{[114]}$; \oplus , $[C_4mim][Tf_2N]^{[41]}$; Δ , $[C_4mim][Tf_2N]^{[114]}$; \blacklozenge , $[C_4mim][Tf_2N]^{[103]}$; \oplus , $[C_6mim][PF_6]^{[119]}$; \bullet , $[C_6mim][PF_6]^{[114]}$. 58

Figure 3.10. Surface tension as a function of temperature for $[C_4mim][Tf_2N]$: \blacklozenge , dry; \blacksquare , water saturated; \bullet , atmospheric saturated.....64

Figure 3.11. Surface tension as a function of temperature for $[C_4mim][PF_6]$: \blacklozenge , dry; \blacksquare , water saturated; \bullet , atmospheric saturated.....64

Figure 3.12. Surface tension as a function of temperature for $[C_8mim][PF_6]$: \blacklozenge , dry; \blacksquare , water saturated; \bullet , atmospheric saturated.....65

Figure 3.13. Surface tension as a function of temperature for $[C_8mim][BF_4]$: \blacklozenge , dry; \blacksquare , water saturated; \bullet , atmospheric saturated.....65

Figure 3.14. (a) $[C_4mim][PF_6]$ surface tension dependence of water mole fraction content at 303.15 K; (b) $[C_8mim][PF_6]$ surface tension dependence of water mole fraction content at 303.15 K.....66

Figure 3.15. Ceff dependency of surface tension for $[C_4mim][BF_4]$, $[C_4mim][CF_3SO_3]$, $[C_4mim][PF_6]$, $[C_8mim][PF_6]$ and $[C_4mim][Tf_2N]$ at 303.15 K: \blacklozenge , this work surface tension data; \blacksquare , Law et al.^[113] surface tension data; \circ , Yang et al.^[110] surface tension data; A, Umecky et al.^[145] Ceff data; B, Tokuda et al.^[87,144] Ceff data.....70

Figure 4.1. Custom made PTFE Wilhelmy plate.....77

Figure 4.2. Perfluorodecalin/water interfacial tension as a function of temperature.....78

1. General Introduction

“We learn wisdom from failure much more than from success. We often discover what will do, by finding out what will not do; and probably he who never made a mistake never made a discovery.”

Samuel Smiles

1.1. General Context

Since its inception, the field of green chemistry has gained swift expansion, with numerous innovative scientific breakthroughs associated with the production and employment of chemical products^[1]. The concept and paradigm of green chemistry goes now beyond chemistry and reaches subjects ranging from energy to social sustainability. The key notion of green chemistry is “efficiency”, including material, energy, man-power, and property efficiency (e.g., desired function *vs.* toxicity). And any “wastes” aside from these efficiencies are to be addressed through innovative green chemistry means. “Atom-economy”^[2] and minimization of auxiliary chemicals, such as protecting groups and solvents, form the pillar of material efficiency in chemical productions.



Figure 1.1. Green Chemistry logo.

By far, the largest amount of “auxiliary wastes” in most chemical productions are associated with solvent usage. In a classical chemical process, solvents are used extensively for dissolving reactants, extracting and washing products, separating mixtures, cleaning reaction apparatus, and dispersing products for practical applications. While the invention of various exotic organic solvents has resulted in some remarkable advances in chemistry, the legacy of such solvents has led to various environmental and health concerns. Consequently, as part of green chemistry efforts, a variety of cleaner solvents have been evaluated as replacements^[3]. Nevertheless, an ideal and universal green solvent for all situations does not exist.

Among the most widely explored greener solvents are ionic liquids^[4], supercritical CO₂^[5], water^[6] and fluorocarbons^[7]. These solvents complement each other subtly and nicely both in properties and applications. Importantly, the study of green solvents goes far beyond just solvent replacement. The use of green solvents has led science to unexplored and inspiring territories. For example, the study of ionic liquids made large-scale supported synthesis possible for the first time^[8], the utilization of supercritical CO₂ has led to breakthroughs in microelectronics and nanotechnologies^[9] and the fluorinated compounds

allowed the coating of volatile elements in radioactive isotope production^[10].

Although water is the most abundant, natural and non-toxic solvent on earth, it has been traditionally considered as a drawback in most chemical productions. However, since Rideout and Breslow's^[11] report on the acceleration of Diels–Alder reactions in aqueous media, the re-examination of this solvent for chemical applications has recovered importance.

Perfluorocarbons (PFCs) are petroleum-based compounds synthesized by replacing hydrogen by fluorine atoms in the analogue hydrocarbons^[12,13]. The fluorine extreme electronegativity gives rise to C-F bonds that possess relatively high ionic bond character, resulting in the strongest single bond with carbon. On the other hand, the high ionization potential of fluorine and relatively low polarizability lead to very weak intermolecular forces^[14]. Therefore, PFCs present weak intermolecular and strong intramolecular forces, which are responsible for their unusual and interesting properties, as for example, large gas solubility (the highest known among organic liquids), exceptional chemical and biological inertness, non-toxicity towards the cells, excellent spreading characteristics, low surface tensions and refractive indexes, densities higher than water and high isothermal compressibilities^[15-17].

Besides their remarkable solubility capacity, they present very low solubilities in water and therefore they do not affect the physical properties of the aqueous phase and can be easily recovered from it^[17]. Another important property of PFCs is their very low surface tension which is particularly important as it contributes to the mass-transfer enhancement in gas-liquid-liquid systems^[18]. Nevertheless, some limitations are found within these compounds when the intent is their use as oxygen carriers in aerobic bioreactors, such as their high vapor pressures, high viscosities and poor solvating capacity for organic compounds. Therefore, a number of physical and chemical properties of fluorocompounds (FCs) should be previously studied to allow the selection of the best FC to be employed.

Recently, the use of “fluorous phase” synthesis^[12], based on the concept that fluorinated compounds will preferentially dissolve in a fluorous solvent, has been advocated^[13,14].

Ionic liquids (ILs) are typically salts composed of relatively large organic cations and inorganic or organic anions where the presence of these large ions tends to reduce the lattice energy of the crystalline structure lowering their melting point, and thus they generally remain liquid at or near room temperature.

During World War I, Walden^[19] was testing new compounds to substitute the explosive-based nitroglycerine, and synthesized what may be considered the first IL, ethylammonium nitrate ([EtNH₃][NO₃]), by the neutralization of ethylamine with concentrated nitric acid. Despite Walden's clear exposition, and his discovery of a new class of liquids, his paper did not gather much interest at the time.

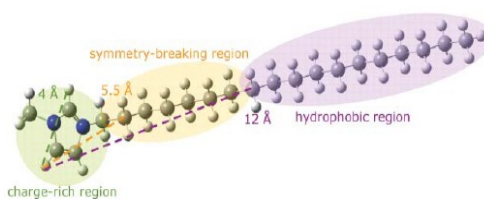


Figure 1.2. An optimized structure of a 1-methyl-3-octadecylimidazolium cation showing the structural regions.

It was not until 1948 that ILs regained the interest of the academia when Hurley and Wier developed, as batch solutions for electroplating, an aluminum based IL with chloroaluminate ions^[20]. Further investigations involving ILs continued but only focused on electrochemical applications. In the early 1980's Seddon and Hussen research groups started to use chloroaluminate melts as nonaqueous polar solvents in the field of transition metal complexes^[21]. In the last decade ILs were recognized as potential “green” solvents and the publications related with these compounds increased in an exponential way (Figure 1.3).

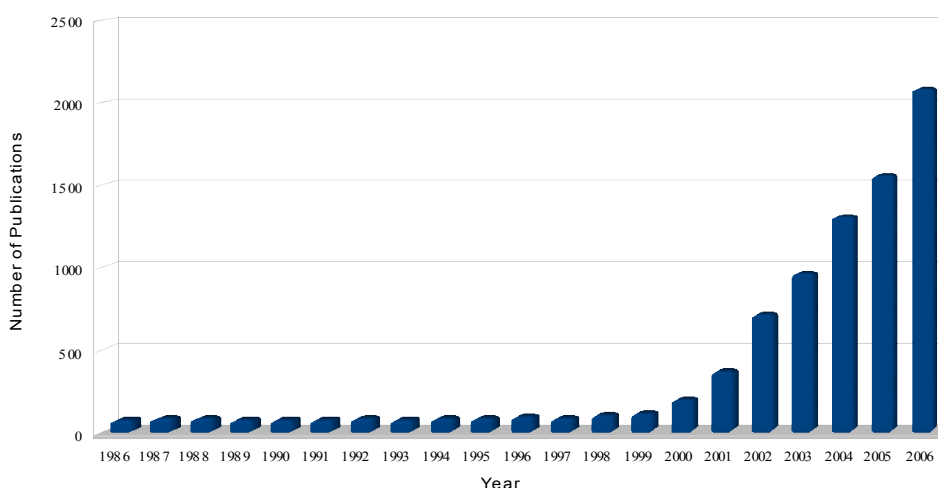


Figure 1.3. Exponential growth of ionic liquid publications, 1986-2006^[22].

Ionic liquids are novel chemical compounds with a wide range of interesting characteristics that are promoting the research in various fields. Their non volatility, high stability, large liquidus range and good solvation properties for both polar and nonpolar compounds make them interesting as solvents for chemical reactions and separations. These outstanding characteristics cataloged ILs as “green” solvents. They are also seen as the paradigm of “designer” solvents due to the possibility of interchangeability between thousands of cations and anions and the possibility of tuning their properties for a given purpose. The ILs great potential already resulted into new innovative processes, such as the BASIL process^[23] and the hydrosilylation process^[24], bridging academia research with chemical industry applications. This convergence is highly notorious in the annual growth of ionic liquids patents shown in Figure 1.5.



Figure 1.4. The BASIL jet stream reactor (©BASF 2007)

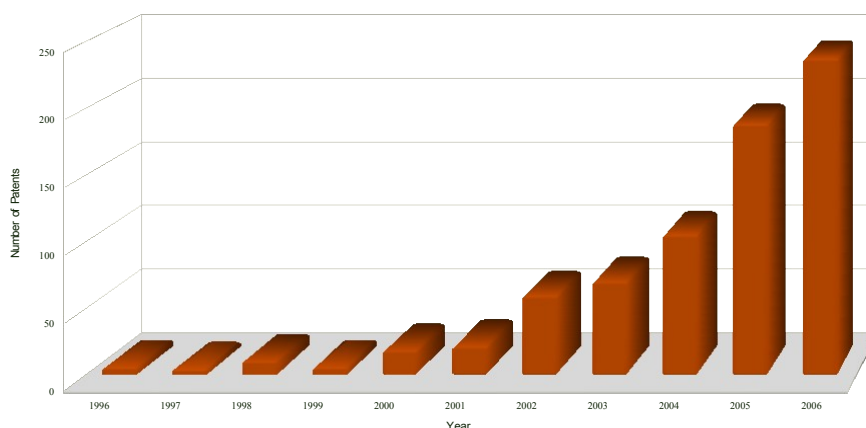


Figure 1.5. Exponential growth of ionic liquid patents, 1986-2006^[22].

Their capabilities as solvents for organic synthesis are well established leading to enhanced yields and selectivities^[20].

Since ionic liquids present negligible vapor pressures^[25], they cannot contribute to a significant atmospheric pollution. This property makes them attractive replacements for organic solvents in several applications in the chemical industry, at a moment when pollution by volatile organic compounds (VOCs) is of great concern. Among the several applications foreseeable for ionic liquids in the chemical industry, there has been

considerable interest in the potential of ILs for separation processes where, among others, ILs have shown promising in the liquid-liquid extraction of organics from water.

Huddleston et al.^[26] showed that 1-butyl-3-methylimidazolium hexafluorophosphate, [C₄mim][PF₆], could be used to extract aromatic compounds from water. Fadeev and Meagher^[27] have shown that two imidazolium ionic liquids with the hexafluorophosphate anion could be used for the extraction of butanol from aqueous fermentation broths. McFarlane et al.^[28] in a recent work presented partition coefficients for a number of organic compounds and discussed the possibilities and limitations of organic liquids for extraction from aqueous media. Other studies have shown that one can use ionic liquids for the extraction of metal ions^[29,30] from solution, aromatics from aromatic-alkane mixtures^[31,32], sulfur-containing aromatics from gasoline^[33] and in the separation of isomeric organic compounds^[34].

In spite of being highly promising, challenging and allowing the complement of each other, both in properties and applications, these solvents are still poorly characterized. In fact, their thermophysical characterization is very limited, inconsistent and discrepant and therefore the gathering of a sufficiently large data bank for process and product design is indispensable.

Reactions involving three-phase systems are frequent in the chemical process industry. Gas-liquid-liquid reactions are gaining importance due to the increase of this type of application in the biotechnology industry and homogeneous catalysis systems^[35]. In this reactions, the addition of dispersed liquid phases changes the transfer rate of the solute gas across the boundary layer and the gas-liquid characteristics can be changed due to the interfacial properties of the dispersed liquid. Nevertheless, the mechanisms involved in the mass transfer in multiphase systems are complex and there are still many gaps to be fulfilled to a complete knowledge of this phenomenon^[35].

The boundary between a liquid phase and a gas phase can be considered a third phase with properties distinct from those of the liquid and gas. A qualitative picture of the microscopic layer shows that there are unequal forces acting upon the molecules, i.e., at low gas densities, the surface molecules are attracted sidewise and toward the bulk liquid

but experience little attraction in the direction of the bulk gas. Thus, the surface layer is in tension and tends to contract to the smallest area still compatible with the mass of material, container restraints, and external forces, e.g., gravity. This tension can be presented in various quantitative ways; the most common is the surface tension, defined as the force exerted in the plane of the surface per unit length.

1.2. Scope and Objectives

Interfacial tension is a property that represents changes in molecular interactions and thus can be used as a mean to achieve a detailed understanding of interfacial behavior. Interfacial tension is crucial to a large set of technological processes, such as coating, adsorption, tertiary oil recovery, liquid-liquid extraction, gas absorption and distillation.

In a search for data of a particular system, one soon realizes that some of the experimental data sets are rather old, and often no specifications for precision, measuring method, accuracy and purity of the substances are given. A critical review of the few available data for fluorocompounds reveals that physical properties such as densities and vapor pressures were recently reported^[15,16,36-38], but scarcely any viscosities and surface tension could be found. On the other hand, ionic liquids domain is prosperous and its growth discloses new publications daily. Nonetheless, large discrepancies among different authors can still be observed. The available data is still scarce but mostly the measurements were until recently carried either using compounds of low purity, without a careful attention towards the preparation of the sample, and often were carried for purposes other than an accurate determination of the thermophysical properties.

Thus, on this work thermophysical properties of PFCs and ILs, such as surface tensions, densities and their related thermodynamic functions, were investigated across a wide temperature range. For ionic liquids it is well established that even low water contents have a great impact on ILs physical properties^[39-42]. Therefore, an extensive study of the water content influence in the surface tension and density was also carried.

2. Fluorocarbons

“The process of scientific discovery is, in effect, a continual flight from wonder.”

Albert Einstein

2.1. Introduction

Surface tension is equivalent to the surface free energy and it is related to the difference between the intermolecular interactions in the bulk and at the surface, accounting for the molecular ordering and structuring of the surface.

Many engineering applications in the chemical process industry, such as mass-transfer operations like distillation, extraction, absorption and adsorption, require surface tension data. Taking into account that fluorocarbons can dissolve large volumes of gases such as carbon dioxide^[38] and oxygen^[15,43], the fluorocarbons interfacial properties are particularly important as they determine the mass transfer enhancement in gas-liquid-liquid systems^[35]. Usually, the addition of fluorocompounds (FCs) in a process aims at enhancing the mass transfer from the gas to the aqueous phase and thus the interfacial properties of FCs clearly play a vital role. For example, the low surface tension of perfluorocompounds (PFCs) is directly responsible for the excellent performance of PFCs in liquid-assisted ventilation^[44]. Thus, it is also clear that lower surface tensions are preferred for the oxygen mass transfer improvement in multiphase biological reactors.

This section aims at studying the surface tension of some linear, aromatic and α -substituted fluorocompounds. Despite its fundamental interest, information about this property is scarce, and the available data are old and present strong discrepancies among each other^[45-54]. Besides, the availability of high purity compounds and improved experimental methods nowadays, allow the accurate surface tension measurements as a function of temperature.

2.2. Experimental Section

2.2.1. Materials

Surface tensions were measured for four *n*-perfluoroalkanes, two cyclic and two aromatic perfluorocompounds, and one α -substituted fluorooctane. The linear perfluorohexane, C₆F₁₄, perfluorooctane, C₈F₁₈ and perfluorononane, C₉F₂₀, were obtained

from Fluorochem with purities verified by Gas Chromatography (GC) of 99.11, 98.36 and 99.18 wt %, respectively. Perfluoroheptane, C_7F_{16} , and the cyclic perfluoromethylcyclohexane, C_7F_{14} , were acquired from Apollo Scientific with a purity of 99.92 and 99.98 wt %, respectively. Perfluorodecalin, $C_{10}F_{18}$, was acquired from Flutec with a purity of 99.88 wt %. The aromatic perfluorobenzene, C_6F_6 , was obtained from Fluorochem and perfluorotoluene, C_7F_8 , from Apollo Scientific with purities of 99.99 and 99.90 wt % respectively. 1-bromo-perfluorooctane, $C_8F_{17}Br$, was acquired from Apollo Scientific with a purity of 99.90 wt %.

The fluorocarbons were used without any further purification, with the exception of $C_{10}F_{18}$ that was purified by passage through a silica column (circa 10 times) according to the suggestions from Gaonkar and Newman^[55] and Goebel and Lunkenheimer^[56]. The initial purity of perfluorodecalin was 97.75 wt % and after purification 99.88 wt % was obtained, as determined by Gas Chromatography (GC).

2.2.2. Apparatus and Procedure

As mentioned before, the purity of each compound was analyzed by GC with a Varian Gas Chromatograph CP 3800 with a flame ionization detector (FID). Chromatographic separations were accomplished with a Varian CP-Wax 52CB column with an internal diameter (ID) of 0.53 mm and equipped with Coating WCot Fused Silica.

The surface tensions of each pure liquid fluorocompound were measured with a *NIMA DST 9005* tensiometer from *NIMA Technology, Ltd.* with a Pt/Ir Du Noüy ring, based on force measurements, for which it has a precision balance able to measure down to 10^{-9} N. The sample surface was cleaned before each measurement by aspiration, to remove the surface active impurities present at the interface, and to allow the formation of a new interface. The measurements were carried in the temperature range (283 to 327) K and at atmospheric pressure.



Figure 2.1. Nima DST 9005 tensiometer from NIMA Technology, Ltd.

The liquid under measurement was kept thermostated in a double-jacketed glass cell

by means of a water bath, using an HAAKE F6 circulator equipped with a Pt100 probe, immersed in the solution, and able to control temperature within ± 0.01 K.

For each sample at least five sets of three immersion/detachment cycles were measured, giving a minimum of at least 15 surface tensions values, which allowed the determination of an average surface tension value for each temperature as well as the corresponding expanded uncertainty^[57-61].

2.3. Results and Discussion

2.3.1. Surface Tension Measurements

Previous measurements have confirmed the ability of the above-described equipment to accurately measure interfacial tensions for hydrocarbons, validating the methodology and experimental procedure adopted in this work^[59-61]. The pure liquid densities necessary for the surface tension measurements were taken from Dias et al.^[36,37] Results for the pure, linear, cyclic, aromatic, and substituted FCs are reported in Tables 2.1 to 2.3. For a better inspection, the surface tension values are presented in Figure 2.2.

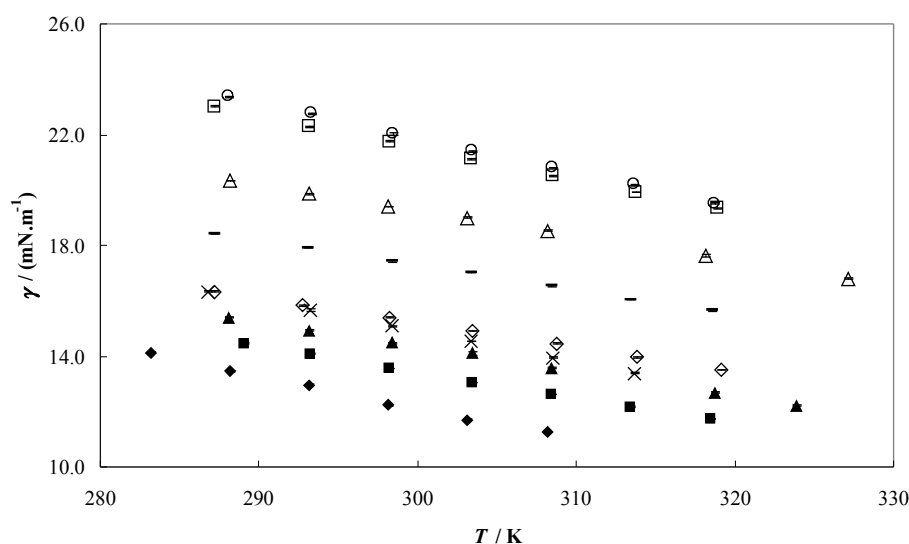


Figure 2.2. Surface tensions as a function of temperature for the FCs: \blacklozenge , C_6F_{14} ; \blacksquare , C_7F_{16} ; \blacktriangle , C_8F_{18} ; \blacklozenge , C_9F_{20} ; \times , C_7F_{14} ; \triangle , $C_{10}F_{18}$; \circ , C_6F_6 ; \square , C_7F_8 ; $-$, $C_8F_{17}Br$.

The measured *n*-perfluoroalkanes surface tensions show that they are strongly dependent on the temperature and only weakly dependent on the carbon number. Also, fluorocarbons present lower surface tensions than the corresponding hydrocarbons, indicating that the van der Waals interactions between fluorinated molecules are usually smaller when compared with the corresponding non-fluorinated molecules. The results obtained are in agreement with other experimental^[45-54] and theoretical evidences^[51], which show their high intramolecular and low intermolecular forces and permit their application in a wide variety of fields.

Table 2.1. Experimental surface tension (γ) of linear perfluoroalkanes.

C ₆ F ₁₄		C ₇ F ₁₆		C ₈ F ₁₈		C ₉ F ₂₀	
$\frac{T}{K}$	$\frac{(\gamma \pm \sigma^a)}{mN.m^{-1}}$						
283.15	14.13 ± 0.03	289.05	14.46 ± 0.01	288.05	15.39 ± 0.02	287.15	16.32 ± 0.03
288.15	13.44 ± 0.02	293.25	14.09 ± 0.02	293.15	14.92 ± 0.02	292.75	15.82 ± 0.02
293.15	12.97 ± 0.03	298.25	13.55 ± 0.01	298.35	14.47 ± 0.02	298.25	15.39 ± 0.02
298.15	12.23 ± 0.02	303.45	13.04 ± 0.01	303.45	14.10 ± 0.06	303.45	14.91 ± 0.01
303.15	11.70 ± 0.03	308.45	12.62 ± 0.02	308.45	13.56 ± 0.02	308.75	14.46 ± 0.03
308.15	11.25 ± 0.01	313.45	12.17 ± 0.02	318.75	12.68 ± 0.02	313.85	13.96 ± 0.01
		318.45	11.73 ± 0.02	323.85	12.22 ± 0.02	319.15	13.51 ± 0.02

^aStandard deviation**Table 2.2.** Experimental surface tension (γ) of cyclic and substituted fluoroalkanes.

C ₇ F ₁₄		C ₁₀ F ₁₈		C ₈ F ₁₇ Br	
$\frac{T}{K}$	$\frac{(\gamma \pm \sigma^a)}{mN.m^{-1}}$	$\frac{T}{K}$	$\frac{(\gamma \pm \sigma^a)}{mN.m^{-1}}$	$\frac{T}{K}$	$\frac{(\gamma \pm \sigma^a)}{mN.m^{-1}}$
286.75	16.33 ± 0.03	288.15	20.34 ± 0.01	287.15	18.42 ± 0.02
293.25	15.65 ± 0.04	293.15	19.85 ± 0.04	292.75	17.92 ± 0.02
298.35	15.10 ± 0.02	298.15	19.41 ± 0.01	298.35	17.43 ± 0.04
303.35	14.54 ± 0.02	303.15	18.99 ± 0.01	303.35	17.01 ± 0.01
308.55	13.95 ± 0.02	308.15	18.53 ± 0.02	308.45	16.54 ± 0.02
313.65	13.38 ± 0.03	318.15	17.61 ± 0.04	313.45	16.04 ± 0.02
		327.15	16.80 ± 0.02	318.55	15.66 ± 0.02

^aStandard deviation

Table 2.3. Experimental surface tension (γ) of aromatic perfluoroalkanes.

C ₆ F ₆		C ₇ F ₈	
$\frac{T}{K}$	$\frac{(\gamma \pm \sigma^a)}{mN.m^{-1}}$	$\frac{T}{K}$	$\frac{(\gamma \pm \sigma^a)}{mN.m^{-1}}$
288.05	23.38 ± 0.02	287.15	23.02 ± 0.02
293.35	22.76 ± 0.03	293.15	22.29 ± 0.02
298.45	22.02 ± 0.03	298.25	21.76 ± 0.03
303.45	21.40 ± 0.02	303.35	21.12 ± 0.02
308.55	20.81 ± 0.01	308.55	20.51 ± 0.02
313.65	20.19 ± 0.02	313.75	19.92 ± 0.02
318.75	19.52 ± 0.03	318.85	19.35 ± 0.02

^aStandard deviation

The relative deviations between the experimental data obtained in this work and those reported by other authors^[45,47,48,50-53] are presented in Figure 2.3. A better agreement can be observed at the higher temperatures with the higher deviations appearing at the lower temperatures. These deviations are larger than those found previously for pure and mixed *n*-alkanes^[59-61] using the same equipment. Note also that large discrepancies exist among the available data from different authors^[45,47,48,50-53], with average absolute deviations ranging from 1 up to 19 %.

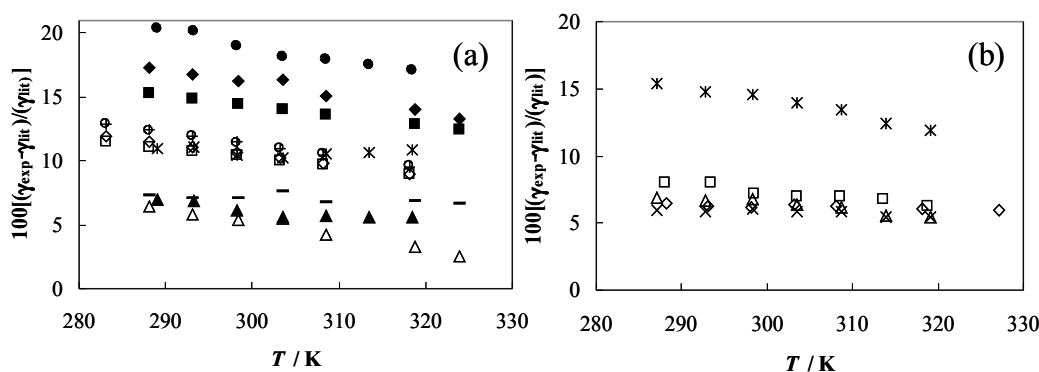


Figure 2.3. Relative deviations between the experimental surface tension data of this work and those reported in the literature. (a) \circ , C₆F₁₄,^[53] \diamond , C₆F₁₄,^[52] \square , C₆F₁₄,^[45] $+$, C₆F₁₄,^[48] $*$, C₇F₁₆,^[52] \bullet , C₇F₁₆,^[45] \blacktriangle , C₇F₁₆,^[50] $-$, C₈F₁₈,^[52] \blacklozenge , C₈F₁₈,^[45] \blacksquare , C₈F₁₈,^[48] \triangle , C₈F₁₈,^[47] (b) \times , C₉F₂₀,^[52] $*$, C₉F₂₀,^[45] \triangle , C₉F₂₀,^[47] \diamond , C₁₀F₁₈,^[47] \square , C₆F₆,^[45]

As indicated in Tables 2.1 to 2.3, the measured data have a good precision, with small associated expanded uncertainties for each compound. Furthermore, the compounds used in this work are of high purity, and the surface was carefully and thoroughly cleaned

between each measurement allowing for a new interface formation. This procedure may explain the systematically higher results obtained in this work when compared to literature data since interface tensions normally decrease with the presence of impurities. Usually, higher interface tensions are an indication of high-purity compounds. Most of the authors who also measured surface tensions of FCs either do not report the purity of the compounds or low purity compounds were used. Haszeldine and Smith^[47] present no indication of the PFCs purity and used the maximum bubble pressure method. McLure et al.^[48] only considered the presence of isomers (< 1 mol % for C₆F₁₄ and < 10 mol % for C₈F₁₈), and Skripov and Firsov^[52] presented no purity statement indicating, however, isomer contamination.

Another fact that has to be taken into account is that surface tension measurements require density data of the compounds under study. Previously authors either obtained these densities from empirical correlations or from experimental measurements with a pycnometer. Finally, due to their unique properties, some surface tension measurement methods are not adequate when working with PFCs. Most authors used the capillary rise method, which is not a good technique for PFCs due to their extremely high hydrophobicity and poor wetting of the hydrophilic glass capillary wall. Also, the drop weight method leads to large uncertainties for these compounds due to the difficulty in the formation of the droplet as a consequence of their large densities. These are the first data reported using the Du Noüy ring method, using compounds with high purity and accurate experimental densities^[36,37].

Another important indication on the quality of the surface tension data available in the literature is given by the work of Sakka and Ogata^[51], who evaluated the parachor assigned to fluorine atoms and concluded that the calculated surface tensions using parachors for PFCs are higher than the available literature data. This may also be an indication of the defective quality of the available data for the surface tension of PFCs.

2.3.2. Thermodynamic Properties

Using the quasi-linear surface tension variation with temperature for all the FCs

observed in the studied temperature range, the surface thermodynamic properties, surface entropy and surface enthalpy, were derived. The surface entropy, S^y , can be obtained from^[62,63]

$$S^y = -\frac{d\gamma}{dT} \quad 2.1$$

And the surface enthalpy, H^y , can be obtained from the following expression^[62,63]

$$H^y = \gamma - T\left(\frac{d\gamma}{dT}\right) \quad 2.2$$

where γ stands for the surface tension and T for the temperature.

The thermodynamic functions for all the ILs studied and the respective expanded uncertainties, derived from the slope of the curve $\gamma = f(T)$ in combination with the law of propagation of uncertainty, are presented in Table 2.4^[64].

Table 2.4. Surface thermodynamic functions for the FCs.

Fluid	$10^5(S^y \pm \sigma^a)$ $N.m^{-1}.K^{-1}$	$10^3(H^y \pm \sigma^a)$ $N.m^{-1}$
C ₆ F ₁₄	11.6 ± 0.4	47.1 ± 1.3
C ₇ F ₁₆	9.3 ± 0.1	41.4 ± 0.5
C ₈ F ₁₈	8.8 ± 0.1	40.8 ± 0.4
C ₉ F ₂₀	8.8 ± 0.1	41.6 ± 0.3
C ₇ F ₁₄	11.0 ± 0.1	47.9 ± 0.2
C ₁₀ F ₁₈	9.0 ± 0.1	46.3 ± 0.2
C ₆ F ₆	12.6 ± 0.1	59.6 ± 0.5
C ₇ F ₈	11.6 ± 0.1	56.3 ± 0.3
C ₈ F ₁₇ Br	8.9 ± 0.2	44.0 ± 0.3

^aStandard deviation

For the linear PFCs, the increase in chain length leads to a slightly decrease in the surface entropy, which is a result of the increase in intermolecular interactions. The combined effect of the surface enthalpy and entropy yields a slight increase in the surface tension with the chain length. A similar behavior is observed for the cyclic compounds with a small decrease in the surface entropy with increasing carbon number that results therefore on the surface tension increase.

Comparing the surface tension of the α -perfluorooctylbromide (Table 2.2) with the respective perfluorooctane (Table 2.1), it can be seen that the inclusion of a less

electronegative heteroatom leads to an increase in surface tension. This substituted compound presents a similar surface entropy to perfluorooctane, and a different surface enthalpy. This increase in surface tension can thus be explained by the increase in surface enthalpy value due to the stronger interactions resulting from the dipole formation at the heteroatom.

The aromatic PFCs show the highest surface enthalpy from all the compounds studied and the methyl substitution on the aromatic ring lowers the surface enthalpy.

2.3.3. *The Methodology of Thermodynamic Similarity*

Both the vaporization process and the process of liquid surface formation are related to the energy required to break down intermolecular forces existent within the liquid. This implies the existence of a relationship between the vaporization enthalpy $\Delta_{vap}H$ and the surface tension γ of the pure liquid. Faizullin^[65] applied the thermodynamic similarity methodology to describe the surface tension of normal (non-associated) liquids for a wide variety of compounds, from gases, alkanes and aromatic compounds, in the temperature range from the triple to the critical point, presenting a one-parameter relation in reduced variables.

Dimensionless quantities for γ , $\Delta_{vap}H$ and liquid molar volume v_L where introduced by the following reduced properties:

$$T_r = \frac{T}{T_c} = 0.6 \quad 2.3$$

where T stands for the temperature and the subscripts r and c for the reduced and critical properties, respectively.

$$\gamma_r = \frac{\gamma}{\gamma_{T_r=0.6}} \quad 2.4$$

$$\Delta_{vap}H_r = \frac{\Delta_{vap}H}{(\Delta_{vap}H)_{T_r=0.6}} \quad 2.5$$

$$(\nu_L)_r = \frac{\nu_L}{(\nu_L)_{T_r=0.6}} \quad 2.6$$

Faizullin's^[65] results show that the surface tensions for a wide range of compounds fall on a common curve, where the point (1,1) in the plot corresponds to the substance "critical" point

$$\gamma_r = \left(\frac{\Delta_{vap} H_r}{(\nu_L)_r} \right)^m \quad 2.7$$

This equation does not require fluid dependent correlation parameters and the only necessary target fluid information is the vaporization enthalpy, the liquid phase molar volume and the surface tension at the reduced temperature of 0.6. These data can be experimentally available or estimated from corresponding states relationships. Faizullin^[65] reported an average value for the exponent m equal to 2.15.

The Faizullin's^[65] approach was used to calculate reduced surface tensions of fluorocarbons and the results were compared with the reduced surface tensions calculated from experimental data measured in this work, as graphically presented in Figure 2.4.

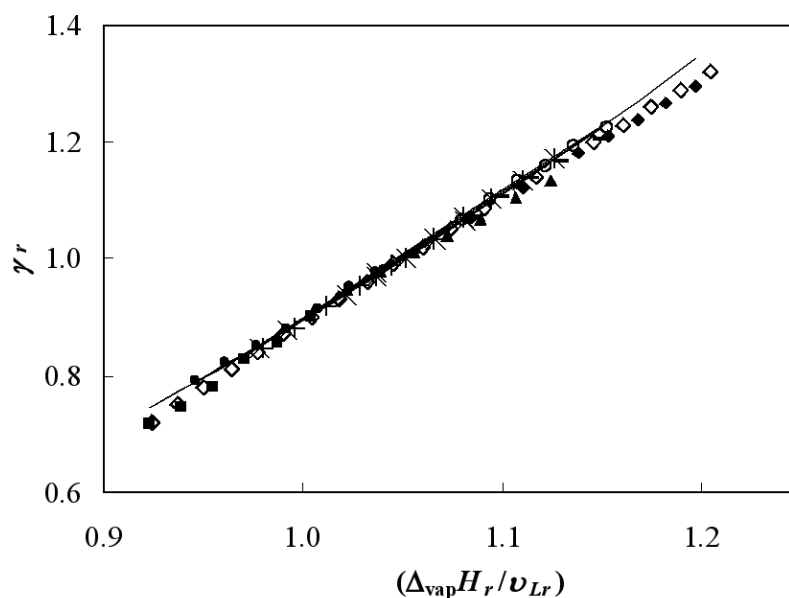


Figure 2.4. Surface tension vs. vaporization enthalpy correlation: ■, C₆F₁₄; ●, C₇F₁₆; ×, C₈F₁₈; *, C₉F₂₀; ▲, C₆F₆; —, C₇F₈; +, C₇F₁₄; ◆, C₁₀F₁₈; ○, C₈F₁₇Br; ◇, C₈H₁₈. The solid line represents the Faizullin correlation^[65].

n-octane^[66] was included to test and validate the procedure, and a plot showing the deviations from the Faizullin's estimated behavior is presented in Figure 2.5.

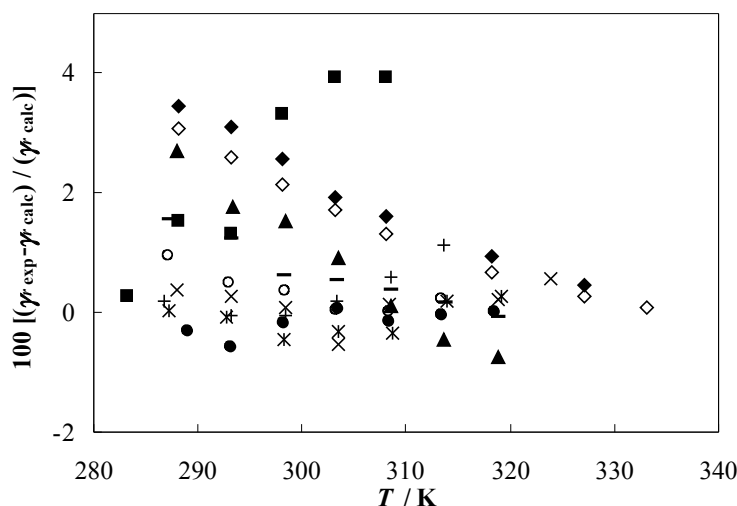


Figure 2.5. Relative deviations between the experimental reduced surface tensions and those calculated with the Faizullin correlation^[65]: ■, C₆F₁₄; ●, C₇F₁₆; ×, C₈F₁₈; *, C₉F₂₀; ▲, C₆F₆; —, C₇F₈; +, C₇F₁₄; ◆, C₁₀F₁₈; ○, C₈F₁₇Br; ◇, C₈H₁₈.

The required experimental information is summarized in Table 2.5. Critical temperatures were either compiled from experimental measurements or obtained from reliable correlations^[16,50,67-78]. Liquid volumes and vaporization enthalpies were obtained from Dias et al.^[36,37] and the required surface tensions at the reduced temperature of 0.6 were obtained from correlations, as a function of temperature, of the experimental data collected for the present work.

Table 2.5. Properties required for the Faizullin correlation^[65].

Fluid	$\frac{T_C}{K}$	$\frac{10^4 (V_{L_{T_r=0.6}})}{m^3 \cdot mol^{-1}}$	$\frac{\gamma_{T_r=0.6}}{mN \cdot m^{-1}}$	$\frac{\Delta_{vap} H_{T_r=0.6}}{kJ \cdot mol^{-1}}$
C ₆ F ₁₄	449.0	1.92	15.68	34.20
C ₇ F ₁₆	474.8	2.20	14.83	37.50
C ₈ F ₁₈	498.0	2.48	14.44	40.65
C ₉ F ₂₀	524.0	2.79	13.93	44.29
C ₇ F ₁₄	485.9	1.94	15.83	35.11
C ₁₀ F ₁₈	566.0	2.52	15.68	39.06
C ₆ F ₆	517.0	1.17	20.59	35.36
C ₇ F ₈	534.5	1.46	19.12	39.17
C ₈ F ₁₇ Br	541.7	2.70	15.06	44.02
C ₈ H ₁₈	569.4	1.73	16.92	39.03

As shown in Figure 2.4, the surface tension relationship with the reduced vaporization enthalpy given by eq 2.5 is also valid for PFCs with the generalized correlation parameter m of 2.15 proposed by Faizullin^[65], who used different fluid families and a broad range of thermodynamic conditions for its determination. The Faizullin correlation provides a good description of the measured surface tension data with typical deviations inferior to 3 % (as shown in Figure 2.5). Larger deviations of 3.9 % were observed for the tetradecafluorohexane and 3.5 % for octadecafluorodecalin, which can be an indication of uncertainties in the critical properties used.

2.4. Conclusions

Experimental data for the surface tensions from C₆F₁₄ to C₉F₂₀ linear perfluoroalkanes, two cyclic, two aromatic and one α -substituted fluorocompound in the temperature range (283 to 327) K using the Du Noüy ring method are presented. New experimental data are presented for the C₇F₁₄, C₇F₈ and C₈F₁₇Br fluorocompounds. PFCs present lower surface tensions than their alkane homologues due to their weaker intermolecular interactions. For the same number of carbon atoms in the molecule, the surface tension increases from linear to cyclic and from cyclic to aromatic PFCs. Substitution of fluorine with bromine in the same chain molecule increases the surface tension, as intermolecular interactions increase.

A generalized correlation between measured surface tension, enthalpy of vaporization and liquid molar volume was verified for PFCs and FCs. It is shown that using a fluid independent exponent m , the description of the reported experimental data is provided with a deviation inferior to 4 %.

3. Ionic Liquids

“The best scientist is open to experience and begins with romance - the idea that anything is possible.”

Ray Bradbury

3.1. Introduction

Room-temperature ionic liquids (RTILs) are a class of organic salts commonly composed of relatively large organic cations and inorganic or organic anions that cannot form an ordered crystal and thus remain liquid at or near room temperature. Unlike molecular liquids, the ionic nature of these compounds results in a unique combination of intrinsic physical properties such as high thermal stability, large liquidus range, high ionic conductivity, negligible vapor pressures, nonflammability and highly solvating capacity, for both polar and nonpolar compounds^[79-87]. These outstanding characteristics, along with their easy manipulation due to the possibility of interchangeability between thousands of cations and anions, cataloged ILs as “green” and “designer” solvents. Among the several applications foreseeable for ionic liquids such as solvents in organic synthesis, as homogeneous and biphasic transfer catalysts, and in electrochemistry, ILs great potential caught the attention of the industry and academia alike.

The design and optimization of industrial processes and new products based on ILs are only possible whenever their thermophysical properties including viscosity, density and interfacial tension are adequately known. Unfortunately, the thermophysical characterization of ILs is limited and it is necessary to accumulate a sufficiently large data bank on the fundamental physical and chemical properties, not only for process and product design, but also for the development of adequate correlations for these properties.

It is the goal of the present work to present reliable data for density and interfacial tensions of a series of ILs and their temperature and pressure dependence. Since it is impossible to measure all the possible combinations of anions and cations, it is necessary to make measurements on selected systems in order to provide results that can be used to develop correlations and to test predictive methods.

3.2. High Pressure Densities

3.2.1. Introduction

The objective of this section is to investigate the relationship between ionic structures and their density, establishing principles for the molecular design of ILs and provide data required for the determination of the ILs interfacial tension. For that purpose, the [C₄mim] cation was studied in combination with two anions, [CF₃SO₃] and [BF₄], and the [C₈mim] cation in combination with the [BF₄] and [PF₆] anions, to conclude about the anion effect. On other hand, the [PF₆] anion was combined with three different cations: [C₄C₁mim], [C₆mim] and [C₈mim], to study the effect of alkyl chain length and the number of substituents on the imidazolium ring on the density and derived properties.

It is well established that the presence of water, even at low concentrations, has a considerable effect in the physical properties of ILs^[40,41]. For that reason, the study of the density of [C₈mim][PF₆] saturated with water at 293.15 K was also investigated, in order to evaluate the extension of the influence of the water content in the density and related derived properties for the most hydrophobic of the ILs studied.

The liquid densities were correlated with the Tait equation^[88] and other thermodynamic properties such as the isothermal compressibility, the isobaric expansivity and the thermal pressure coefficient were calculated and showed in some examples.

3.2.2. Materials

Experimental densities were measured for six imidazolium-based ILs, namely, [C₄mim][BF₄], [C₈mim][BF₄], [C₆mim][PF₆], [C₈mim][PF₆], [C₄C₁mim][PF₆] and [C₄mim][CF₃SO₃]. [C₄mim][BF₄] was acquired at Solvent Innovation with a mass fraction purity > 98 % and a mole fraction of chloride ion of 100×10^{-6} . [C₈mim][BF₄] and [C₄mim][CF₃SO₃] were acquired at IoLiTec with mass fraction purities > 99 %. The bromide impurity mole fraction in the [C₈mim][BF₄] is 64×10^{-6} and the [C₄mim][CF₃SO₃] is halogen free since it was produced directly from butylimidazole and methyltriflate. The [C₆mim][PF₆] was acquired at Merck with a mass fraction purity ≥ 99 % and a mole

fraction of chloride ion $\leq (100 \times 10^{-6})$. $[\text{C}_8\text{mim}][\text{PF}_6]$ and $[\text{C}_4\text{C}_1\text{mim}][\text{PF}_6]$ were acquired at Solchemar with mass fraction purities $> 99 \%$. The chloride mole fraction content in both ILs is $< (80 \times 10^{-6})$.

In order to reduce the water content and volatile compounds to negligible values, vacuum (0.1 Pa) at moderate temperature (353 K) for at least 48 h was applied to all the ILs samples prior to their use. After this proceeding, the water content in the ILs was determined with a Metrohm 831 Karl-Fischer coulometer indicating very low levels of water mass fraction content, as $(485, 371, 181, 311, 87 \text{ and } 18) \times 10^{-6}$ for $[\text{C}_4\text{mim}][\text{BF}_4]$, $[\text{C}_8\text{mim}][\text{BF}_4]$, $[\text{C}_4\text{mim}][\text{CF}_3\text{SO}_3]$, $[\text{C}_4\text{C}_1\text{mim}][\text{PF}_6]$, $[\text{C}_6\text{mim}][\text{PF}_6]$ and $[\text{C}_8\text{mim}][\text{PF}_6]$, respectively.

The influence of water content in density was studied for $[\text{C}_8\text{mim}][\text{PF}_6]$. For that purpose, this IL was saturated with ultra pure water, maintaining the two phases in equilibrium, at 293.15 K for at least 48 h, which was previously found to be the necessary time to achieve equilibrium^[89]. The water mass fraction content in the saturated $[\text{C}_8\text{mim}][\text{PF}_6]$ was $(11905 \pm 98) \times 10^{-6}$. The water used was double distilled, passed by a reverse osmosis system and further treated with a Milli-Q plus 185 water purification apparatus. It has a resistivity of 18.2 $\text{M}\Omega\cdot\text{cm}$, a TOC smaller than 5 $\mu\text{g}\cdot\text{dm}^{-3}$ and it is free of particles greater than 0.22 μm .

Experimental densities were measured using an Anton Paar DMA 60 digital vibrating tube densimeter, with a DMA 512P measuring cell in the temperature range (293.15 to 393.15) K and pressure range (0.10 to 10.0) MPa. The temperature in the vibrating tube cell was measured with a platinum resistance probe which has a temperature uncertainty of ± 0.01 K coupled with a GW Instek Dual Display Digital Multimeter GDM-845. A Julabo FP-50 thermostatic bath with silicone oil as circulating fluid was used in the thermostat circuit of the measuring cell which was held constant to ± 0.01 K. The diameter of tube is 1/16" and the buffer is more than 1 m in length which guarantees the inexistence of diffusion of the hydraulic liquid in the liquid contained in the cell of densimeter.

The required pressure was generated and controlled with a Pressure Generator Model 50-6-15, Mftd. from High Pressure Equipment Co., using acetone as the hydraulic fluid.

Pressures were measured with a pressure transducer (Wika Transmitter S-10, Mftd. from WIKA Alexander Wiegand GmbH & Co.) with a maximum uncertainty of ± 0.025 MPa. Figure 3.1 shows the installation of the DMA 512P cell and the peripheral equipment used.

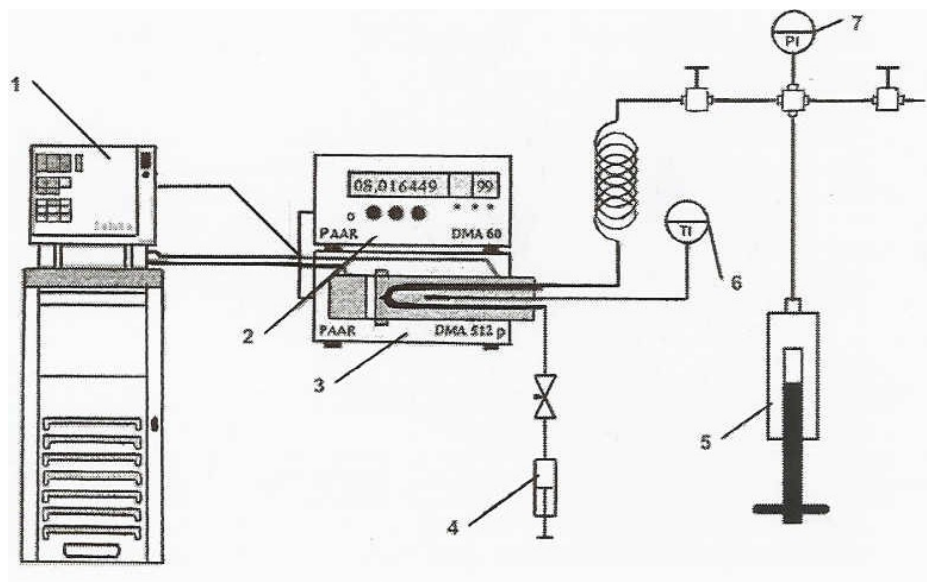


Figure 3.1. Experimental setup for the measurement of ionic liquid densities at high pressures. **1**, Julabo FP-50 thermostatic bath; **2**, DMA 60 (Anton Paar) device for the measuring the period of oscillation; **3**, measuring cell DMA 512P (Anton Paar); **4**, syringe for sample introduction; **5**, pressure generator model HIP 50-6-15; **6**, Pt probe; **7**, pressure transducer WIKA, S-10.

3.2.3. Results and Discussion

3.2.3.1. Density Measurements

Water, *n*-perfluorohexane and *n*-perfluorononane were used as reference fluids for the calibration of the vibrating tube densimeter, in order to guarantee an interpolation besides an extrapolation of the ILs densities^[90-92].

The reference fluids density data were used to fit the calibration equation proposed by Niesen^[93] and has a solid theoretical basis as discussed by Holcom and Outcalt^[94], and it can be described as follow:

$$\rho(T, p, \tau) = A_1 + A_2 T + A_3 p + \left[\frac{\tau^2(T, p) (A_4 + A_5 T + A_6 T^2)}{\tau^2(T_0, p_0 = 0)} \right] \quad 3.1$$

where $\rho(T, p)$ and $\tau(T, p)$ are the density and the oscillation period respectively, which are both function of the temperature T and of the pressure p . The oscillation period $\tau(T_0, p_0)$ is a function of the reference temperature T_0 and vacuum. In this work $T_0 = 303.15$ K and the measured period at $p = 0$ is $\tau(T_0, p_0) = 0.388074$ μs .

For water, the density data from Saul et al.^[90] and those taken from National Institute of Science and Technology (NIST)^[91], in the temperature range of (293.15 K to 393.15) K and pressures from (0.1 to 35) MPa were used, while for the *n*-perfluorohexane and *n*-perfluorononane reference fluids density data were taken from Piñeiro et al.^[92], in the same pressure and temperature range of this work. The standard deviation of the fitting σ is defined as,

$$\sigma = \left[\frac{\sum_{i=1}^{N_p} (\rho_{cal} - \rho_{exp})_i^2}{N_p - k} \right]^{1/2} \quad 3.2$$

where ρ_{calc} and ρ_{exp} are respectively the density data from eq 3.1 and the experimental data for the measurement i , N_p represents the number of points used ($N_p = 174$) and k is the number of adjusted parameters ($k = 6$), obtaining a standard deviation of the fitting of the order of ± 1 $\text{kg}\cdot\text{m}^{-3}$. The percentage average absolute deviation, AAD (%), from the experimental data to the fitting is defined accordingly to eq 3.3 as follow,

$$AAD(\%) = \frac{\sum_{i=1}^{N_p} \left| \frac{\rho_{calc} - \rho_{exp}}{\rho_{calc}} \right|_i}{N_p} \times 100 \quad 3.3$$

from where an average AAD (%) of 0.002 % was obtained for all the ILs studied.

The influence of the viscosity on the measured densities was evaluated. In order to check the effect of viscosity in the density, a viscosity correction for compounds with viscosities lower than 100 $\text{mPa}\cdot\text{s}$ was applied with the equation proposed for the density uncertainty of an Anton Paar DMA 512 densimeter^[95]. For compounds with viscosities higher than 400 $\text{mPa}\cdot\text{s}$ the correction factor becomes constant^[96] and equal to 0.5 $\text{kg}\cdot\text{m}^{-3}$, and between 100 and 400 $\text{mPa}\cdot\text{s}$ the viscosities correction follow an intermediate behavior.

Considering for example, the available viscosity data for $[\text{C}_4\text{mim}][\text{BF}_4]$ ^[97,98] and for $[\text{C}_4\text{mim}][\text{CF}_3\text{SO}_3]$ ^[97,98] at atmospheric pressure and between (298.15 to 343.15) K, where the viscosities of both ILs are inferior to 100 mPa·s, there is an average density uncertainty of $0.3 \text{ kg}\cdot\text{m}^{-3}$ for both. For other ILs and/or other higher pressures where the viscosity increases, the correction value $0.5 \text{ kg}\cdot\text{m}^{-3}$ was assumed, being inferior to the uncertainty in the overall density data of $1 \text{ kg}\cdot\text{m}^{-3}$, and for that reason the viscosity corrections were neglected in the present work.

Density measurements were carried out at temperatures ranging from (293.15 to 393.15) K and pressures from (0.10 to 10.0) MPa. The experimental data obtained are reported in Tables 3.1 and 3.2 for all the ILs studied. For $[\text{C}_4\text{C}_1\text{mim}][\text{PF}_6]$ the density was measured only for temperatures higher than 313.15 K, due to the high melting point of this compound ($\approx 303.15 \text{ K}$).

Table 3.1. Experimental density data, ρ , for $[\text{C}_4\text{mim}][\text{BF}_4]$, $[\text{C}_8\text{mim}][\text{BF}_4]$ and $[\text{C}_4\text{mim}][\text{CF}_3\text{SO}_3]$

$\frac{P}{\text{MPa}}$	$\rho / \text{Kg}\cdot\text{m}^{-3}$ at T / K									
	293.15	303.15	313.15	323.15	333.15	343.15	353.15	363.15	373.15	393.15
$[\text{C}_4\text{mim}][\text{BF}_4]$										
0.10	1206.9	1198.6	1190.8	1183.0	1175.8	1168.4	1161.3	1154.7	1148.2	1136.1
1.00	1207.3	1199.1	1191.3	1183.5	1176.3	1168.9	1161.8	1155.3	1148.8	1136.7
2.00	1207.7	1199.6	1191.8	1184.0	1176.9	1169.3	1162.4	1155.8	1149.3	1137.3
3.00	1208.2	1200.1	1192.2	1184.5	1177.4	1169.8	1163.0	1156.4	1149.9	1137.9
4.00	1208.7	1200.7	1192.7	1185.0	1177.9	1170.3	1163.5	1156.9	1150.4	1138.4
5.00	1209.1	1201.1	1193.2	1185.5	1178.4	1170.8	1164.1	1157.5	1151.0	1139.0
10.0	1211.3	1203.5	1195.5	1187.8	1181.0	1173.1	1166.6	1160.1	1153.6	1141.9
$[\text{C}_8\text{mim}][\text{BF}_4]$										
0.10	1108.7	1100.7	1092.9	1085.4	1078.2	1071.4	1064.7	1058.6	1052.4	1040.9
1.00	1109.1	1101.1	1093.4	1085.9	1078.7	1072.0	1065.2	1059.1	1053.0	1041.5
2.00	1109.6	1101.6	1093.9	1086.4	1079.3	1072.5	1065.8	1059.8	1053.7	1042.1
3.00	1110.0	1102.1	1094.4	1087.0	1079.8	1073.1	1066.4	1060.4	1054.3	1042.8
4.00	1110.5	1102.6	1094.9	1087.5	1080.3	1073.7	1067.0	1061.0	1054.9	1043.4
5.00	1110.9	1103.1	1095.4	1088.0	1080.9	1074.2	1067.6	1061.6	1055.5	1044.1
10.0	1113.1	1105.4	1097.9	1090.6	1083.5	1076.9	1070.3	1064.4	1058.5	1047.2
$[\text{C}_4\text{mim}][\text{CF}_3\text{SO}_3]$										
0.10	1306.1	1296.6	1287.6	1278.7	1270.5	1262.5	1254.0	1246.8	1239.6	1225.3
1.00	1306.6	1297.1	1288.1	1279.3	1271.1	1263.1	1254.7	1247.5	1240.3	1226.1
2.00	1307.1	1297.7	1288.7	1280.0	1271.7	1263.8	1255.3	1248.3	1241.1	1226.8
3.00	1307.7	1298.3	1289.3	1280.7	1272.4	1264.5	1256.0	1249.0	1241.8	1227.6
4.00	1308.2	1298.9	1289.9	1281.3	1273.1	1265.2	1256.7	1249.7	1242.5	1228.4
5.00	1308.8	1299.5	1290.5	1282.0	1273.8	1265.8	1257.4	1250.4	1243.2	1229.1
10.0	1311.5	1302.3	1293.3	1285.0	1276.9	1269.1	1260.7	1253.8	1246.6	1232.7

Table 3.2. Experimental density data, ρ , for [C₄C₁mim]PF₆, [C₆mim]PF₆ and dry and water saturated [C₈mim][PF₆]

$\frac{P}{\text{MPa}}$	$\rho / (\text{kg}\cdot\text{m}^{-3})$ at T / K										
	293.15	303.15	313.15	323.15	333.15	343.15	353.15	363.15	373.15	383.15	393.15
[C ₄ C ₁ mim]PF ₆											
0.10			1339.6	1330.9	1321.9	1313.5	1305.4	1297.6	1290.6	1283.4	1276.1
1.00			1340.0	1331.4	1322.4	1314.1	1306.0	1298.2	1291.2	1284.0	1276.8
2.00			1340.7	1331.9	1323.0	1314.6	1306.6	1298.8	1291.9	1284.7	1277.4
3.00			1341.2	1332.5	1323.5	1315.2	1307.2	1299.4	1292.5	1285.3	1278.1
4.00			1341.6	1333.1	1324.1	1315.8	1307.8	1300.1	1293.2	1286.0	1278.8
5.00			1342.1	1333.6	1324.6	1316.3	1308.3	1300.7	1293.8	1286.6	1279.4
10.0			1344.6	1336.2	1327.2	1319.1	1311.1	1303.6	1296.7	1289.7	1282.6
[C ₆ mim][PF ₆]											
0.10	1299.8	1290.6	1281.5	1272.7	1264.2	1256.1	1248.0	1240.6	1233.4	1226.4	1219.4
1.00	1300.3	1291.1	1282.0	1273.2	1264.8	1256.7	1248.6	1241.2	1234.1	1227.2	1220.1
2.00	1300.8	1291.7	1282.6	1273.9	1265.4	1257.3	1249.2	1242.0	1234.9	1227.9	1220.9
3.00	1301.4	1292.2	1283.1	1274.5	1266.0	1258.0	1249.9	1242.6	1235.6	1228.7	1221.7
4.00	1301.9	1292.7	1283.7	1275.0	1266.6	1258.6	1250.5	1243.3	1236.3	1229.4	1222.5
5.00	1302.4	1293.2	1284.3	1275.6	1267.3	1259.2	1251.2	1244.0	1237.0	1230.1	1223.3
10.0	1304.9	1295.8	1287.0	1278.5	1270.3	1262.0	1254.2	1247.2	1240.3	1233.6	1227.0
[C ₈ mim][PF ₆]											
0.10	1242.4	1233.8	1225.3	1217.6	1209.1	1201.0	1193.6	1186.2	1179.2	1172.7	1166.0
1.00	1242.9	1234.4	1225.9	1218.2	1209.7	1201.6	1194.3	1186.9	1179.9	1173.5	1166.8
2.00	1243.5	1235.0	1226.5	1218.8	1210.3	1202.3	1195.0	1187.6	1180.6	1174.2	1167.5
3.00	1244.1	1235.6	1227.1	1219.4	1211.0	1203.0	1195.7	1188.3	1181.3	1174.9	1168.3
4.00	1244.6	1236.1	1227.7	1220.0	1211.6	1203.6	1196.3	1189.0	1182.0	1175.6	1169.1
5.00	1245.1	1236.7	1228.3	1220.6	1212.2	1204.3	1197.1	1189.7	1182.7	1176.3	1169.8
10.0	1247.8	1239.5	1231.1	1223.4	1215.1	1207.4	1200.3	1193.0	1186.1	1179.8	1173.5
[C ₈ mim][PF ₆] saturated with water at 293.15 K											
0.10	1237.2	1228.1	1219.9	1211.0	1202.6	1194.6	1186.89	1179.3	1172.6	1165.4	
1.00	1237.7	1228.7	1220.5	1211.5	1203.1	1195.2	1187.53	1180.0	1173.3	1166.1	
2.00	1238.3	1229.2	1221.1	1212.1	1203.8	1195.9	1188.22	1180.7	1174.0	1166.8	
3.00	1238.8	1229.8	1221.7	1212.7	1204.4	1196.6	1188.91	1181.4	1174.7	1167.5	
4.00	1239.3	1230.4	1222.2	1213.3	1205.0	1197.2	1189.59	1182.1	1175.4	1168.2	
5.00	1239.8	1231.0	1222.8	1213.9	1205.6	1197.9	1190.28	1182.8	1176.0	1169.0	
10.0	1242.4	1233.7	1225.7	1216.8	1208.7	1201.0	1193.60	1186.2	1179.5	1172.4	

Density data for some of the studied ILs are already available in the open literature but almost only at atmospheric pressure^[84,86,98-103] and the relative deviations between the experimental data obtained in this work and those reported by the other authors at 0.10 MPa and from this work and Azevedo et al.^[98] at 10.0 MPa are presented in Figure 3.2.

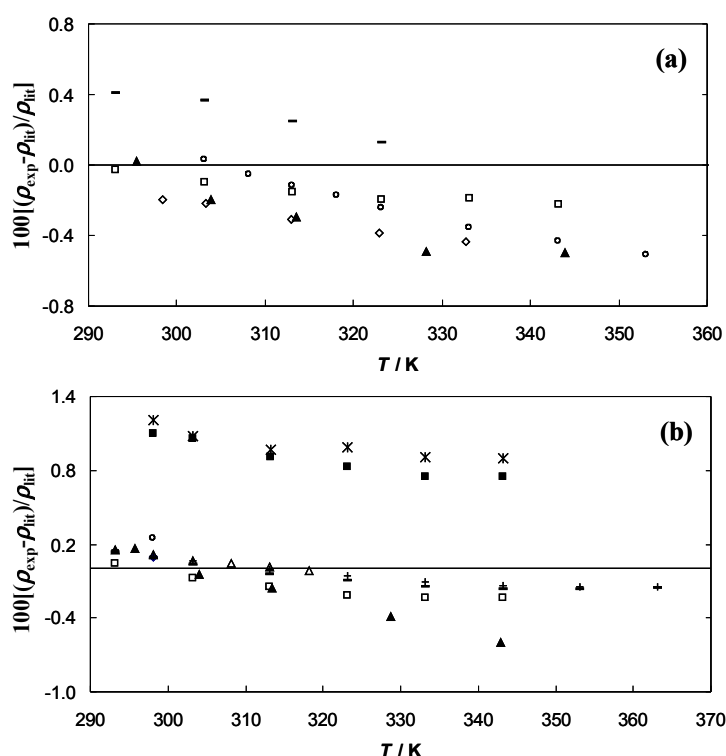


Figure 3.2. Relative deviations between the experimental density data of this work and those reported in the literature as a function of temperature. **(a)** $[\text{C}_4\text{mim}][\text{BF}_4]$ at 0.10 MPa: \blacktriangle , Fredakle et al.^[84]; \square , Tokuda et al.^[86]; \diamond , Azevedo et al.^[98]; \circ , Zhou et al.^[99]; $[\text{C}_4\text{mim}][\text{BF}_4]$ at 10.0 MPa: $-$, Azevedo et al.^[98]; **(b)** $[\text{C}_4\text{mim}][\text{CF}_3\text{SO}_3]$ at 0.10 MPa: \blacktriangle , Fredakle et al.^[84]; \square , Tokuda et al.^[86]; $[\text{C}_8\text{mim}][\text{BF}_4]$ at 0.10 MPa: \times , Gu and Brennecke^[100]; $-$, Harris et al.^[101]; $[\text{C}_6\text{mim}][\text{PF}_6]$ at 0.10 MPa: Δ , Pereiro et al.^[102]; \circ , Dzyuba and Bartsch^[103]; $[\text{C}_8\text{mim}][\text{PF}_6]$ at 0.10 MPa: \blacksquare , Gu and Brennecke^[100]; $+$, Harris et al.^[101]; \blacklozenge , Dzyuba and Bartsch^[103].

From Figure 3.2 it can be seen that no systematic errors are present, where the maximum deviations found are in the order of 1.2 and 1.1 % for $[\text{C}_4\text{mim}][\text{BF}_4]$ and $[\text{C}_8\text{mim}][\text{PF}_6]$, respectively, and appearing at the lower temperatures in respect to Gu and Brennecke^[100]. However, a better agreement can be observed at higher temperatures. In general, the deviations from our data and the literature are ranging from (-0.6 to 1.2) %, and they can be due essentially to the salts purity including water and halides content, and also from the experimental technique adopted.

From the experimental densities for a given anion, it is observed that as the alkyl chain length in the imidazolium cation increases, the density of the corresponding IL decreases. The inclusion of a new third substitution in the imidazolium cation of

[C₄C₁mim][PF₆] follows the same trend, presenting lower densities when compared to [C₄mim][PF₆] reported by Azevedo et al.^[98] and higher density values when compared to [C₆mim][PF₆] and [C₈mim][PF₆]. The average change of $(33.88 \pm 0.01) \text{ cm}^3 \cdot \text{mol}^{-1}$ by the addition of two $-\text{CH}_2$ groups observed in the measured data is in good agreement with that reported by Azevedo et al.^[98,104] and Esperança et al.^[105] and are anion independent.

The molar volumes for a series of ionic liquids with the same cation seem to increase with the effective anion size from $[\text{BF}_4] < [\text{PF}_6] < [\text{CF}_3\text{SO}_3]$. Due to differences in molecular weight this effect is not directly translated in a similar dependence in the densities.

For the most hydrophobic IL, [C₈mim][PF₆], an increase of the water mass fraction content of $(11905 \pm 98) \times 10^{-6}$ causes an average density decrease of 0.53 % compared to the dry IL. The water content does not affect the [C₈mim][PF₆] density across the pressure and temperature range investigated, as much as other properties such as viscosity and surface tensions^[40,41,106].

Esperança et al.^[105] have developed and demonstrated the ability of a simple model for ILs molar volume prediction, where the molar volume, V_m , of a given ionic liquid is considered as the sum of the effective molar volumes occupied by the cation, V_c^* , and the anion, V_a^* :

$$V_m = V_c^* + V_a^* \quad 3.4$$

Using this approach, for a given IL, knowing the effective size of the anion it is possible to determine the molar volume of the cation and *vice-versa*. Moreover, it was verified that there is a proportional increment with the methyl groups and that is irrespective to the anion identity. Thus, it was possible to use the molar volumes presented by Esperança et al.^[105] for the estimation of the volume of a new anion group ([CF₃SO₃]) and a new cation group ([C₄C₁mim]). The effective molar volumes of these new groups are reported in Table 3.3 along with predictions of the molar volumes of the studied ILs.

Table 3.3. Effective molar volume of anion, V_a^* , cation, V_c^* , and estimated molar volumes, V_m , at 298.15 K

Anion	$\frac{V_a^*}{\text{cm}^3 \cdot \text{mol}^{-1}}$	Cation	$\frac{V_c^*}{\text{cm}^3 \cdot \text{mol}^{-1}}$	Estimated $\frac{V_m}{\text{cm}^3 \cdot \text{mol}^{-1}}$	Experimental $\frac{V_m}{\text{cm}^3 \cdot \text{mol}^{-1}}$	% of V_m Relative Deviation
[BF ₄]	53.4	[C ₄ mim]	133.58	187.0	187.9	0.5
[BF ₄]	53.4	[C ₈ mim]	202.34	255.7	255.4	0.1
[CF ₃ SO ₃]	88.0 ^a	[C ₄ mim]	133.58	---	221.5	---
[PF ₆]	73.7	[C ₄ C ₁ mim]	147.33a	---	221.0	---
[PF ₆]	73.7	[C ₆ mim]	167.96	241.7	241.1	0.2
[PF ₆]	73.7	[C ₈ mim]	202.34	276.0	274.8	0.4

^aEstimated in this work

Deviations from experimental values are less than 0.5 %, showing the good predictive capability of this simple model proposed by Esperança et al.^[105].

3.2.3.2. Thermodynamic Properties

The experimental density values can be used to derive some thermodynamic properties, such as the isothermal compressibility, κ_T , the isobaric thermal expansion coefficient, α_p and the thermal pressure coefficient, γ_p .

The fitting of the isobaric density data was performed using a Tait equation^[88] as described by eq 3.5,

$$\rho = \rho^* - A \ln \left(\frac{(B+0.1)/\text{MPa}}{(B+p)/\text{MPa}} \right) \quad 3.5$$

where ρ^* is the density at a given temperature and at a reference pressure of 0.1 MPa, and A and B are coefficients of the Tait equation^[88] that are temperature and IL dependent. This equation is known to represent very well the density behavior of liquids over pressure at constant temperature. The correlation parameters for each isotherm and the maximum relative deviations from experimental data are reported in Tables 3.4 to 3.6.

Table 3.4. Coefficients of the Tait equation (eq 3.5) for the density at each isotherm between 0.10 and 10.0 MPa for [C₄mim][BF₄], [C₈mim][BF₄] and [C₄mim][CF₃SO₃]

$\frac{T}{K}$	$\frac{A}{(kg \cdot m^{-3})}$	$\frac{B}{MPa}$	% Maximum Relative Deviation
[C ₄ mim][BF ₄]			
293.15	40.43	85.94	0.0017
303.15	41.76	86.87	0.0008
313.15	46.73	95.41	0.0033
323.15	30.99	59.12	0.0014
333.15	29.49	54.78	0.0008
343.15	43.25	78.30	0.0008
353.15	26.76	47.34	0.0005
363.15	39.25	67.75	0.0010
373.15	41.27	70.43	0.0022
383.15	45.49	74.77	0.0013
393.15	47.88	77.59	0.0029
[C ₈ mim][BF ₄]			
293.15	62.76	134.84	0.0006
303.15	61.45	122.05	0.0008
313.15	73.92	143.10	0.0021
323.15	73.68	136.94	0.0006
333.15	73.00	132.81	0.0008
343.15	60.94	104.76	0.0004
353.15	64.37	108.05	0.0004
363.15	66.05	106.66	0.0003
373.15	60.64	94.35	0.0009
383.15	65.37	97.91	0.0002
393.15	74.61	110.71	0.0013
[C ₄ mim][CF ₃ SO ₃]			
293.15	60.33	105.54	0.0025
303.15	63.82	104.53	0.0023
313.15	58.61	96.48	0.0005
323.15	38.87	56.30	0.0018
333.15	52.67	75.63	0.0044
343.15	40.82	56.53	0.0030
353.15	67.55	94.36	0.0044
363.15	66.30	90.02	0.0018
373.15	52.38	69.40	0.0018
383.15	57.60	73.06	0.0028
393.15	67.34	85.05	0.0024

Table 3.5. Coefficients of the Tait equation (eq 3.5) for the density at each isotherm between 0.10 and 10.0 MPa for [C₄C₁mim]PF₆, [C₆mim]PF₆ and [C₈mim][PF₆]

$\frac{T}{K}$	$\frac{A}{(kg \cdot m^{-3})}$	$\frac{B}{MPa}$	% Maximum Relative Deviation
[C ₄ C ₁ mim][PF ₆]			
313.15	41.35	76.13	0.0055
323.15	54.06	94.39	0.0028
333.15	38.30	66.62	0.0016
343.15	48.67	81.81	0.0034
353.15	43.99	71.07	0.0020
363.15	53.88	84.57	0.0021
373.15	43.12	65.05	0.0159
383.15	38.14	55.15	0.0005
393.15	48.77	69.81	0.0009
[C ₆ mim][PF ₆]			
293.15	61.71	115.45	0.0027
303.15	38.93	69.68	0.0009
313.15	54.42	93.33	0.0006
323.15	57.67	92.33	0.0036
333.15	61.73	95.62	0.0009
343.15	30.44	46.48	0.0011
353.15	53.84	80.61	0.0020
363.15	49.41	68.78	0.0033
373.15	35.19	45.90	0.0016
383.15	36.97	46.15	0.0037
393.15	62.23	75.92	0.0005
[C ₈ mim][PF ₆]			
293.15	53.59	93.49	0.0046
303.15	50.76	84.49	0.0035
313.15	47.99	75.99	0.0040
323.15	37.16	58.61	0.0006
333.15	35.39	53.86	0.0040
343.15	39.21	56.40	0.0022
353.15	44.55	61.18	0.0066
363.15	48.90	66.86	0.0053
373.15	46.99	62.62	0.0007
383.15	50.11	65.21	0.0072
393.15	46.78	56.81	0.0046

Table 3.6. Coefficients of the Tait equation (eq 3.5) for the density at each isotherm between 0.10 and 10.0 MPa for water saturated $[\text{C}_8\text{mim}][\text{PF}_6]$

$\frac{T}{K}$	$\frac{A}{(\text{kg} \cdot \text{m}^{-3})}$	$\frac{B}{\text{MPa}}$	% Maximum Relative Deviation
$[\text{C}_8\text{mim}][\text{PF}_6]$ saturated with water at 293.15 K			
293.15	37.25	66.27	0.8339
303.15	50.52	84.43	0.9071
313.15	78.49	129.15	0.9456
323.15	56.51	91.66	0.9519
333.15	73.60	114.85	1.0064
343.15	54.40	79.71	1.0604
353.15	94.06	133.91	1.1236
363.15	72.95	100.44	1.1556
373.15	71.92	98.34	1.1720
383.15	75.67	102.15	1.1933

The experimental density isotherms for $[\text{C}_4\text{mim}][\text{CF}_3\text{SO}_3]$ along with the fitting lines obtained with eq 3.5 are illustrated in Figure 3.3.

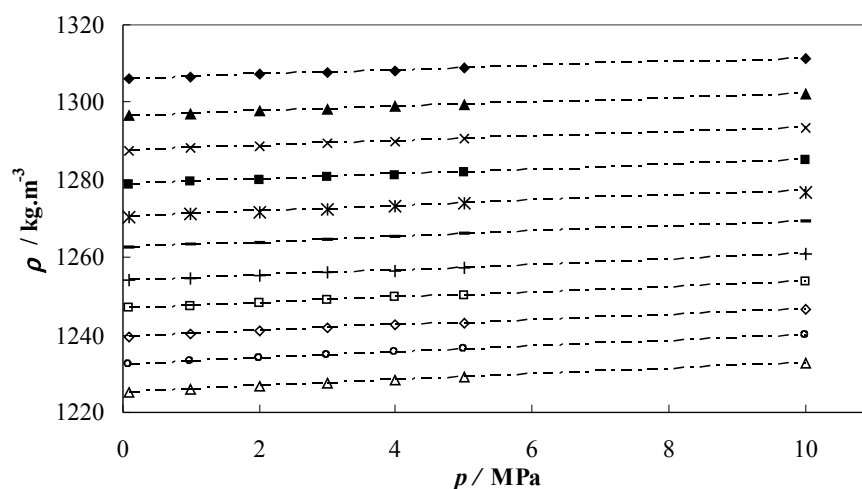


Figure 3.3. Isotherms of the experimental density of $[\text{C}_4\text{mim}][\text{CF}_3\text{SO}_3]$: \blacklozenge , 293.15 K; \blacktriangle , 303.15 K; \times , 313.15 K; \blacksquare , 323.15 K; \times , 333.15 K; $-$, 343.15 K; $+$, 353.15 K; \square , 363.15 K; \diamond , 373.15 K; \circ , 383.15 K; \triangle , 393.15 K. The lines correspond to the fit of the data by eq 3.5.

The Tait equation was found to adequately describe the dry ILs isothermal experimental densities with a maximum deviation of 0.02 %. Larger deviations for the densities of the water saturated $[\text{C}_8\text{mim}][\text{PF}_6]$ were observed with maximum deviations from experimental data of 1.2 %.

The Tait equation is an integrated form of an empirical equation representative of the

isothermal compressibility behavior *versus* pressure. The isothermal compressibility, k_T , is the effect of pressure in density that is calculated using the isothermal pressure derivative of density according to the following equation,

$$k_T = \left(\frac{\partial \ln \rho}{\partial p} \right)_T = - \left(\frac{\partial \ln V}{\partial p} \right)_T \quad 3.6$$

where ρ is the density and p the pressure at constant temperature, T . The isothermal compressibilities can be thus easily calculated using the fitting of eq 3.5 to the density data. For illustration purposes the isothermal compressibilities of $[\text{C}_6\text{mim}][\text{PF}_6]$ are shown in Figure 3.4.

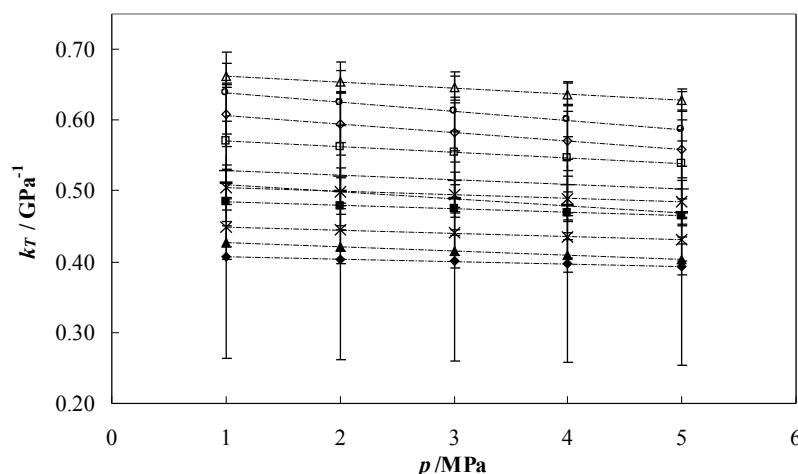


Figure 3.4. Isothermal compressibilities of $[\text{C}_6\text{mim}][\text{PF}_6]$: \blacklozenge , 293.15 K; \blacktriangle , 303.15 K; \times , 313.15 K; \blacksquare , 323.15 K; \star , 333.15 K; $-$, 343.15 K; $+$, 353.15 K; \square , 363.15 K; \diamond , 373.15 K; \circ , 383.15 K; \triangle , 393.15 K.

The standard deviations presented were calculated with the law of propagation of errors from the standard deviations of each constant of eq 3.5. Although the associated uncertainty is quite large, as shown by the error bars in Figure 3.4, it seems that the ILs become more compressible with increasing temperatures. On the other hand it would seem that the ILs become less compressible with increasing pressure, but if the large standard deviations associated to these values are considered, the isothermal compressibilities should be considered constant in the pressure range studied. For example, for $[\text{C}_6\text{mim}][\text{PF}_6]$ the isothermal compressibilities range from $(0.41 \pm 0.14) \text{ GPa}^{-1}$ at 293.15 K to $(0.66$

± 0.02) GPa^{-1} at 393.15 K and at a constant pressure of 1.0 MPa.

The ILs isothermal compressibilities are similar to those of water and high temperature molten salts and are smaller than those of organic solvents, due to the strong Coulombic interactions between the ions^[91,100].

For $[\text{C}_4\text{mim}][\text{BF}_4]$ in the range (303.15 to 323.15) K and (0.1 to 10.0) MPa there is an average deviation of isothermal compressibilities of - 3 % from Azevedo et al.^[98]. For $[\text{C}_8\text{mim}][\text{BF}_4]$ and $[\text{C}_8\text{mim}][\text{PF}_6]$ at 0.10 MPa and 323.15 K it was found a deviation of -21 % and 5 %, respectively, from the data reported by Gu and Brennecke^[100]. It should be noted that there is a strong dependence of the derivation method from the fitting to the experimental data, and to determine accurate derivative properties, a large number of experimental density points should be collected.

The function $\ln(\rho)=f(T)$ was used to describe the volume variations *versus* temperature as recommended by Esperança et al.^[105], because it avoids the mathematical violation that can arise from the assumption of considering the density as a linear function of temperature, and the isobaric expansivity is described by eq 3.7,

$$\alpha_p = -\left(\frac{\partial \ln \rho}{\partial T}\right)_p = \left(\frac{\partial \ln V}{\partial T}\right)_p \quad 3.7$$

If this function is linear, then $\ln(V)=f(T)$ should also be linear, and α_p constant, since it is temperature independent^[105]. To investigate α_p temperature independence, relatively to other compounds reported in literature^[98,100,104,105], a second-order polynomial function for the temperature dependence of the $\ln(\rho)$ was chosen,

$$\ln\left(\frac{\rho}{\rho_0}\right) = C + D(T) + E(T)^2 \quad 3.8$$

where ρ is the experimental density at each pressure and temperature, ρ_0 is assumed to be $1.0 \text{ kg}\cdot\text{m}^{-3}$, T is the temperature, and C , D and E are constant parameters determined from the experimental data using a second-order polynomial equation at constant pressure, p . The fitting coefficients of the second-order polynomial equation for each IL at constant pressure are presented in Tables 3.7 and 3.8.

Table 3.7. Parameters of the isobaric second-order polynomial fitting (eq 3.8) for [C₄mim][BF₄], [C₈mim][BF₄] and [C₄mim][CF₃SO₃]

$\frac{p}{MPa}$	$(C \pm \sigma^a)$	$\frac{10^3(D \pm \sigma^a)}{K^{-1}}$	$\frac{10^7(E \pm \sigma^a)}{K^{-2}}$
[C ₄ mim][BF ₄]			
0.10	7.373 ± 0.004	-1.20 ± 0.03	8.6 ± 0.4
1.00	7.373 ± 0.004	-1.20 ± 0.03	8.6 ± 0.4
2.00	7.372 ± 0.005	-1.19 ± 0.03	8.6 ± 0.4
3.00	7.372 ± 0.004	-1.19 ± 0.03	8.6 ± 0.4
4.00	7.372 ± 0.004	-1.19 ± 0.03	8.6 ± 0.4
5.00	7.373 ± 0.004	-1.19 ± 0.03	8.6 ± 0.4
10.0	7.374 ± 0.004	-1.19 ± 0.03	8.8 ± 0.4
[C ₈ mim][BF ₄]			
0.10	7.319 ± 0.003	-1.36 ± 0.02	10.7 ± 0.3
1.00	7.318 ± 0.003	-1.36 ± 0.02	10.7 ± 0.3
2.00	7.318 ± 0.004	-1.36 ± 0.02	10.7 ± 0.3
3.00	7.318 ± 0.004	-1.36 ± 0.02	10.7 ± 0.3
4.00	7.318 ± 0.004	-1.35 ± 0.02	10.7 ± 0.3
5.00	7.317 ± 0.004	-1.35 ± 0.02	10.6 ± 0.3
10.0	7.316 ± 0.004	-1.34 ± 0.02	10.6 ± 0.4
[C ₄ mim][CF ₃ SO ₃]			
0.10	7.464 ± 0.007	-1.25 ± 0.04	8.9 ± 0.6
1.00	7.464 ± 0.006	-1.25 ± 0.04	9.0 ± 0.6
2.00	7.463 ± 0.007	-1.24 ± 0.04	8.8 ± 0.6
3.00	7.461 ± 0.007	-1.23 ± 0.04	8.7 ± 0.6
4.00	7.461 ± 0.007	-1.22 ± 0.04	8.7 ± 0.6
5.00	7.460 ± 0.006	-1.22 ± 0.04	8.7 ± 0.6
10.0	7.458 ± 0.007	-1.20 ± 0.04	8.5 ± 0.6

^aStandard deviation

Table 3.8. Parameters of the isobaric second-order polynomial fitting (eq 3.8) for [C₄C₁mim][PF₆], [C₆mim][PF₆] and dry and water saturated [C₈mim][PF₆]

$\frac{p}{MPa}$	$(C \pm \sigma^a)$	$\frac{10^3(D \pm \sigma^a)}{K^{-1}}$	$\frac{10^7(E \pm \sigma^a)}{K^{-2}}$
[C ₄ C ₁ mim][PF ₆]			
0.10	7.51 ± 0.01	-1.30 ± 0.07	9.9 ± 0.9
1.00	7.51 ± 0.01	-1.29 ± 0.07	9.7 ± 0.9
2.00	7.51 ± 0.01	-1.31 ± 0.07	10.1 ± 0.9
3.00	7.51 ± 0.01	-1.31 ± 0.07	10.0 ± 0.9
4.00	7.51 ± 0.01	-1.30 ± 0.07	10.0 ± 0.9
5.00	7.51 ± 0.01	-1.30 ± 0.07	10.0 ± 0.9
10.0	7.51 ± 0.01	-1.30 ± 0.08	10.0 ± 0.9
[C ₆ mim][PF ₆]			
0.10	7.467 ± 0.004	-1.29098	9.5 ± 0.3
1.00	7.468 ± 0.004	-1.29630	9.6 ± 0.4
2.00	7.468 ± 0.004	-1.29817	9.7 ± 0.4
3.00	7.469 ± 0.004	-1.30319	9.8 ± 0.4
4.00	7.469 ± 0.004	-1.30295	9.82554
5.00	7.470 ± 0.005	-1.30526	9.9 ± 0.4
10.0	7.474 ± 0.005	-1.32533	10.3 ± 0.5
[C ₈ mim][PF ₆]			
0.10	7.403 ± 0.009	-1.18 ± 0.05	7.9 ± 0.7
1.00	7.405 ± 0.009	-1.19 ± 0.05	8.1 ± 0.7
2.00	7.404 ± 0.008	-1.18 ± 0.05	8.0 ± 0.7
3.00	7.405 ± 0.008	-1.19 ± 0.05	8.1 ± 0.7
4.00	7.404 ± 0.008	-1.18 ± 0.05	8.1 ± 0.7
5.00	7.404 ± 0.008	-1.18 ± 0.05	8.1 ± 0.7
10.0	7.408 ± 0.008	-1.20 ± 0.04	8.5 ± 0.6
[C ₈ mim][PF ₆] saturated with water at 293.15 K			
0.10	7.417 ± 0.009	-1.27 ± 0.04	9.0 ± 0.6
1.00	7.416 ± 0.009	-1.27 ± 0.04	9.0 ± 0.6
2.00	7.416 ± 0.008	-1.27 ± 0.04	8.9 ± 0.5
3.00	7.415 ± 0.008	-1.26 ± 0.04	8.9 ± 0.6
4.00	7.414 ± 0.008	-1.25 ± 0.04	8.8 ± 0.5
5.00	7.413 ± 0.008	-1.25 ± 0.04	8.8 ± 0.5
10.0	7.409 ± 0.008	-1.22 ± 0.03	8.5 ± 0.6

^aStandard deviation

Using eqs 3.7 and 3.8 the following equation is obtained,

$$\alpha_p = -(D + 2E(T)) \quad 3.9$$

At a first approach, α_p seems to decrease with temperature as shown in Figure 3.5 for [C₈mim][BF₄].

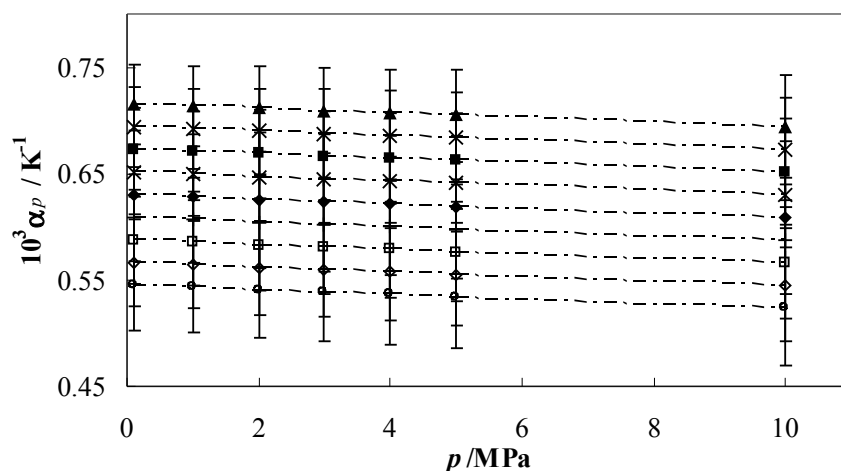


Figure 3.5. Isotherms for the isobaric expansivity of $[\text{C}_8\text{mim}][\text{BF}_4]$: ▲, 303.15 K; ×, 313.15 K; ■, 323.15 K; ✱, 333.15 K; ◆, 343.15 K; +, 353.15 K; □, 363.15 K; ◇, 373.15 K; ○, 383.15 K.

If the combined uncertainties determined with the law of propagation of uncertainties from the standard deviation due to each adjusted parameter are considered, they show to be very large and no statistically significant temperature dependence can be assigned to this property for most of the ILs studied, even in the large temperature range used in this work. It can nevertheless be shown that the ILs studied do not expand significantly with temperature.

There are some ILs that present more significant decreases in α_p with temperature, if obtained from eq 3.9, but in fact, ILs seem not to expand markedly with temperature, and present α_p values lower than most organic liquids and similar to those of water^[91]. For example, from eq 3.9, for $[\text{C}_8\text{mim}][\text{BF}_4]$ the thermal expansion coefficient range from $(0.72 \pm 0.04) \times 10^{-3} \text{ K}^{-1}$ at 303.15 K to $(0.54 \pm 0.04) \times 10^{-3} \text{ K}^{-1}$ at 383.15 K and at constant pressure of 0.1 MPa.

Several authors have determined the thermal expansion coefficient for ILs studied on this work^[98,100] and an average deviation of 12 % within the data for $[\text{C}_4\text{mim}][\text{BF}_4]$ at several pressures and at 303.15 K presented by Azevedo et al.^[98], and 6 % from the $[\text{C}_8\text{mim}][\text{BF}_4]$ and 12 % from the $[\text{C}_8\text{mim}][\text{PF}_6]$ data at 0.10 MPa and several temperatures reported by Gu and Brennecke^[100] was observed.

The thermal pressure coefficient, γ_V , may be calculated for all the ILs studied according to the following equation,

$$\gamma_V = \frac{\alpha_p}{k_T} \quad 3.10$$

The thermal pressure coefficients as function of pressure obtained for $[\text{C}_8\text{mim}][\text{PF}_6]$, as well as the associated uncertainties, are depicted in Figure 3.6.

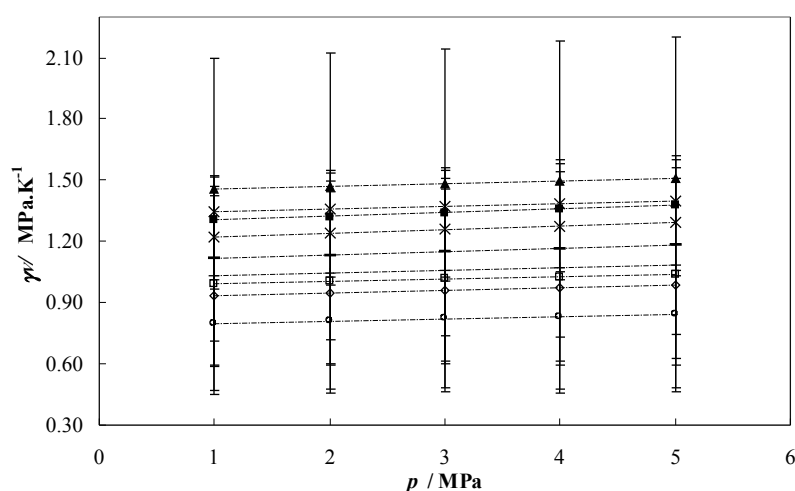


Figure 3.6. Isotherms for the thermal pressure coefficient of $[\text{C}_8\text{mim}][\text{PF}_6]$: ▲, 303.15 K; ×, 313.15 K; ■, 323.15 K; ✱, 333.15 K; -, 343.15 K; +, 353.15 K; □, 363.15 K; ◇, 373.15 K; ○, 383.15 K.

The γ_V decreases with temperature and increases slightly with pressure for all the ILs studied, if the uncertainties are not taken into account. However if this is done, it can be seen that the γ_V is almost constant in the temperature and pressure range studied. The uncertainties were determined with the law of propagation of errors from the standard deviation of α_p and k_T .

A comparison for the isothermal compressibilities and isobaric thermal expansivities as a function of temperature at a constant pressure of 5.0 MPa for the ILs studied is presented in Figure 3.7. The standard deviations were not included in these derived properties in order to facilitate the identification of the ILs, however it should be noted that as mentioned before, they are quite large as shown in Figures 3.4 and 3.5.

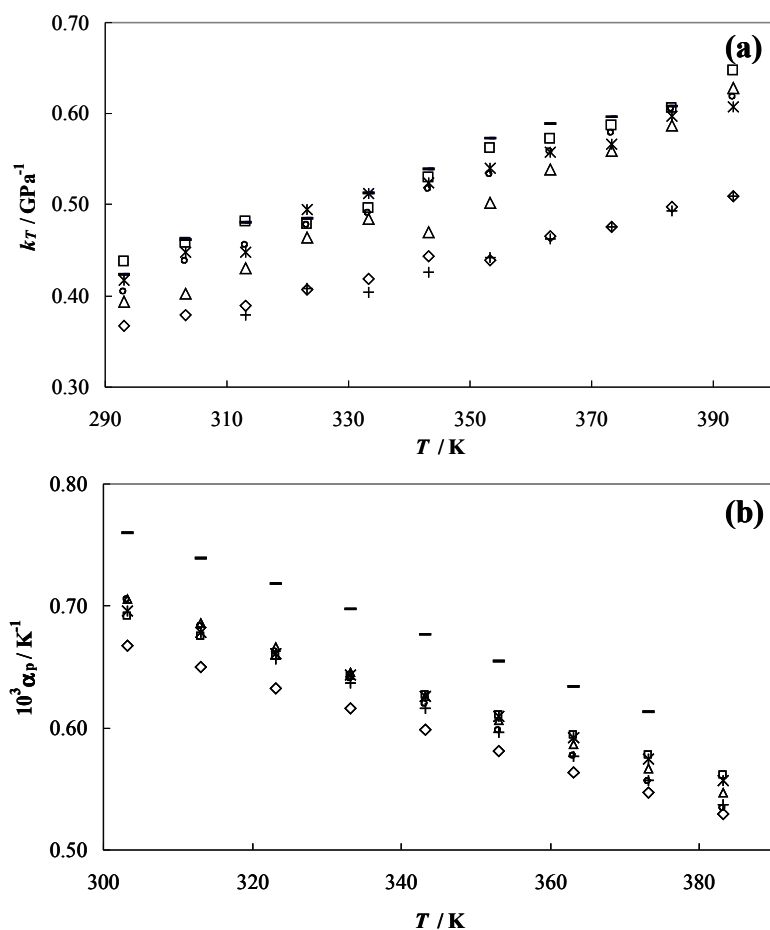


Figure 3.7. (a) Isothermal compressibility at 5.0 MPa as a function of temperature; (b) Thermal expansion coefficient at 5.0 MPa as a function of temperature: \diamond , [C₄mim][BF₄]; \circ , [C₈mim][BF₄]; \ast , [C₄mim][CF₃SO₃]; $+$, [C₄C₁mim][PF₆]; Δ , [C₆mim][PF₆]; \square , [C₈mim][PF₆] dried; $-$, [C₈mim][PF₆] saturated with water at 293.15 K.

Some conclusions can nevertheless be drawn. From Figure 3.7(a) there is an indication that the ILs with higher molar volumes are generally more compressible, since the κ_T increases with the alkyl chain length of the cation and with the effective anion size. On the other side, Figure 3.7(b) shows that the thermal expansion coefficient decreases with the alkyl chain length of the cation and with the effective anion size. For both cases it can also be seen that there is an increase in the derived properties with the presence of water in the IL.

3.2.4. Conclusions

Experimental density data for six pure ILs in the temperature range (293.15 to 393.15) K and pressure range (0.10 to 10.0) MPa were presented, and the water content influence in the density of the most hydrophobic IL was also assessed. Density results show that this property can be tailored by structural variations in the cation and anion. From the experimental data it was observed a proportional molar volume increase with the $-\text{CH}_2$ addition to the alkyl chain length of the 1- C_n -3-methylimidazolium based ILs, and a molar volume increase with the effective anion size. A simple ideal-volume model previously proposed by Esperança et al.^[105] was employed here for the prediction of the imidazolium molar volumes at ambient conditions and proved to agree well with the experimental results. Water content, anion identity and alkyl chain length can be a significant factor when considering the applications of a particular IL.

The liquid densities were correlated with the Tait equation^[88] that has shown to describe extremely well all the pure dried ILs studied with deviations from experimental data inferior to 0.02 %. However, larger deviations were found for the correlation of the water saturated IL isothermal densities, presenting a maximum deviation from the experimental data of 1.2 %.

The experimental results were also used to derive some thermodynamic properties such as the isothermal compressibility, the isobaric expansivity and the thermal pressure coefficient.

3.3. Surface Tensions

3.3.1. Introduction

In this section the influence of temperature, anion, cation and water content on the surface tension of eight imidazolium-based ionic liquids: $[\text{C}_4\text{mim}][\text{BF}_4]$, $[\text{C}_8\text{mim}][\text{BF}_4]$, $[\text{C}_4\text{mim}][\text{Tf}_2\text{N}]$, $[\text{C}_4\text{mim}][\text{PF}_6]$, $[\text{C}_8\text{mim}][\text{PF}_6]$, $[\text{C}_6\text{mim}][\text{PF}_6]$, $[\text{C}_4\text{C}_1\text{mim}][\text{PF}_6]$ and $[\text{C}_4\text{mim}][\text{CF}_3\text{SO}_3]$ were investigated. An extensive study of the effect of the water content in the surface tension was also carried.

Using the quasi-linear surface tension variation with temperature observed for all the ILs, the surface thermodynamic properties, such as surface entropy and surface enthalpy were derived, as well as the critical temperature, by means of the Eötvös^[107] and Guggenheim^[108] equations.

Since the thermophysical properties of the ionic liquids are related to their ionic nature, the surface tensions were correlated with the molar conductivity ratio, expressed as the effective ionic concentration.

3.3.2. Experimental Section

3.3.2.1. Materials

Surface tensions were measured for eight imidazolium based ILs, namely, 1-butyl-3-methyl-imidazolium tetrafluoroborate, [C₄mim][BF₄], 3-methyl-1-octyl-imidazolium tetrafluoroborate, [C₈mim][BF₄], 1-butyl-3-methyl-imidazolium bis(trifluoromethylsulfonyl)imide, [C₄mim][Tf₂N], 1-butyl-3-methyl-imidazolium hexafluorophosphate, [C₄mim][PF₆], 3-methyl-1-octyl-imidazolium hexafluorophosphate, [C₈mim][PF₆], 1-hexyl-3-methyl-imidazolium hexafluorophosphate, [C₆mim][PF₆], 1-butyl-2,3-dimethyl-imidazolium hexafluorophosphate, [C₁C₄mim][PF₆], and 1-butyl-3-methyl-imidazolium trifluoromethanesulfonate, [C₄mim][CF₃SO₃]. The [C₄mim][BF₄] was acquired at Solvent Innovation with a stated mass fraction purity state >98 % and a mole fraction of chloride ion of 100×10^{-6} . The [C₄mim][PF₆], [C₆mim][PF₆], [C₈mim][BF₄] and [C₄mim][CF₃SO₃] were acquired at IoLiTec with mass fraction purities >99 %. The bromide impurity mole fraction in the [C₄mim][PF₆] is 85×10^{-6} , in the [C₆mim][PF₆] is 100×10^{-6} , in the [C₈mim][BF₄] is 64×10^{-6} and the [C₄mim][CF₃SO₃] is halogen free since it was produced directly from butylimidazole and methyltriflate. The [C₈mim][PF₆] and [C₁C₄mim][PF₆] were acquired at Solchemar with mass fraction purities >99 %. The chloride mole fraction content in both ILs is $< (80 \times 10^{-6})$. The [C₄mim][Tf₂N] was synthesized in our laboratory based on a metathesis anion exchange reaction of 1-butyl-3-methylimidazolium bromide, [C₄mim][Br], with 1.2 equivalent amount of [Li][Tf₂N] in

water, followed by repeatedly washing, as described in literature^[40,86]. The reagents [C₄mim][Br] and [Li][Tf₂N] were acquired at IoLiTec with purities of >99 % and >98%, respectively. The mole fraction bromide impurity in the [C₄mim][Tf₂N], determined by ion chromatography, is 37×10^{-6} . The purities of each ionic liquid were checked by ¹H NMR, ¹³C NMR and ¹⁹F NMR. The water used was double distilled, passed by a reverse osmosis system and further treated with a Milli-Q plus 185 water purification apparatus. It has a resistivity of 18.2 MΩ•cm, a TOC smaller than 5 µg•L⁻¹ and it is free of particles greater than 0.22 µm.

In order to reduce the water content and volatile compounds to negligible values, vacuum (0.1 Pa), steering and moderate temperature (353 K) for at least 48 h were applied to all the ILs samples prior to the measurements. After this procedure, the water content in the ILs was determined with a Metrohm 831 Karl-Fischer coulometer indicating very low levels of water mass fraction content, as (485, 371, 181, 87, 18, 601, 121, 21) × 10⁻⁶ for [C₄mim][BF₄], [C₈mim][BF₄], [C₄mim][CF₃SO₃], [C₁C₄mim][PF₆], [C₈mim][PF₆], [C₄mim][PF₆], [C₄mim][Tf₂N] and [C₆mim][PF₆] respectively.

The influence of water content in the surface tensions was studied for both water saturated and atmospheric saturated ILs. With this purpose two highly hydrophobic, [C₈mim][PF₆] and [C₄mim][Tf₂N], and two less hydrophobic and highly hygroscopic ILs, [C₈mim][BF₄] and [C₄mim][PF₆] were studied. These compounds were saturated with ultra pure water, maintaining the two phases in equilibrium, at 293.15 K for at least 48 h, which was previously found to be the necessary time to achieve equilibrium^[89]. Between each temperature measurements the ILs were kept in equilibrium with ultra pure water inside the measurement cell, being the water removed and the interface carefully cleaned, by aspiration, and the water content determined before each new measurement. At saturation, for the same temperature, the ILs present a water mass fraction content of (15259, 14492, 25621, 171789) × 10⁻⁶ for [C₄mim][Tf₂N], [C₈mim][PF₆], [C₄mim][PF₆] and [C₈mim][BF₄] respectively^[89,109].

The atmospherically saturated ILs were dried and kept in contact with atmospheric air covered with a permeable membrane for several days, for each temperature measured. The

water mass fraction content of $[\text{C}_8\text{mim}][\text{PF}_6]$, $[\text{C}_4\text{mim}][\text{Tf}_2\text{N}]$, $[\text{C}_8\text{mim}][\text{BF}_4]$ and $[\text{C}_4\text{mim}][\text{PF}_6]$ was $(1340, 1252, 3530 \text{ and } 3381) \times 10^{-6}$ respectively, as determined by Karl Fisher coulometry.

To have a more complete picture of the effect of water concentration in the ionic liquid surface tension, the surface tensions of $[\text{C}_4\text{mim}][\text{PF}_6]$ and $[\text{C}_8\text{mim}][\text{PF}_6]$ for various water concentrations were also studied.

3.3.2.2. Apparatus and Procedure

The surface tension of each IL was measured with a *NIMA DST 9005* tensiometer from *NIMA Technology, Ltd.* with a Pt/Ir Du Noüy ring, based on force measurements, for which it has a precision balance able to measure down to 10^{-9} N. Prior to the measurements, vacuum (0.1 Pa), steering and moderate temperature (353 K) were applied to the sample. The sample surface was also cleaned before each measurement, by aspiration, in order to remove surface active impurities present at the interface and to allow the formation of a new interface. The measurements were carried in the temperature range from (293 to 353) K and at atmospheric pressure. The sample under measurement was kept thermostated in a double-jacketed glass cell by means of a water bath, using an HAAKE F6 circulator equipped with a Pt100 probe, immersed in the solution, and able to control temperature within ± 0.01 K.

For each sample and temperature at least five sets of three immersion/detachment cycles were performed, giving a minimum of at least 15 surface tension values, which allow the determination of an average surface tension value as well as the associated expanded uncertainty^[57,58]. Further details about the equipment and method can be found elsewhere^[59-61].

For mass spectrometry ionic liquids were used as acetonitrile solutions (1.5×10^{-4} M). Electrospray ionization mass spectrometry (ESI-MS) and tandem spectrometry (ESI-MS-MS) were acquired with Micromass Q-ToF 2 operating in the positive ion mode. Source and desolvation temperatures were 80 °C and 100 °C, respectively. Capillary voltage was 2600 V and cone voltage 25 V. ESI-MS-MS spectra were acquired by selecting the

precursor ion with the quadrupole, performing collisions with argon at energies of 2-30 eV in the hexapole, followed by mass analysis of product ions by the TOF analyzer. N₂ was used as nebulization gas. The ionic liquid solutions were introduced at a 10 mL.min⁻¹ flow. The breakdown graphs were obtained by acquiring the ESI-MS-MS spectra of each ion investigated at increasing collision energies and plotting the relative abundance of precursor and fragment ions as a function of collision energy. The relative order of hydrogen bond strength between cation and anion in each ion-pair studied, was obtained by acquiring the ESI-MS-MS spectra, at 10 eV collision energy, of the cluster ions [C₁...A...C₂]⁺ and measuring the relative abundances of the two fragment ions observed.

3.3.3. Results and Discussion

3.3.3.1. Surface Tension Measurements

Previous measurements have confirmed the ability of the equipment used to accurately measure interfacial tensions for hydrocarbons and fluorocarbon systems, validating the methodology and experimental procedure adopted in this work^[18,59-61]. The liquid densities of the pure compounds necessary for the surface tension measurements using the Du Noüy ring were obtained from the literature^[100,110-112], when available, or measured, as described in section 3.2.

The surface tension data of the dry ILs are reported in Table 3.9 and presented in Figure 3.8 for a better inspection. The relative deviations between the experimental data obtained in this work and those reported by other authors^[41,103,110,113-115] are presented in Figure 3.9.

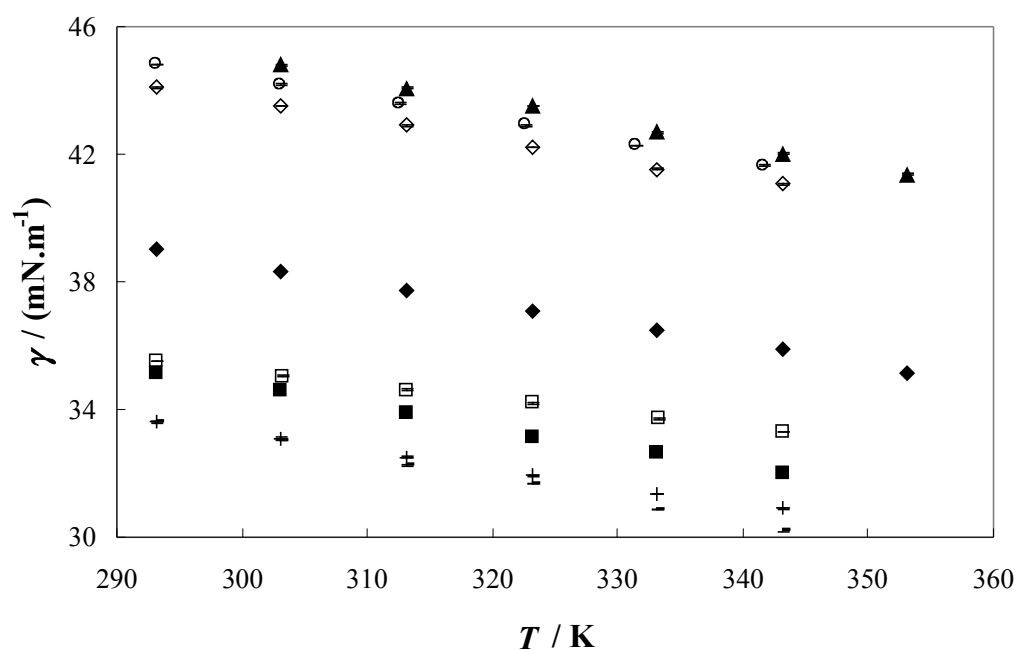


Figure 3.8. Experimental surface tension as a function of temperature for the dry ionic liquids studied: ○, [C₄mim][BF₄]; ◇, [C₄mim][PF₆]; +, [C₄mim][Tf₂N]; □, [C₄mim][CF₃SO₃]; ◆, [C₆mim][PF₆]; ■, [C₈mim][PF₆]; ▲, [C₄C₁mim][PF₆]; -, [C₈mim][BF₄].

The data measured shows average deviations of 4%, in respect with the available literature data. These deviations are larger than those previously observed for hydrocarbon and fluorocarbon compounds^[18,59-61] using the same equipment, but it must also be stressed that large discrepancies were also observed among the data from different authors^[41,103,110,113-115] as can be observed in Figure 3.9.

Table 3.9. Experimental surface tension (γ) of the dry ionic liquids studied.

[C ₄ mim][BF ₄]		[C ₄ mim][PF ₆]		[C ₄ mim][Tf ₂ N]		[C ₄ mim][CF ₃ SO ₃]	
$\frac{T}{K}$	$\frac{(\gamma \pm \sigma^a)}{mN.m^{-1}}$	$\frac{T}{K}$	$\frac{(\gamma \pm \sigma^a)}{mN.m^{-1}}$	$\frac{T}{K}$	$\frac{(\gamma \pm \sigma^a)}{mN.m^{-1}}$	$\frac{T}{K}$	$\frac{(\gamma \pm \sigma^a)}{mN.m^{-1}}$
293.15	44.81 ± 0.02	293.15	44.10 ± 0.02	293.15	33.60 ± 0.01	293.20	35.52 ± 0.03
303.15	44.18 ± 0.02	303.15	43.52 ± 0.04	303.15	33.09 ± 0.02	303.20	35.05 ± 0.03
312.65	43.58 ± 0.02	313.15	42.90 ± 0.03	313.15	32.50 ± 0.01	313.20	34.62 ± 0.02
322.65	42.90 ± 0.02	323.15	42.21 ± 0.03	323.15	31.92 ± 0.01	323.20	34.19 ± 0.02
331.45	42.27 ± 0.03	333.15	41.53 ± 0.03	333.15	31.35 ± 0.02	333.20	33.71 ± 0.02
341.65	41.64 ± 0.02	343.15	41.07 ± 0.01	343.15	30.90 ± 0.02	343.20	33.30 ± 0.03
[C ₆ mim][PF ₆]		[C ₈ mim][PF ₆]		[C ₄ C ₁ mim][PF ₆]		[C ₈ mim][BF ₄]	
$\frac{T}{K}$	$\frac{(\gamma \pm \sigma^a)}{mN.m^{-1}}$	$\frac{T}{K}$	$\frac{(\gamma \pm \sigma^a)}{mN.m^{-1}}$	$\frac{T}{K}$	$\frac{(\gamma \pm \sigma^a)}{mN.m^{-1}}$	$\frac{T}{K}$	$\frac{(\gamma \pm \sigma^a)}{mN.m^{-1}}$
293.15	39.02 ± 0.02	293.15	35.16 ± 0.01	303.15	44.80 ± 0.03	288.15	34.15 ± 0.03
303.15	38.35 ± 0.02	303.15	34.60 ± 0.02	313.15	44.07 ± 0.01	293.15	33.62 ± 0.02
313.15	37.71 ± 0.01	313.15	33.89 ± 0.02	323.15	43.52 ± 0.04	303.15	33.04 ± 0.02
323.15	37.09 ± 0.01	323.15	33.14 ± 0.02	333.15	42.68 ± 0.02	313.15	32.26 ± 0.01
333.15	36.47 ± 0.01	333.15	32.67 ± 0.01	343.15	42.02 ± 0.02	323.15	31.67 ± 0.01
343.15	35.91 ± 0.04	343.15	31.98 ± 0.01	353.15	41.37 ± 0.02	333.15	30.87 ± 0.02
353.15	35.15 ± 0.02					343.15	30.20 ± 0.02

^aStandard deviation

Not only the surface tension data available today for ionic liquids are rather scarce but also most of the measurements were carried either using compounds of low purity or without a careful attention towards the preparation of the sample, in particular drying, and often those measurements have been carried for purposes other than an accurate determination of the surface tensions.

The experimental values show that both the anion and cation have an influence on the surface tensions. Within the imidazolium family, the increase in the cation alkyl chain length reduces the surface tension values. Both compounds with the octyl chain present surface tensions lower than the corresponding butyl homologue. Surprisingly the introduction of a methyl group on the [C₄mim][PF₆] IL, substituting the most acidic hydrogen at the C₂ position in the imidazolium ring^[116], leads to an increase in the surface tension values of the [C₁C₄mim][PF₆], when compared with [C₄mim][PF₆]. Hunt^[117] reported the same odd behavior for melting points and viscosity and hypothesized that the effects due to the loss in hydrogen bonding are less significant than those due to the loss of entropy. The loss of entropy enhance the alkyl chain interactions by lowering the amount of disorder in the system, eliminating the ion-pair conformers, and increasing the rotational

barrier of the alkyl chain. Thus, the reduction in the entropy leads to a greater ordering within the liquid and consequently to the surface, leading to a slight increase in the surface tension.

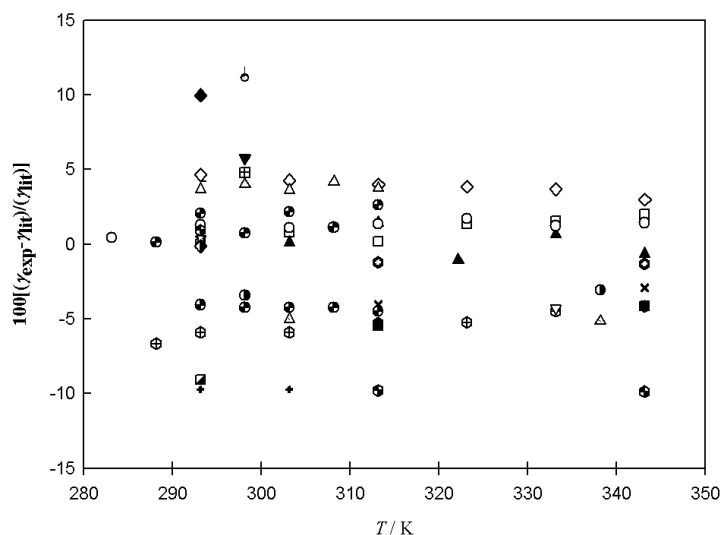


Figure 3.9. Relative deviations between the experimental surface tension data of this work and those reported in literature: \square , [C₄mim][BF₄]^[110]; $+$, [C₄mim][BF₄]^[113]; \blacktriangledown , [C₄mim][BF₄]^[41]; \blacksquare , [C₄mim][BF₄]^[118]; \odot , [C₄mim][BF₄]^[114]; \diamond , [C₄mim][PF₆]^[113]; $|$, [C₄mim][PF₆]^[41]; $-$, [C₄mim][PF₆]^[118]; \oplus , [C₄mim][PF₆]^[119]; \blacklozenge , [C₄mim][PF₆]^[103]; \blacktriangle , [C₄mim][PF₆]^[115]; \times , [C₄mim][PF₆]^[114]; \circ , [C₈mim][PF₆]^[113]; \boxplus , [C₈mim][PF₆]^[41]; \odot , [C₈mim][PF₆]^[118]; \triangle , [C₈mim][PF₆]^[119]; \star , [C₈mim][PF₆]^[103]; \odot , [C₈mim][PF₆]^[114]; \oplus , [C₈mim][BF₄]^[113]; ∇ , [C₈mim][BF₄]^[118]; \blacksquare , [C₈mim][BF₄]^[114]; \odot , [C₄mim][Tf₂N]^[41]; \triangle , [C₄mim][Tf₂N]^[114]; \blacklozenge , [C₄mim][Tf₂N]^[103]; \oplus , [C₆mim][PF₆]^[119]; \odot , [C₆mim][PF₆]^[114].

Similarly, an increase in the size of the anion leads to a decrease on the surface tensions with their values following the sequence [BF₄]⁻ > [PF₆]⁻ > [CF₃SO₃]⁻ > [Tf₂N]⁻, which agrees with Deetlefs et al.^[120] hypothesis that the increase of the anion size and the increase of the diffuse nature of the anion negative charge leads to a more delocalized charge and therefore to a decrease on the ability to hydrogen bonding. This is an odd result as, usually, the surface tension of organic compounds increase with the size of the molecules. However, these changes are actually a result of the energetic rather than steric interactions, contrary to the suggestion of Law and Watson^[113]. Since the surface tension is a measure of the surface cohesive energy, it is thus related to the strength of the interactions that are established between the anions and cations in an ionic liquid. The

increase in surface tensions with size in most organic compounds results from an increase in the forces between the molecules with their size. Ionic liquids are complex molecules where coulombic forces, hydrogen bonds and Van der Waals forces are all present in the interaction between molecules, with the hydrogen bonds being probably the most important forces in ionic liquids^[40,120,121]. Although the increase in size of the molecule leads to an increase of the Van der Waals forces it will also contribute to a dispersion of the ion charge and a reduction on the hydrogen bond strength.

The measured data presents surface tension values well above those of conventional organic solvents, such as methanol (22.07 mN.m^{-1})^[77] and acetone (23.5 mN.m^{-1})^[77], as well as those of *n*-alkanes^[59-61], but still lower than those of water (71.98 mN.m^{-1})^[77].

Complex molecules tend to minimize their surface energies by exposing to the vapor phase their parts with lower surface energy. An alcohol will have a surface tension close to an alkane and not to water as the alkyl chains will be facing upwards at surface to minimize the surface energy. Yet the surface tensions for the ionic liquids are close to those of imidazole extrapolated to the same temperatures^[118]. According to Langmuir's principle of independent surface action^[122] this is an indication of the presence of the imidazolium ring at the surface rather than the alkyl chain as usual in compounds with alkyl chains. That the surface may be made up of mainly anions is also precluded by the surface tensions that the surface would present in this case. The $[\text{PF}_6]$ should have a surface tension close to $[\text{SF}_6]$ that has a value of circa 10 mN.m^{-1} at -50°C ^[123], other fluorinated ions should also have very low surface tensions. The only explanation for these high surface tensions are the hydrogen bonds that exist between the cations, and the anions and cations, as discussed below, that increase the interactions between the ions leading to enhanced values of surface tension.

3.3.3.2. Thermodynamic Properties

Using the quasi-linear surface tension variation with temperature for all the ILs observed in the studied temperature range, the surface thermodynamic properties, surface entropy and surface enthalpy, were derived^[62,63]. The surface entropy, S^g , and the surface

enthalpy, H^y , were determined accordingly to eqs 2.1 and 2.2 described in *section 2.3.2*.

The thermodynamic functions for all the ILs studied and the respective expanded uncertainties, derived from the slope of the curve $\gamma = f(T)$ in combination with the law of propagation of uncertainty, are presented in Table 3.10^[64].

Table 3.10. Surface thermodynamic functions for the ionic liquids studied

IL	Dry ILs		Saturated ILs	
	$10^5(S^y \pm \sigma^a)$	$10^2(H^y \pm \sigma^a)$	$10^5(S^y \pm \sigma^a)$	$10^2(H^y \pm \sigma^a)$
	$N.m^{-1}.K^{-1}$	$N.m^{-1}$	$N.m^{-1}.K^{-1}$	$N.m^{-1}$
[C ₄ mim][PF ₆]	6.2 ± 0.1	6.23 ± 0.05	6.4 ± 0.4	6.3 ± 0.2
[C ₆ mim][PF ₆]	6.34 ± 0.08	5.76 ± 0.03	---	---
[C ₈ mim][PF ₆]	6.7 ± 0.1	5.49 ± 0.05	6.3 ± 0.2	5.30 ± 0.07
[C ₄ C ₁ mim][PF ₆]	6.9 ± 0.1	6.57 ± 0.05	---	---
[C ₄ mim][BF ₄]	6.35 ± 0.07	6.34 ± 0.02	---	---
[C ₈ mim][BF ₄]	7.1 ± 0.1	5.44 ± 0.04	6.9 ± 0.4	5.4 ± 0.1
[C ₄ mim][Tf ₂ N]	5.5 ± 0.1	4.97 ± 0.03	5.4 ± 0.2	4.96 ± 0.06
[C ₄ mim][CF ₃ SO ₃]	4.45 ± 0.04	4.86 ± 0.01	---	---

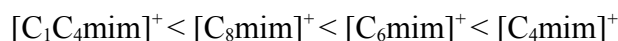
^aStandard deviation

The most important indication from the surface thermodynamic properties is the low surface entropies. Compared to other organic compounds the surface entropies are remarkably low. Even the *n*-alkanes, which are an example of surface organization^[124] have surface entropies that are 50 to 100% higher than the ionic liquids here studied. This is a clear indication of high surface organization in these fluids in agreement with the simulation results by Lynden-Bell^[125] and the surface studies of Watson and Law^[113,118,126] using Direct Recoil Spectroscopy, Iimori et al.^[127] using Sum Frequency Generation, Bowers et al.^[128] using neutron reflectometry measurements, and Slouskin et al.^[129] using X-Ray reflectometry measurements. On a previous work^[130], using a completely different approach, it was also shown that the surface of ionic liquids was highly organized. Using experimental and simulation values of heats of vaporization for imidazolium based ionic liquids with alkyl chain lengths ranging from ethyl to octyl, and with the [Tf₂N] anion, it was shown that a high degree of organization was present in the ionic liquids. Although that work put the emphasis on the bulk organization rather than on the surface, the direct relation between the heats of vaporization and the surface tensions makes those results even more significant to the understanding of surface structure and indicate that a great

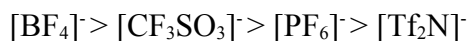
organization is present at surface as well. Although all these studies do not fully agree on the model of the surface structure, all of them indicate that a significant degree of surface ordering would be present and thus would be the cause for the reduced surface entropy observed. It is thus not surprising that the surface entropies increase with the size of the alkyl chain as can be seen in Table 3.10 for the $[\text{PF}_6]$ and $[\text{BF}_4]$ compounds. The surface cannot be made up just of cations, but both cations and anions should be present, and the surface entropies seem to be more affected by the anion type than by the cation chain length. The surface enthalpy by its turn seems to decrease with the increasing chain length of the cation and also to suffer an important dependence on the anion. The change in the surface enthalpies seems to follow the decrease in strength of the hydrogen bonding observed for these ionic liquids with, again, the curious exception of the $[\text{bmim}][\text{PF}_6]$. More good quality data for other ionic liquids, however, are required to make reliable generalizations of these observations.

3.3.3.3. Mass Spectrometry and Hydrogen Bonding

Mass spectrometry measurements have been carried out as described above to establish the relative strength of the hydrogen bonds in ionic liquids for the anions and cations studied here. A higher abundance of ion C_1^+ in the ESI-MS-MS spectra of the heterodimer $[\text{C}_1\dots\text{A}\dots\text{C}_2]^+$ will imply a stronger bond between the cation C_2^+ and the anion $\text{A}^{[131]}$. The analysis of the ESI-MS-MS spectra obtained for the binary mixtures of ionic liquids used to form the clusters, shows that the relative strength of the hydrogen bonds observed in $[\text{C}_1\dots\text{BF}_4\dots\text{C}_2]^+$ and in $[\text{C}_1\dots\text{PF}_6\dots\text{C}_2]^+$ is the following



while that observed in $[\text{A}\dots\text{C}_4\text{mim}\dots\text{A}]^-$ is



The relative strength of the hydrogen bonds observed for the cations can be rationalized in terms of chain length increase on the N^1 -alkyl group of the imidazolium, which reduces the $\text{H}\dots\text{F}$ distance, and of the introduction of a second methyl group, which removes the most acidic hydrogen from carbon 2. Both factors contribute to a reduction in

the interactions between cations and anions. For the anions, the relative position of CF_3SO_3^- will probably be explained by the larger negative charge on the oxygen atoms as compared with the fluorine atoms^[132].

The relative strength of the hydrogen bonds observed is, with two exceptions, in agreement with the surface tensions measured showing that the surface tension data measured and reported in Table 3.9 and in Figure 3.8 are dependent on the strength of the interactions established between the anions and cations. A possible explanation for the increase in surface tensions of $[\text{C}_1\text{C}_4\text{mim}][\text{PF}_6]$, contrary to what was expected based on relative hydrogen bond strength, has already been discussed above. The second exception refers to the relative position of anions PF_6^- and CF_3SO_3^- , which is reversed when compared with surface tension values of $[\text{C}_4\text{mim}][\text{PF}_6]$ and $[\text{C}_4\text{mim}][\text{CF}_3\text{SO}_3]$. This may be due to entropic rather than energetic effects due to the shape and symmetry of the PF_6^- anion, which could lead to a greater ordering within the liquid.

3.3.3.4. Influence of the Water Content on the Surface Tension of Ionic Liquids

A major issue concerning ionic liquids thermophysical properties is the influence of the water content on their values. This is well established for densities^[41,42,103,113,114,133], viscosities^[40,41], melting points, glass transitions^[41], and gas solubilities^[134], among others. Although Hudlleston et al.^[41] showed some results on the influence of water on the surface tensions, the surface tension data available do not allow any discussion on the effect of water on the surface tensions of ionic liquids. Also some references^[135,136] seem to indicate that the water content has little or no influence on the surface tension values. In this work, besides a careful determination of the surface tensions of dry ionic liquids, the surface tensions of four water saturated ionic liquids ($[\text{C}_4\text{mim}][\text{Tf}_2\text{N}]$, $[\text{C}_8\text{mim}][\text{BF}_4]$, $[\text{C}_4\text{mim}][\text{PF}_6]$ and $[\text{C}_8\text{mim}][\text{PF}_6]$) were measured along with the dependence on the water content for two ionic liquids ($[\text{C}_4\text{mim}][\text{PF}_6]$ and $[\text{C}_8\text{mim}][\text{PF}_6]$) and are reported in Table 3.11.

Table 3.11. Experimental surface tension, γ , of water saturated ionic liquids

[C ₄ mim][Tf ₂ N]		[C ₄ mim][PF ₆]		[C ₈ mim][PF ₆]		[C ₈ mim][BF ₄]	
$\frac{T}{K}$	$\frac{(\gamma \pm \sigma^a)}{mN.m^{-1}}$	$\frac{T}{K}$	$\frac{(\gamma \pm \sigma^a)}{mN.m^{-1}}$	$\frac{T}{K}$	$\frac{(\gamma \pm \sigma^a)}{mN.m^{-1}}$	$\frac{T}{K}$	$\frac{(\gamma \pm \sigma^a)}{mN.m^{-1}}$
293.15	33.73 ± 0.02	303.15	43.57 ± 0.01	298.05	34.01 ± 0.02	293.15	33.75 ± 0.04
303.15	33.20 ± 0.01	313.15	42.66 ± 0.01	303.25	33.78 ± 0.02	303.15	32.58 ± 0.01
313.15	32.47 ± 0.02	323.15	42.36 ± 0.01	313.35	33.01 ± 0.01	313.15	32.35 ± 0.03
323.15	32.06 ± 0.02	333.15	41.56 ± 0.01	323.25	32.51 ± 0.02	323.15	31.45 ± 0.03
333.15	31.56 ± 0.02	343.15	40.89 ± 0.01	335.05	31.70 ± 0.01	333.15	31.00 ± 0.03
343.15	31.01 ± 0.02						

^aStandard deviation**Table 3.12.** Experimental surface tension, γ , of ILs as a function of the water mole fraction (x_{H_2O}) at 303.15 K

[C ₄ mim][PF ₆]		[C ₈ mim][PF ₆]	
x_{H_2O}	$\frac{(\gamma \pm \sigma^a)}{mN.m^{-1}}$	x_{H_2O}	$\frac{(\gamma \pm \sigma^a)}{mN.m^{-1}}$
0.0031	43.27 ± 0.02	0.0020	34.19 ± 0.02
0.0104	43.08 ± 0.02	0.0027	34.15 ± 0.02
0.0123	43.09 ± 0.02	0.0135	34.10 ± 0.02
0.0144	43.02 ± 0.02	0.0466	34.07 ± 0.01
0.0318	42.69 ± 0.02	0.1018	34.17 ± 0.08
0.0329	42.57 ± 0.02	0.1045	34.19 ± 0.02
0.0530	41.74 ± 0.02		
0.0578	41.65 ± 0.02		
0.0732	40.95 ± 0.02		
0.1452	43.57 ± 0.01		

^aStandard deviation

The measured surface tension values of saturated ILs indicate that, for the more hydrophobic ILs, the surface tensions of the saturated ILs are very similar to those obtained for the dry ones, as can be seen in Figures 3.10 to 3.13.

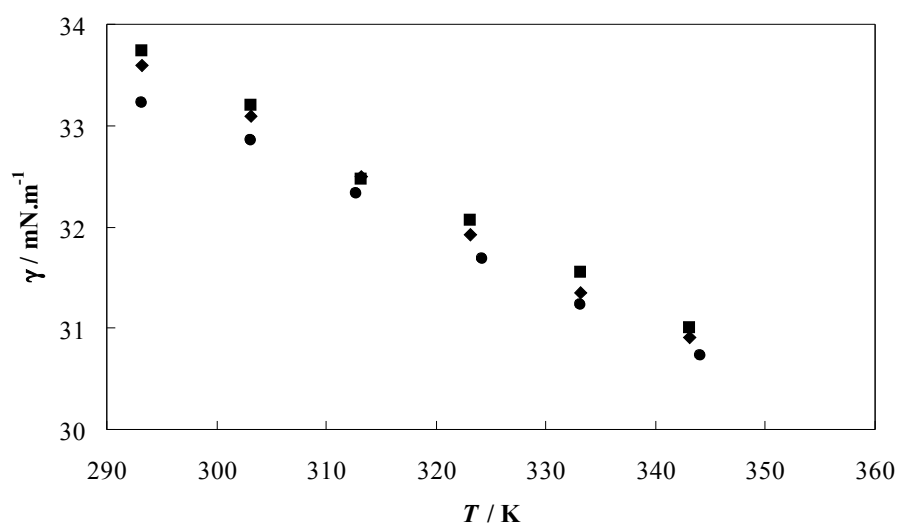


Figure 3.10. Surface tension as a function of temperature for $[\text{C}_4\text{mim}][\text{Tf}_2\text{N}]$: \blacklozenge , dry; \blacksquare , water saturated; \bullet , atmospheric saturated.

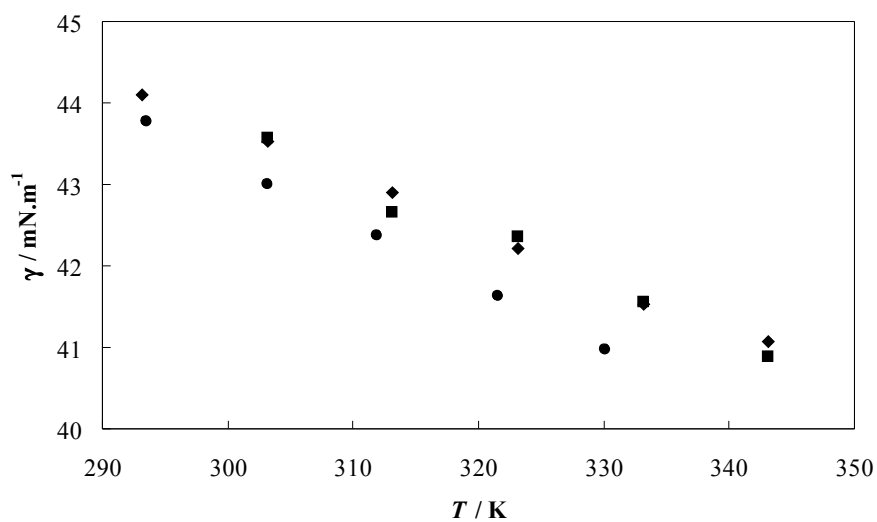


Figure 3.11. Surface tension as a function of temperature for $[\text{C}_4\text{mim}][\text{PF}_6]$: \blacklozenge , dry; \blacksquare , water saturated; \bullet , atmospheric saturated.

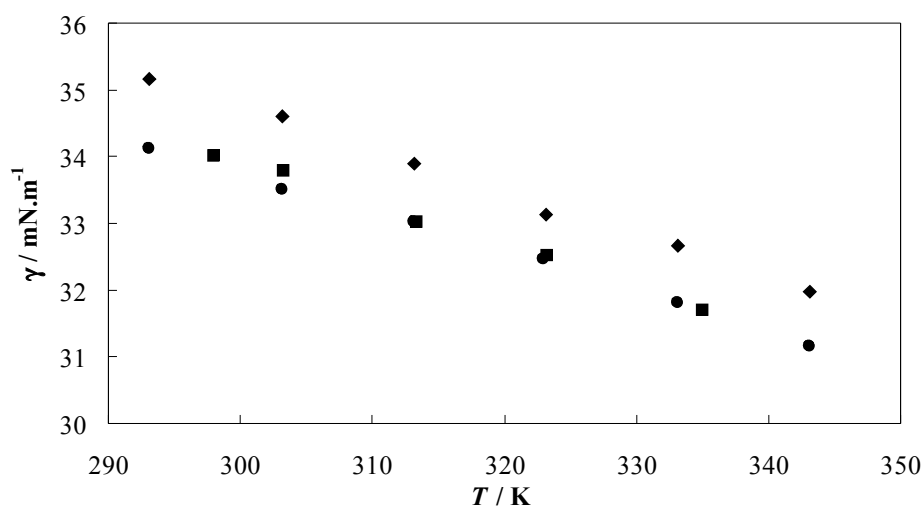


Figure 3.12. Surface tension as a function of temperature for [C₈mim][PF₆]: ♦, dry; ■, water saturated; ●, atmospheric saturated.

In all cases there is a decrease in the surface tension values for low water content. The same behavior can be seen for [C₄mim][PF₆], [C₈mim][PF₆] and [C₈mim][BF₄] as well as for the hydrophobic (yet somewhat hygroscopic) [C₄mim][Tf₂N] IL, with a decrease in the surface tension for low water contents.

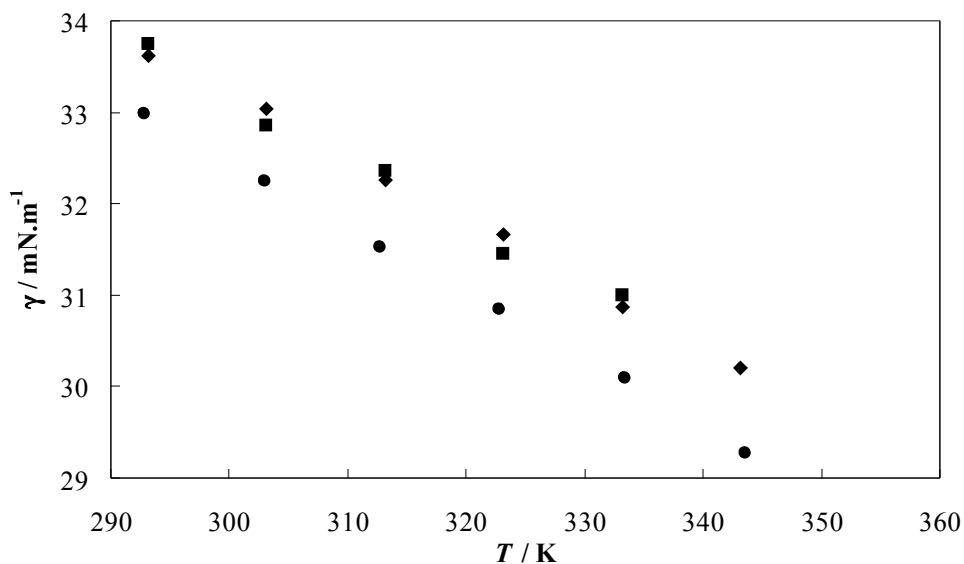


Figure 3.13. Surface tension as a function of temperature for [C₈mim][BF₄]: ♦, dry; ■, water saturated; ●, atmospheric saturated.

For a more complete understanding on the effect of the water content in the surface tension values, measurements have been carried for $[C_4mim][PF_6]$ and $[C_8mim][PF_6]$ as a function of the water content at 303 K, and are shown in Figure 3.14.

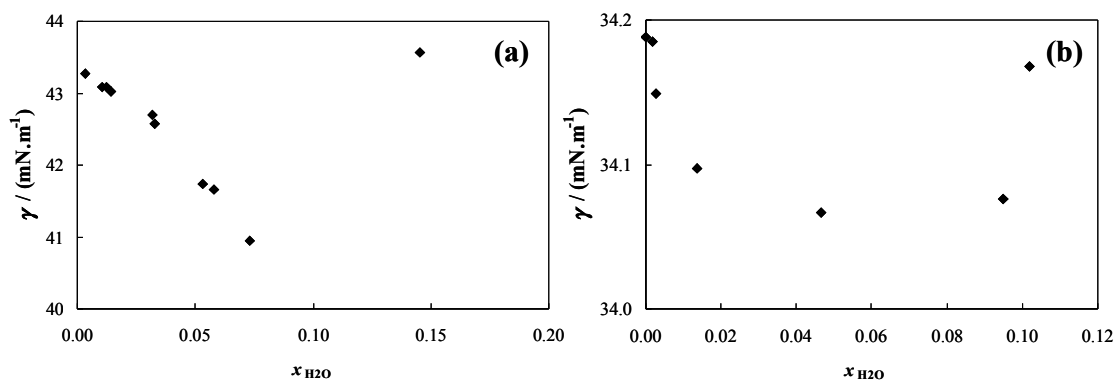


Figure 3.14. (a) $[C_4mim][PF_6]$ surface tension dependence of water mole fraction content at 303.15 K; (b) $[C_8mim][PF_6]$ surface tension dependence of water mole fraction content at 303.15 K.

Both ILs studied present a minimum in the surface tension for low water contents increasing for a higher and constant value. The effect of the water on the surface tensions seems to be more important for the more hydrophilic ionic liquids. In effect, for $[C_8mim][PF_6]$ this variation is almost insignificant, while for $[C_4mim][PF_6]$ this variation is quite considerable, in the order of 6 %. It is well established that water accommodates in the ionic liquid structure by establishing hydrogen bonds with both the anion and the cation, leading to the decrease of the IL physical properties by means of the reduction of the electrostatic attractions between the ions, and therefore to a decrease on the overall cohesive energy. The presence of low water content forces the ionic liquid to rearrange into a new different internal order in which more water can be accommodated, till a point where further addition of water leads to a complete solvation of the ions and to the appearance of water molecules not hydrogen-bonded to the IL, and thus to a new structural rearrangement leading to an increase in the physical properties^[40,137,138].

This IL surface tension dependence on the water content may explain the discrepancies between some results of this work when compared to literature data. Most authors who measured ILs surface tensions neither report the ILs water content and

impurity levels nor make reference to any drying methodology^[103,113,118]. Only Huddleston et al.^[41] seem to have dried the ILs used, although for a short period of just 4 hours, leading to a final water content higher than those achieved in this work and, as consequence, obtaining values of surface tensions lower than those obtained for dry ILs.

The respective surface thermodynamic properties are reported in Table 3.10. It is possible to observe that both the surface entropies and the surface enthalpies are not significantly affected by the water content of the saturated ionic liquids.

3.3.3.5. Estimated Critical Temperatures

Critical temperatures (T_c) are one of the most relevant thermophysical properties since they can be used in many corresponding states correlations for equilibrium and transport properties of fluids^[78]. Due to ILs intrinsic nature, with negligible vapor pressures and relatively low decomposition temperatures, the determination of critical temperature is impossible. Nonetheless several methods for critical temperature estimation based on surface tension data can be found in literature^[78,107,108]. The estimation of the critical temperature of the used ionic liquids based on the temperature dependence of the surface tension and liquid density were carried by means of the Eötvös^[107] and Guggenheim^[108] empirical equations described below and are reported in Table 3.13.

$$\gamma \left(\frac{M}{\rho} \right)^{\frac{2}{3}} = K (T_c - T) \quad 3.11$$

$$\gamma = K \left(1 - \frac{T}{T_c} \right)^{\frac{11}{9}} \quad 3.12$$

respectively, where γ is the surface tension, T_c the critical temperature, M the molecular weight and ρ the density of the ionic liquid. Both equations reflect the fact that γ becomes null at the critical point and are based on corresponding states correlations^[78]. The critical temperature values estimated in this work are compared in Table 3.13 with the values reported by Rebelo et al.^[114], estimated using the same approach and the values reported by Valderrama and Robles^[139] estimated using an extended group contribution

method, based on the models of Lydersen^[140] and Joback^[141] and Reid^[142].

Table 3.13. Estimated critical temperatures, T_c , using both Eötvös^[107] (Eot) and Guggenheim^[108] (Gug) equations, comparison and relative deviation from literature data

ILs	This work		Rebello et al. ^[114]				Valderrama and Robles ^[139]		
	$\frac{Eot}{T_c/K}$	$\frac{Gug}{T_c/K}$	$\frac{Eot}{T_c/K}$	$\frac{RD}{\%}$	$\frac{Gug}{T_c/K}$	$\frac{RD}{\%}$	$\frac{GCM^a}{T_c/K}$	$\frac{Eot}{RD/\%}$	$\frac{Gug}{RD/\%}$
[C ₄ mim][PF ₆]	977 ± 22	958 ± 17	1187	17.7	1102	13.1	544.0	-79.6	-76.1
[C ₆ mim][PF ₆]	1116 ± 15	1039 ± 10	1109	-0.6	1050	1.0	589.7	-89.2	-76.2
[C ₈ mim][PF ₆]	977 ± 22	958 ± 17	997	2.0	972	1.4	625.5	-53.7	-50.7
[C ₄ C ₁ mim][PF ₆]	1159 ± 19	1091 ± 16							
[C ₄ mim][BF ₄]	1183 ± 12	1113 ± 8	1240	4.6	1158	3.9	632.3	-87.1	-76.0
[C ₈ mim][BF ₄]	870 ± 16	873 ± 11	1027	15.3	990	11.8	726.1	-19.8	-20.2
[C ₄ mim][Tf ₂ N]	1110 ± 18	1032 ± 13	1077	-3.1	1012	-2.0	851.8	-30.3	-21.2
[C ₄ mim][CF ₃ SO ₃]	1628 ± 55	1264 ± 8					697.1	-133.5	-81.3

^aGroup Contribution Method

Rebello's values are in good agreement with the critical temperatures here reported unlike Valderrama and Robles critical temperatures that are much lower than the values obtained from the surface tension data. It is well established that this approach of extrapolating the surface tension data (at 1 atm) to estimate the critical temperature provides estimations of the critical temperatures that are lower than those directly measured since it does not take into account the influence of the critical pressure on the surface tension^[140]. This implies that the estimated values for the critical temperatures using the Valderrama and Robles approach are unreliable.

Based on what is known today concerning the relative volatilities of ionic liquids^[25,134] it is hard to trust the values of critical temperatures obtained, since predictions of relative volatilities based on these data are contrary to the experimental observations for a number of cases. This approach to the estimation of the critical temperatures, using data from a limited temperature range, and requiring a too large extrapolation, towards the estimation of meaningful values for the critical temperatures introduces an important error in the estimation of the critical temperature values.

3.3.3.6. *Effective Ionic Concentration and Surface Tension Relation*

Being the surface tensions dependent on the interactions between the IL molecules it should be possible to relate those values to obtain a correlation for the surface tensions. The technique used above cannot however establish a quantitative value for the hydrogen bond energies in spite of the attempts carried by some authors^[143] in this direction. Nevertheless, recently, a new approach on the direction of correlating thermophysical properties of ionic liquids with molecular interactions was proposed by Tokuda et al.^[144] They suggested that ILs thermophysical properties are related to their ionic nature and thus used the molar conductivity ratio (A_{imp}/A_{NMR}), where A_{imp} is the molar conductivity obtained by electrochemical impedance measurements and A_{NMR} is that calculated from the pulse-field-gradient spin-echo NMR ionic self-diffusion coefficients and the Nernst-Einstein equation, expressed as the effective ionic concentration (C_{eff}), to correlate properties such as viscosities and glass transitions. The C_{eff} illustrates the degree of the cation-anion aggregation at equilibrium and can be explained by the effects of anionic donor and cationic acceptor abilities and by the inductive and dispersive forces for the alkyl chain lengths in the cations^[144]. In this work, this approach was extended to the surface tensions using C_{eff} values obtained from literature^[87,144,145]. As shown in Figure 3.15 there is a correlation of the surface tension with the effective ionic concentration described by the following equation

$$\gamma = 12.115 e^{0.2215C_{eff}} \quad 3.13$$

Although it should be noted that it is possible to obtain a correlation between the measured surface tensions and the effective ionic concentration (C_{eff}) this does not imply that the surface tensions are solely controlled by the electrostatic forces alone. Instead, a subtle balance between these and other intermolecular forces are acting in ionic liquids resulting in the observed surface tension. Although more data are required for developing a sound correlation, the results here obtained indicate that the C_{eff} could be an useful parameter for the estimation of the ILs surface tensions.

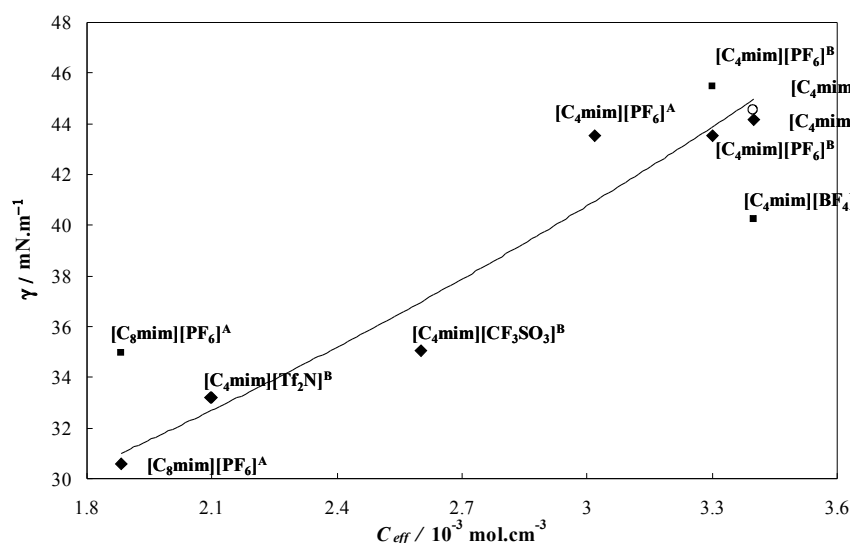


Figure 3.15. C_{eff} dependency of surface tension for $[C_4mim][BF_4]$, $[C_4mim][CF_3SO_3]$, $[C_4mim][PF_6]$, $[C_8mim][PF_6]$ and $[C_4mim][Tf_2N]$ at 303.15 K: \blacklozenge , this work surface tension data; \blacksquare , Law et al.^[113] surface tension data; \circ , Yang et al.^[110] surface tension data; ^A, Umecky et al.^[145] C_{eff} data; ^B, Tokuda et al.^[87,144] C_{eff} data.

3.3.4. Conclusions

Many engineering applications in the chemical process industry, such as the mass-transfer operations like distillation, extraction, absorption and adsorption, require surface tension data. The ILs interfacial properties are particularly important as they determine the mass transfer enhancement in gas-liquid-liquid or liquid-liquid extraction systems.

New experimental data are reported for the surface tensions of eight ionic liquids in the temperature range from (288 to 353) K and at atmospheric pressure. The ILs present surface tensions lower than those observed for conventional salts but still much higher than those reported for common organic solvents. Very low surface entropies were observed for all ionic liquids indicating an high surface ordering.

The results presented indicate that the anion-cation interactions are more relevant for the understanding of the surface tensions than the interactions between the ion pairs. Similarly to what is commonly observed for most organic compounds, the increase in size of the ionic liquid molecule leads to an increase of the interaction forces between the IL ion pairs^[129] but this size increase leads to a decrease of the surface tension due to the

dispersion of the ion charge and the reduction on the hydrogen bond strength between the anion and cation as observed from mass spectrometry. This peculiar behavior precludes the application of the Stefan equation to obtain a relation between the surface tensions and the heats of vaporization for ionic liquids. The surface interactions of ionic liquids are however a very complex matter and exceptions to the rule of increasing surface tensions with increasing cation-anion interaction were observed notably with the [bmmim] cation. The substitution of the most acidic hydrogen, on the carbon 2, by a methyl group, leads to a state of less entropy and therefore to an enhancement of the alkyl chain interactions. Lowering the disorder in the surface leads to an increase on the surface tensions of this ionic liquid when compared with the homologous unsubstituted compound.

The influence of the water content on the surface tensions was also investigated. Low water contents contribute to a decrease on the surface tension of ionic liquids. This decrease is more prominent for the less hydrophobic ionic liquids being almost insignificant for the most hydrophobic ones. Nevertheless, the decrease on the surface tension is followed by an increase to a higher and constant value, that for the more hydrophobic ionic liquids is similar to the surface tension values of the dry IL. The surface tension decrease is due to the water accommodation in the ionic liquid structure, by establishing hydrogen bonds with both the anion and cation, leading to a reduction of the electrostatic attractions between the ions and therefore to a decrease on the overall cohesive energy.

Being shown that the surface tensions depend on the strength of the interactions between anion and cation, and in particular that they could be related with the hydrogen bond strength as measured by mass spectrometry, it was attempted to develop a correlation for surface tensions with the cation-anion interactions. For that purpose, a correlation with the effective ionic concentration (C_{eff}) was developed showing that this could be a useful parameter for the estimation of the surface tension of ionic liquids.

4. Final Remarks and Future Work

"A man's limitations are not the things he wants to do and can't; they are the things he ought to do but doesn't. The difficult we will do eventually, the impossible will just take a little more time."

Source Unknown

The work developed provide new insights about PFCs and ILs molecular interactions and thus can act as a mean of achieving a detailed understanding of the interfacial behavior. Nonetheless, vapor-liquid interfacial tension is only the beginning of the path to understand more complex systems. Thus, the study of liquid-liquid interfaces rises as an inspiring challenge for future work.

The most important drawback on liquid-liquid interfacial tension measurements resides in the preference plate wettability of one compound over the other. In systems where the bottom phase presents lower wettability, towards the plate, than the top phase the traditional Pt/Ir plate faces extreme difficulties on maintaining the precision along the detachment/immersion cycles. The impossibility of assuring a correct and accurate measurement of the system property forces the experimentalist to repeat the plate cleaning process and system preparation (plate and top phase placement) after each detachment cycle, leading to an extremely time consuming process and thus a not viable process.

In order to develop a methodology able to accurately measure interfacial tensions of such systems an PTFE plate was engineered (Figure 4.1).



Figure 4.1. Custom made PTFE Wilhelmy plate.

The plate's development is still in its beginning and presents several handicaps. To start, the plate thickness is excessive not ensuring that the plate's buoyancy term is small and a short under-cutting of the meniscus, before rupture occurs, is achieved.

Nevertheless, to have a perspective of the developed PTFE plate potential, the system perfluorodecalin/water was studied.

Although they do not present the well-established linear trend decrease with temperature, as achieved for the surface tension when using the Du Noüy ring, the interfacial tension values obtained (Figure 4.2) indicate that a successful measurement

method can be developed.

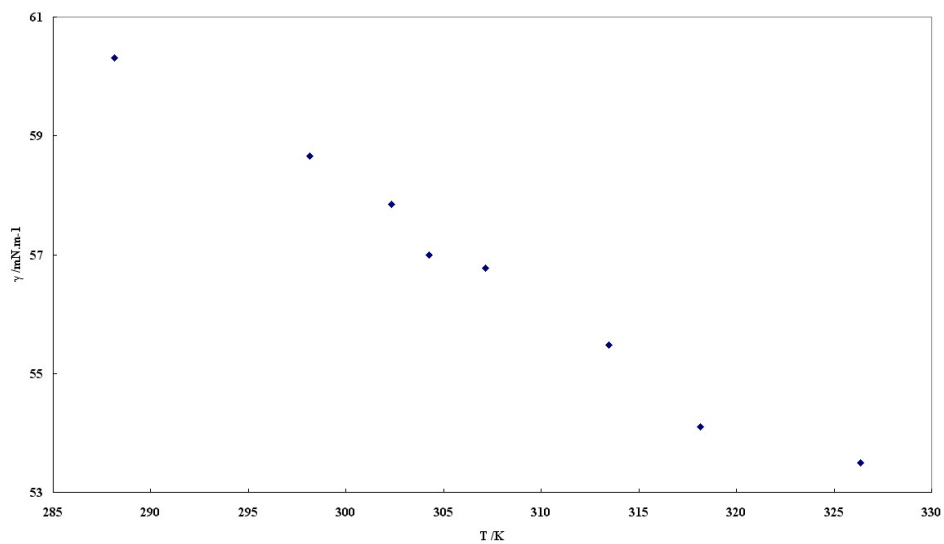


Figure 4.2. Perfluorodecalin/water interfacial tension as a function of temperature.

5. References

“I shall never be ashamed of citing a bad author if the line is good”

Seneca

References

- [1] P.T. Anastas, J.C. Warner, *Green chemistry theory and practice*, Oxford University Press, New York (Ed.) (1998)
- [2] B. Trost "**The atom economy--a search for synthetic efficiency**" *Science* 254 (1991) 1471
- [3] R.A. Sheldon "**Green solvents for sustainable organic synthesis: state of the art**" *Green Chem.* 7 (2005) 267
- [4] R.D. Rogers, G.A. Voth "**Ionic liquids**" *Acc. Chem. Res.* 40 (2007) 1077
- [5] J.M. DeSimone, W. Tumas, *Green chemistry using liquid and supercritical carbon dioxide*, Oxford University Press, New York, (2003)
- [6] C. Li "**Organic reactions in aqueous media with a focus on carbon-carbon bond formations: a decade update**" *Chem. Rev.* 105 (2005) 3095
- [7] P.F.F. Amaral, M.G. Freire, M.H.M. Rocha-Leão, I.M. Marrucho, J.A.P. Coutinho, M.A.Z. Coelho "**Optimization of oxygen mass transfer in a multiphase bioreactor with perfluorodecalin as a second liquid phase**" *Biotechnol. Bioeng.* 99(3) (2008) 588
- [8] W. Miao, T. Chan "**Ionic-liquid-supported synthesis: a novel liquid-phase strategy for organic synthesis**" *Acc. Chem. Res.* 39 (2006) 897
- [9] D.A. Britz, A.N. Khlobystov, J. Wang, A.S. O'Neil, M. Poliakoff, A. Ardavan, G.A.D. Briggs "**Selective host-guest interaction of single-walled carbon nanotubes with functionalised fullerenes**" *Chem. Commun.* (2004) 176
- [10] L.C.J. Clark, F. Gollan "**Survival of mammals breathing organic liquids equilibrated with oxygen at atmospheric pressure**" *Science* 152 (1966) 1755
- [11] D.C. Rideout, R. Breslow "**Hydrophobic acceleration of diels-alder reactions**" *JACS* 102 (1980) 7816
- [12] J.W. Sargent, R.J. Seffl "**Properties of perfluorinated liquids**" *Fed. Proc.* 29 (1970) 1699
- [13] F.G. Drakesmith "**Electrofluorination of organic compounds**" *Top. Curr. Chem.* 193 (1997) 197
- [14] H.C. Fielding, *Organofluorine surfactants and textile chemicals*, in Banks, R. E., "*Organofluorine Chemicals and Their Industrial Applications*", Ellis Horwood for the Society of Chemical Industry C (Ed.) (1979)
- [15] A.M.A. Dias, M.G. Freire, J.A.P. Coutinho, I.M. Marrucho "**Solubility of oxygen in liquid perfluorocarbons**" *Fluid Phase Equilib.* 222-223 (2004) 325
- [16] A.M. Dias. *Gas solubilities in blood substitutes*. University of Aveiro, Portugal. 2005.
- [17] M. Freire, A. Razzouk, I. Mokbel, J. Jose, I. Marrucho, J. Coutinho "**Solubility of hexafluorobenzene in aqueous salt solutions from (280 to 340) k**" *J. Chem. Eng. Data* 50 (2005) 237
- [18] M.G. Freire, P.J. Carvalho, A.J. Queimada, I.M. Marrucho, J.A.P. Coutinho "**Surface tension of liquid fluorocompounds**" *J. Chem. Eng. Data* 51 (2006) 1820
- [19] P. Walden "" *Bull. Acad. Imper. Sci. St. Petersburg* 8 (1914) 405

- [20] P. Wasserscheid, W. Keim "Ionic liquids - new ?olutions? for transition metal catalysis" *Angew. Chem., Int. Ed.* 39 (2000) 3772
- [21] T.B. Scheffler, C.L. Hussey, K.R. Seddon, C.M. Kear, P.D. Armitage "Molybdenum chloro complexes in room-temperature chloroaluminate ionic liquids: stabilization of hexachloromolybdate(2-) and hexachloromolybdate(3-)" *Inorg. Chem.* 22 (1983) 2099
- [22] N.V. Plechkova, K.R. Seddon "Applications of ionic liquids in the chemical industry" *Chem. Soc. Rev.* 37 (2008) 123
- [23] M. Freemantle "" *Chem. Eng. News* 81 (2003) 9
- [24] B. Weyershausen, K. Hell, U. Hesse "Industrial application of ionic liquids as process aid" *Green Chem.* 7 (2005) 283
- [25] M.J. Earle, J.M.S.S. Esperanca, M.A. Gilea, J.N. Canongia Lopes, L.P.N. Rebelo, J.W. Magee, K.R. Seddon, J.A. Widegren "The distillation and volatility of ionic liquids" *Nature* 439 (2006) 831
- [26] J.G. Huddleston, H.D. Willauer, R.P. Swatloski, A.E. Visser, R.D. Rogers "Room temperature ionic liquids as novel media for clean liquid-liquid extraction" *Chem. Commun.* 16 (1998) 1765
- [27] A.G. Fadeev, M.M. Meagher "Opportunities for ionic liquids in recovery of biofuels" *Chem. Commun.* (2001) 1765
- [28] J. McFarlane, W.B. Ridenour, H. Luo, R.D. Hunt, D.W. DePaoli, R.X. Ren "Room temperature ionic liquids for separating organics from produced water" *Sep. Sci. Technol.* 40 (2005) 1245
- [29] G.T. Wei, Z.S. Yang, C.J. Chen "Room temperature ionic liquid as a novel medium for liquid/liquid extraction of metal ions" *Anal. Chim. Acta* 488 (2003) 183
- [30] N. Kozonoi, Y. Ikeda "Extraction mechanism of metal ion from aqueous solution to the hydrophobic ionic liquid, 1-butyl-3-methylimidazolium nonafluorobutanesulfonate" *Monatsh. Chem.* 138 (2007) 1145
- [31] M.S. Selvan, M.D. McKinley, R.H. Dubois, J.L. Atwood "Liquid-liquid equilibria for toluene plus heptane+1-ethyl-3-methylimidazolium triiodide and toluene plus heptane+1-butyl-3-methylimidazolium triiodide" *J. Chem. Eng. Data* 45 (2000) 841
- [32] T.M. Letcher, N. Deenadayalu, B. Soko, D. Ramjugernath, P.K. Naicker "Ternary liquid-liquid equilibria for mixtures of 1-methyl-3-octylimidazolium chloride plus an alkanol plus an alkane at 298.2 K and 1 bar" *J. Chem. Eng. Data* 48 (2003) 904
- [33] S.G. Zhang, Z.C. Zhang "Novel properties of ionic liquids in selective sulfur removal from fuels at room temperature" *Green Chem.* 4 (2002) 376
- [34] L.C. Branco, J.G. Crespo, C.A.M. Afonso "Highly selective transport of organic compounds by using supported liquid membranes based on ionic liquids" *Angew. Chem., Int. Ed.* 41 (2002) 2771
- [35] E. Dumont, H. Delmas "Mass transfer enhancement of gas absorption in oil-in-water systems: a review" *Chem. Eng. Process.* 42 (2003) 419
- [36] A.M.A. Dias, A.I. Caco, J.A.P. Coutinho, L.M.N.B.F. Santos, M.M. Pineiro, L.F. Vega, M.F.C. Gomes, I.M. Marrucho "Thermodynamic properties of perfluoro-n-octane" *Fluid Phase Equilib.* 225 (2004) 39
- [37] A.M.A. Dias, C.M.B. Goncalves, A.I. Caco, L.M.N.B.F. Santos, M.M. Pineiro, L.F. Vega, J.A.P. Coutinho, I.M. Marrucho "Densities and vapor pressures of highly fluorinated compounds" *J. Chem. Eng. Data* 50 (2005) 1328

- [38] A.M.A. Dias, H. Carrier, J.L. Daridon, J.C. Pamiés, L.F. Vega, J.A.P. Coutinho, I.M. Marrucho "Vapor-liquid equilibrium of carbon dioxide-perfluoroalkane mixtures: experimental data and soft modeling" *Ind. Eng. Chem. Res* 45 (2006) 2341
- [39] M.G. Freire, P.J. Carvalho, A.M. Fernandes, I.M. Marrucho, A.J. Queimada, J.A. Coutinho "Surface tensions of imidazolium based ionic liquids: anion, cation, temperature and water effect" *J. Colloid Interface Sci.* 314(2) (2007) 621
- [40] K.R. Seddon, A. Stark, M. Torres "Influence of chloride, water, and organic solvents on the physical properties of ionic liquids" *Pure Appl. Chem.* 72 (12) (2000) 2275
- [41] J.G. Huddleston, A.E. Visser, W.M. Reichert, H.D. Willauer, G.A. Broker, R.D. Rogers "Characterization and comparison of hydrophilic and hydrophobic room temperature ionic liquids incorporating the imidazolium cation" *Green Chem.* 3 (2001) 156
- [42] R.L. Gardas, M.G. Freire, P.J. Carvalho, I.M. Marrucho, I.M.A. Fonseca, A.G.M. Ferreira, Coutinho, Joao, A P "High pressure densities and derived thermodynamic properties of imidazolium based ionic liquids" *J. Chem. Eng. Data* 52(1) (2007) 80
- [43] M.G. Freire, A.M.A. Dias, M.A.Z. Coelho, J.A.P. Coutinho, I.M. Marrucho "Enzymatic method for determining oxygen solubility in perfluorocarbon emulsions" *Fluid Phase Equilib.* 231 (2005) 109
- [44] M.R. Wolfson, J.S. Greenspan, T.H. Shaffer "Liquid-assisted ventilation: an alternative respiratory modality" *Pediatr. Pulm.* 26 (1998) 42
- [45] G.V. Ermakov, V.P. Skripov "Thermodynamic properties of perfluorocarbons" *Russ. J. Phys. Chem.* 43 (1967) 726
- [46] T. Handa, P. Mukerjee "Surface tensions of nonideal mixtures of fluorocarbons and hydrocarbons and their interfacial tensions against water" *J. Phys. Chem.* 85 (1981) 3916
- [47] R.N. Haszeldine, F. Smith "Organic fluorides. part vi. the chemical and physical properties of certain fluorocarbons" *J. Chem. Soc.* 1 (1951) 603
- [48] I.A. McLure, V.A.M. Soares, B. Edmonds "Surface tension of perfluoropropane, perfluoro-n-butane, perfluoro-n-hexane, perfluoro-octane, perfluorotributylamine and n-pentane. application of the principle of corresponding states to the surface tension of perfluoroalkanes" *J. Chem. Soc., Faraday Trans. 1* 78 (1982) 2251
- [49] N. Nishikido, W. Mahler, P. Mukerjee "Interfacial tensions of perfluorohexane and perfluorodecalin against water" *Langmuir* 5 (1989) 227
- [50] G.D. Oliver, S. Blumkin, C.W. Cunningham "Some physical properties of hexadecafluoroheptane_{1a,1b}" *JACS* 73 (1951) 5722
- [51] T. Sakka, Y.H. Ogata "Surface tension of fluoroalkanes in a liquid phase" *J. Fluorine Chem.* 126 (2005) 371
- [52] V.P. Skripov, V.V. Firsov "Surface tension of perfluoroalkanes" *Russ. J. Phys. Chem.* 42 (1968) 653
- [53] V.E. Stiles, G.H. Cady "Physical properties of perfluoro-n-hexane and perfluoro-2-methylpentane" *JACS* 74 (1952) 3771
- [54] J.K. Yoon, D.J. Burgess "Comparison of dynamic and static interfacial tension at aqueous perfluorocarbon interfaces" *J. Colloid Interface Sci.* 151 (1992) 402
- [55] A.G. Gaonkar, R.D. Neuman "The effect of wettability of wilhelmy plate and du nouy ring on interfacial tension measurements in solvent extraction systems" *J. Colloid Interface Sci.* 98 (1984) 112

- [56] A. Goebel, K. Lunkenheimer "Interfacial tension of the water/n-alkane interface" *Langmuir* 13 (1997) 369
- [57] R. Chirico, M. Frenkel, V. Diky, K. Marsh, R. Wilhoit "Thermoml-an xml-based approach for storage and exchange of experimental and critically evaluated thermophysical and thermochemical property data. 2. uncertainties" *J. Chem. Eng. Data* 48 (2003) 1344
- [58] The NIST Reference on Constants, Units, and Uncertainty; <http://www.physics.nist.gov/cuu/>
- [59] L.I. Rolo, A.I. Caco, A.J. Queimada, I.M. Marrucho, J.A.P. Coutinho "Surface tension of heptane, decane, hexadecane, eicosane, and some of their binary mixtures" *J. Chem. Eng. Data* 47 (2002) 1442
- [60] A.J. Queimada, A.I. Caco, I.M. Marrucho, J.A.P. Coutinho "Surface tension of decane binary and ternary mixtures with eicosane, docosane, and tetracosane" *J. Chem. Eng. Data* 50 (2005) 1043
- [61] A.J. Queimada, F.A.E. Silva, A.I. Caco, I.M. Marrucho, J.A.P. Coutinho "Measurement and modeling of surface tensions of asymmetric systems: heptane, eicosane, docosane, tetracosane and their mixtures" *Fluid Phase Equilib.* 214(2) (2003) 211
- [62] A.D. McNaught, A. Wilkinson, Compendium of chemical terminology, iupac recommendations, Blackwell Science: Cambridge, UK, (1997) 2nd ed.
- [63] A.W. Adamson, A.P. Gast, Physical chemistry of surfaces, John Wiley, (1997) 6th ed.
- [64] J.C. Miller, J.N. Miller, Statistics for analytical chemistry, PTR Prentice Hall: Chichester, (1993) 3rd ed.
- [65] M.Z. Faizullin "New universal relationships for surface tension and vaporization enthalpy of non-associated liquids" *Fluid Phase Equilib.* 211 (2003) 75
- [66] J.J. Jasper, E.R. Kerr, F. Gregorich "The orthobaric surface tensions and thermodynamic properties of the liquid surfaces of the n-alkanes, c5 to c28" *JACS* 75 (1953) 5252
- [67] A.H.N. Mousa "Study of vapor pressure and critical properties of perfluoro-n-hexane" *J. Chem. Eng. Data* 23 (1978) 133
- [68] A.E.H.N. Mousa, W.B. Kay, A. Kreglewski "The critical constants of binary mixtures of certain perfluoro-compounds with alkanes" *J. Chem. Thermodyn.* 4(2) (1972) 301
- [69] V.P. Skripov, G.N. Muratov "Data on surface-tension of liquids and their processing by thermodynamic similarity methods" *Zh. Fiz. Khim.* 51 (1977) 1369
- [70] R.D. Dunlap, C.J. Murphy, R.G. Bedford "Some physical properties of perfluoro-n-hexane" *JACS* 80 (1958) 83
- [71] V. Vandana, D.J. Rosenthal, A.S. Teja "The critical properties of perfluoro n-alkanes" *Fluid Phase Equilib.* 99 (1994) 209
- [72] W.V. Steele, R.D. Chirico, S.E. Knipmeyer, A. Nguyen "Vapor pressure, heat capacity, and density along the saturation line, measurements for cyclohexanol, 2-cyclohexen-1-one, 1,2-dichloropropane, 1,4-di-tert-butylbenzene, (+-)-2-ethylhexanoic acid, 2-(methylamino)ethanol, perfluoro-n-heptane, and sulfolane" *J. Chem. Eng. Data* 42 (1997) 1021
- [73] H.T. Milton, G.D. Oliver "High vapor pressure of n-hexadecafluoroheptane" *JACS* 74 (1952) 3951
- [74] D. Ambrose, B.E. Broderick, R. Townsend "The critical temperatures and pressures of thirty organic compounds" *J. Appl. Chem. Biotechnol.* 24 (1974) 359
- [75] J.L. Hales, R. Townsend "Liquid densities from 293 to 490 K of eight fluorinated aromatic

compounds" *J. Chem. Thermodyn.* 6 (1974) 111

- [76] G.D. Oliver, J.W. Grisard "Some thermodynamic properties of hexadecafluoroheptane" *JACS* 73 (1951) 1688
- [77] H.Y. Afeefy, J.F. Liebman, Stein, S. E. Neutral Thermochemical Data in NIST Chemistry WebBook, NIST Standard Reference Database Number 69, Eds. P. J. Linstrom and W. G. Mallard, June 2005, National Institute of Standards and Technology, Gaithersburg MD, 20899; <http://webbook.nist.gov/chemistry/>
- [78] B.E. Poling, J.M. Prausnitz, J.P. O'Connell, The properties of gases and liquids, McGraw-Hill: New York, (2000) Fifth Edition
- [79] R.D. Rogers, K.R. Seddon "Ionic liquids--solvents of the future?" *Science* 302 (2003) 792
- [80] K.N. Marsh, J.A. Boxall, R. Lichtenthaler "Room temperature ionic liquids and their mixtures--a review" *Fluid Phase Equilib.* 219 (2004) 93
- [81] C. Chiappe, D. Pieraccini "Ionic liquids: solvent properties and organic reactivity" *J. Phys. Org. Chem.* 18 (2005) 275
- [82] J.D. Holbrey, K.R. Seddon "The phase behaviour of 1-alkyl-3-methylimidazolium tetrafluoroborates; ionic liquids and ionic liquid crystals" *J. Chem. Soc., Dalton Trans.* 13 (1999) 2133
- [83] M.J. Earle, K.R. Seddon "Ionic liquids. green solvents for the future" *Pure Appl. Chem.* 72 (2000) 1391
- [84] C.P. Fredakle, J.M. Crosthwaite, D.G. Hert, S.N.V.K. Aki, J.F. Brennecke "Thermophysical properties of imidazolium-based ionic liquids" *J. Chem. Eng. Data* 49 (2004) 954
- [85] J.L. Anthony, E.J. Maginn, J.F. Brennecke "Solution thermodynamics of imidazolium-based ionic liquids and water" *J. Phys. Chem. B* 105 (2001) 10942
- [86] H. Tokuda, K. Hayamizu, K. Ishii, M. Susan, M. Watanabe "Physicochemical properties and structures of room temperature ionic liquids. 1. variation of anionic species" *J. Phys. Chem. B* 108 (2004) 16593
- [87] H. Tokuda, K. Hayamizu, K. Ishii, M. Susan, M. Watanabe "Physicochemical properties and structures of room temperature ionic liquids. 2. variation of alkyl chain length in imidazolium cation" *J. Phys. Chem. B* 109 (2005) 6103
- [88] J.H. Dymond, R. Malhotra "The tait equation: 100 years on" *Int. J. Thermophys.* 9 (1988) 941
- [89] M.G. Freire, C.M.S.S. Neves, P.J. Carvalho, R.M. Gardas, A.M. Fernandes, I.M. Marrucho, L.M.N.B.F. Santos, J.A.P. Coutinho "Mutual solubilities of water and hydrophobic ionic liquids" *J. Phys. Chem. B* 111(45) (2007) 13082
- [90] A. Saul, W. Wagner "New international skeleton tables for the thermodynamic properties of ordinary water substance" *J. Phys. Chem. Ref. Data* 17 (1988) 1439
- [91] H.Y. Afeefy, J.F. Liebman, S.E. Stein "Neutral thermochemical data in nist chemistry webbook" *NIST Standard Reference Database* Number 69 Eds. P. J. Linstrom and W. G. Mallard (June 2005) National Institute of Standards and Technology, Gaithersburg MD, 20899 (<http://webbook.nist.gov>)
- [92] M.M. Piñeiro, D. Bessières, J.M. Gacio, H. Saint-Guirons, J.L. Legido "Determination of high-pressure liquid density for n-perfluorohexane and n-perfluorononane" *Fluid Phase Equilib.* 220 (2004) 127
- [93] V.G. Niesen "(vapor + liquid) equilibria and coexisting densities of (carbon dioxide + n-butane) at 311 to 395 k" *J. Chem. Thermodyn.* 22 (1990) 777

- [94] C.D. Holcomb, S.L. Outcalt "A theoretical-based calibration and evaluation procedure for vibrating-tube densimeters" *Fluid Phase Equilib.* 150-151 (1998) 815
- [95] O. Fandiño, A.S. Pensado, L. Lugo, M.P.J. Comuñas, J. Fernández "Compressed liquid densities of squalane and pentarythritol tetra(2-ethylhexanoate)" *J. Chem. Eng. Data* 50 (2005) 939
- [96] O. Fandiño, J. Garcia, M.P.J. Comuñas, E.R. López, J. Fernández "Ppt measurements and equation of state (eos) predictions of ester lubricants up to 45 mpa" *Ind. Eng. Chem. Res.* 45 (2006) 1172
- [97] O.O. Okoturo, T.J. VanderNoot "Temperature dependence of viscosity for room temperature ionic liquids" *J. Electroanal. Chem.* 568 (2004) 167
- [98] R.G. Azevedo, J.M.S.S. Esperança, V. Najdanovic-Visak, Z.P. Visak, H.J.R. Guedes, M. Nunes da Ponte, L.P.N. Rebelo "Thermophysical and thermodynamic properties of 1-butyl-3-methylimidazolium tetrafluoroborate and 1-butyl-3-methylimidazolium hexafluorophosphate over an extended pressure range" *J. Chem. Eng. Data* 50 (2005) 997
- [99] H. Zhou, H. Lu, B. Liang "Solubility of multicomponent systems in the biodiesel production by transesterification of jatropha curcas l. oil with methanol" *J. Chem. Eng. Data* 51 (2006) 1130
- [100] Z. Gu, J.F. Brennecke "Volume expansivities and isothermal compressibilities of imidazolium and pyridinium-based ionic liquids" *J. Chem. Eng. Data* 47 (2002) 339
- [101] K.R. Harris, M. Kanakubo, L.A. Woolf "Temperature and pressure dependence of the viscosity of the ionic liquids 1-methyl-3-octylimidazolium hexafluorophosphate and 1-methyl-3-octylimidazolium tetrafluoroborate" *J. Chem. Eng. Data* 51 (2006) 1161
- [102] A.B. Pereiro, E. Tojo, A. Rodríguez, J. Canosa, J. Tojo "Properties of ionic liquid hmimpf6 with carbonates, ketones and alkyl acetates" *J. Chem. Thermodyn.* 38 (2006) 651
- [103] S.V. Dzyuba, R.A. Bartsch "Influence of structural variations in 1-alkyl(aralkyl)-3-methylimidazolium hexafluorophosphates and bis(trifluoromethylsulfonyl)imides on physical properties of the ionic liquids" *ChemPhysChem* 3 (2002) 161
- [104] R. Gomes De Azevedo, J.M.S.S. Esperança, J. Szydłowski, Z.P. Visak, P.F. Pires, H.J.R. Guedes, L.P.N. Rebelo "Thermophysical and thermodynamic properties of ionic liquids over an extended pressure range: [bmim][ntf2] and [hmim][ntf2]" *J. Chem. Thermodyn.* 37 (2005) 888
- [105] J.M.S.S. Esperança, H.J.R. Guedes, M. Blesic, L.P.N. Rebelo "Densities and derived thermodynamic properties of ionic liquids. 3. phosphonium-based ionic liquids over an extended pressure range" *J. Chem. Eng. Data* 51 (2006) 237
- [106] E. Gómez, B. González, A. Domínguez, E. Tojo, J. Tojo "Dynamic viscosities of a series of 1-alkylimidazolium chloride ionic liquids and their binary mixtures with water at several temperatures" *J. Chem. Eng. Data* 51 (2006) 696
- [107] J.L. Shereshefsky "Surface tension of saturated vapors and the equation of eotvos" *J. Phys. Chem.* 35 (1931) 1712
- [108] E.A. Guggenheim "The principle of corresponding states" *J. Chem. Phys.* 13 (1945) 253
- [109] M.G. Freire, P.J. Carvalho, R.L. Gardas, I.M. Marrucho, L.M.N.B.F. Santos, J.A.P. Coutinho "Mutual solubilities of water and the [cnmim][tf2n] hydrophobic ionic liquids" *J. Phys. Chem. B* in press (2008)
- [110] J. Yang, J. Gui, X. Lu, Q. Zhang, H. Li "Study on properties of ionic liquid bmibf4" *Acta Chim. Sin.* 63 (2005) 577

- [111] R. Gomes de Azevedo, J.M.S.S. Esperanca, J. Szydłowski, Z.P. Visak, P.F. Pires, H.J.R. Guedes, L.P.N. Rebelo "Thermophysical and thermodynamic properties of ionic liquids over an extended pressure range: [bmim][ntf2] and [hmim][ntf2]" *J. Chem. Thermodyn.* 37 (2005) 888
- [112] M. Krummen, P. Wasserscheid, J. Gmehling "Measurement of activity coefficients at infinite dilution in ionic liquids using the dilutor technique" *J. Chem. Eng. Data* 47 (2002) 1411
- [113] G. Law, P.R. Watson "Surface tension measurements of n-alkylimidazolium ionic liquids" *Langmuir* 17 (2001) 6138
- [114] L.P.N. Rebelo, J.N. Canongia Lopes, J.M.S.S. Esperanca, E. Filipe "On the critical temperature, normal boiling point, and vapor pressure of ionic liquids" *J. Phys. Chem. B* 109 (2005) 6040
- [115] V. Halka, R. Tsekov, W. Freyland "Peculiarity of the liquid/vapour interface of an ionic liquid: study of surface tension and viscoelasticity of liquid bmimpf6 at various temperatures" *Phys. Chem. Chem. Phys.* 9 (2005) 2038
- [116] L. Crowhurst, P.R. Mawdsley, J.M. Perez-Arlandis, P.A. Salter, T. Welton "Solvent-solute interactions in ionic liquids" *Phys. Chem. Chem. Phys.* 5 (2003) 2790
- [117] P. Hunt "Why does a reduction in hydrogen bonding lead to an increase in viscosity for the 1-butyl-2,3-dimethyl-imidazolium-based ionic liquids?" *J. Phys. Chem. B* 111(18) (2007) 4844
- [118] G. Law, P.R. Watson "Surface orientation in ionic liquids" *Chem. Phys. Lett.* 345 (2001) 1
- [119] A. Pereiro, P. Verdia, E. Tojo, A. Rodriguez "Physical properties of 1-butyl-3-methylimidazolium methyl sulfate as a function of temperature" *J. Chem. Eng. Data* 52(2) (2007) 377
- [120] M. Deetlefs, C. Hardacre, M. Nieuwenhuyzen, A. Padua, O. Sheppard, A. Soper "Liquid structure of the ionic liquid 1,3-dimethylimidazolium bis((trifluoromethyl)sulfonyl)amide" *J. Phys. Chem. B* 110 (2006) 12055
- [121] K. Dong, S. Zhang, D. Wang, X. Yao "Hydrogen bonds in imidazolium ionic liquids" *J. Phys. Chem. A* 110 (2006) 9775
- [122] Langmuir, I., In phenomena atoms and molecules, Philosophical Library, New York, (1950)
- [123] DIPPR Design Institute for Physical Properties: DIPPR 801 database Brigham Young University; 1998
- [124] E. Sloutskin, C.D. Bain, B.M. Ocko, M. Deutsch "Surface freezing of chain molecules at the liquid-liquid and liquid-air interfaces" *Faraday Disc.* 129 (2005) 339
- [125] R.M. Lynden-Bell "Gas-liquid interfaces of room temperature ionic liquids" *Mol. Phys.* 101 (2003) 2625
- [126] G. Law, P.R. Watson, A.J. Carmichael, K.R. Seddon "Molecular composition and orientation at the surface of room-temperature ionic liquids: effect of molecular structure" *Phys. Chem. Chem. Phys.* 3 (2001) 2879
- [127] T. Iimoria, T. Iwahashi, H. Ishiib, K. Seki, Y. Ouchi, R. Ozawac, H. Hamaguchic, D. Kim "Orientational ordering of alkyl chain at the air/liquid interface of ionic liquids studied by sum frequency vibrational spectroscopy" *Chem. Phys. Lett.* 389 (2004) 321
- [128] J. Bowers, C.P. Butts, P.J. Martin, M.C. Vergara-Gutierrez, R.K. Heenan "Aggregation behavior of aqueous solutions of ionic liquids" *Langmuir* 20 (2004) 2191
- [129] E. Slouskin, B. Ocko, L. Tamam, I. Kuzmenko, T. Gog, M. Deutsch "Surface layering in ionic liquids: an x-ray reflectivity study" *J. Am. Chem. Soc.* 127 (2005) 7796

- [130] L.M.N.B.F. Santos, J.N. CanongiaLopes, J.A.P. Coutinho, J.M.S.S. Esperanca, L.R. Gomes, I.M. Marrucho, L.P.N. Rebelo "Ionic liquids: first direct determination of their cohesive energy" *J. Am. Chem. Soc* 192(2) (2006) 284
- [131] R.G. Cooks, J.T. Koskinen, P.D. Thomas "The kinetic method of making thermochemical determinations" *Int. J. Mass Spectrom.* 34 (1999) 85
- [132] S. Tsuzuki, H. Tokuda, K. Hayamizu, M. Watanabe "Magnitude and directionality of interaction in ion pairs of ionic liquids: relationship with ionic conductivity" *J. Phys. Chem. B* 109 (2005) 16474
- [133] R.L. Gardas, M.G. Freire, P.J. Carvalho, I.M. Marrucho, I.M.A. Fonseca, A.G.M. Ferreira, J.A.P. Coutinho "P, r, t measurements of imidazolium based ionic liquids" *J. Chem. Eng. Data* in press (2007) corrected proof
- [134] D. Fu, X. Sun, J. Pu, S. Zhao "Effect of water content on the solubility of co2 in the ionic liquid [bmim][pf6]" *J. Chem. Eng. Data* 51 (2006) 371
- [135] I. Malham, P. Letellier, M. Turmine "Evidence of a phase transition in water-1-butyl-3-methylimidazolium tetrafluoroborate and water-1-butyl-2,3-dimethylimidazolium tetrafluoroborate mixtures at 298 K: determination of the surface thermal coefficient, bt,p" *J. Phys. Chem. B* 110 (2006) 14212
- [136] J. Sung, Y. Jeon, D. Kim, T. Iwahashi, T. Iimori, K. Seki, Y. Ouchi "Air-liquid interface of ionic liquid + h2o binary system studied by surface tension measurement and sum-frequency generation spectroscopy" *Chem. Phys. Lett.* 406 (2005) 495
- [137] L. Cammarata, S.G. Kazarian, P.A. Salter, T. Welton "Molecular states of water in room temperature ionic liquids" *Phys. Chem. Chem. Phys.* 3 (2001) 5192
- [138] S. Rivera-Rubero, S. Baldelli "Influence of water on the surface of hydrophilic and hydrophobic room-temperature ionic liquids" *J. Am. Chem. Soc.* 126 (2004) 11788
- [139] J. Valderrama, P. Robles "Critical properties, normal boiling temperatures, and acentric factors of fifty ionic liquids" *Ind. Eng. Chem. Res.* 46 (2007) 1338
- [140] A.L. Lydersen, Estimation of critical properties of organic compounds. report 3, Engineering Experimental Station: Madison, WI, University of Wisconsin COE (Ed.) (1955)
- [141] K.K. Joback, R. Reid "Estimation of pure component properties from group contribution" *Chem. Eng. Commun.* 57 (1987) 233
- [142] K M Klineciewicz, R C Reid, "Estimation of critical properties with group contribution methods" *AIChE Journal* 30 (1984) 137
- [143] F.C. Gozzo, L.S. Santos, R. Augusti, C.S. Consorti, J. Dupont, M.N. Eberlin "Gaseous supramolecules of imidazolium ionic liquids: "magic" numbers and intrinsic strengths of hydrogen bonds" *Chem.--Eur. J.* 10 (2004) 6187
- [144] H. Tokuda, S. Tsuzuki, M. Susan, K. Hayamizu, M. Watanabe "How ionic are room-temperature ionic liquids? an indicator of the physicochemical properties" *J. Phys. Chem. B* 110 (2006) 19593
- [145] T. Umecky, M. Kanakubo, Y. Ikushima "Effects of alkyl chain on transport properties in 1-alkyl-3-methylimidazolium hexafluorophosphates" *J. Mol. Liq.* 119 (2005) 77